

Characterization of the pro-inflammatory activity of short-chain fatty acids (SCFAs)

Doctoral thesis
to obtain a doctorate (PhD)
from the Faculty of Medicine
of the University of Bonn

Wei Wang
from Henan, China
2021

Written with authorization of
the Faculty of Medicine of the University of Bonn

First reviewer: Prof. Dr. med. Eicke Latz

Second reviewer: Prof. Dr. med. Joachim Schultze

Day of oral examination: 06.10.2021

For the institute of Innate Immunity
Director: Prof. Dr. med. Eicke Latz

Table of Contents

1. Abstract	6
2. Introduction.....	7
2.1 The immune system: an overview.....	7
2.1.1 The functions of the immune system	7
2.1.2 Pathogen recognition machinery	8
2.1.3 The NLRP3 inflammasome	10
2.1.4 Apoptosis, pyroptosis, necroptosis, and PANoptosis - programmed cell death (PCD) and inflammation.....	13
2.2 Short-chain fatty acids (SCFAs).....	16
2.2.1 Commensal bacteria and metabolites in the gut	16
2.2.2 The category and molecular functions of SCFAs	17
2.2.3 The role of SCFAs in health and diseases.....	18
2.3 Inflammatory bowel disease (IBD)	19
2.3.1 The pathogenesis of IBD.....	19
2.3.2 Clinical treatment and therapeutic targets of IBD.....	21
2.4 Objective of this study.....	22
3 Materials and Methods.....	24
3.1 Materials	24
3.1.1 Devices	24
3.1.2 Consumables.....	25
3.1.3 Chemical and Reagents.....	25
3.1.4 Kits	27
3.1.5 Antibodies.....	28
3.1.6 siRNAs for electroporation	29
3.1.7 qPCR primers	30
3.1.8 Cell culture media	30
3.1.9 Buffers and Solutions.....	31
3.1.10 Primary cells and Cell lines	32
3.1.11 Mice.....	33
3.2 Methods.....	33
3.2.1 Cell culture and counting.....	33
3.2.2 Cultivation and stimulation of THP-1 monocytes.....	33
3.2.3 Cultivation, differentiation and stimulation of THP-1 macrophages.....	34
3.2.4 Purification and stimulation of human PBMCs	34
3.2.5 Purification, differentiation and stimulation of primary human monocyte-derived macrophages (hMDMs)	34

3.2.6 Homogeneous Time Resolved Fluorescence (HTRF).....	35
3.2.7 Western blot	35
3.2.8 WES.....	37
3.2.9 Small interfering RNA (siRNA) electroporation in primary human macrophages.....	37
3.2.10 Caspase-8 activity assay	38
3.2.11 Intracellular ROS production assay	38
3.2.12 Lactate dehydrogenase (LDH) assay	38
3.2.13 Live cell imaging for cell death analysis by incuCyte.....	39
3.2.14 Reverse transcription quantitative real-time PCR.....	39
3.2.15 ASC specks imaging.....	40
3.2.16 Multiple immunoassay by Luminex.....	41
3.2.17 RNA-sequencing (RNA-Seq).....	41
3.2.18 Mass Spectrometry (MS)	43
4. Results.....	45
4.1 Characterization of the effects of short-chain fatty acids (SCFAs) on TLR-induced cellular responses through transcriptomic and proteomic analysis.....	45
4.1.1 Transcriptomic analysis reveals regulatory functions of SCFAs on the TLR-induced gene expression profile	45
4.1.2 DE Genes regulated by SCFAs are associated with diverse cellular processes	48
4.1.3 Dissecting the influence of SCFAs on TLR-mediated cellular responses through proteomic analysis.....	50
4.2 SCFAs regulate the LPS-induced cytokine secretion profile in primary human macrophages.....	53
4.2.1 SCFAs modulate the production of multiple LPS-induced cytokines	53
4.2.2 Butyrate in combination with LPS induce IL-1 β secretion in macrophages but not in monocytes.....	56
4.2.3 Butyrate induces IL-1 β release in concert with TLR activation	58
4.2.4 LPS + butyrate induce IL-1 β secretion in a NLRP3 inflammasome-dependent manner.....	58
4.2.5 Butyrate does not impair the priming of primary human macrophages in response to TLR activation.....	61
4.2.6 LPS + butyrate drive NLRP3 inflammasome activation dependently on potassium efflux ..	63
4.2.7 LPS + butyrate trigger NLRP3 inflammasome activation but not pyroptosis and ASC speck formation.....	65
4.3 Multiple mediators are involved in the induction of IL-1 β in response to LPS + butyrate in primary human macrophages.....	68
4.3.1 Butyrate inhibits the expression of cFLIP, an endogenous inhibitor of caspase-8.....	68
4.3.2 LPS + butyrate induce IL-1 β secretion in a caspase-8-dependent manner.....	70
4.3.3 RIPK3 is involved in the IL-1 β secretion induced by LPS + butyrate	72
4.3.4 RIPK1 negatively regulates IL-1 β secretion driven by LPS + butyrate.....	73

4.3.5 STAT3 is a negative regulator of the IL-1 β response to LPS + butyrate	75
4.3.6 TBK1 downregulates the IL-1 β secretion driven by LPS + butyrate.....	76
4.3.7 HDAC11 modulates IL-1 β processing triggered by LPS + butyrate through the regulation of NLRP3 and pro-IL-1 β expression.....	78
4.4 SCFAs exacerbate the inflammatory response through inhibition of the IL-10 signaling pathway	79
4.4.1 Butyrate inhibits TLR-induced IL-10 production in primary human macrophages	80
4.4.2 Butyrate regulates STAT3 activity through IL-10 suppression	81
4.4.3 Butyrate inhibits phosphorylation of STAT1 and p38 independently of IL-10	83
4.4.4 Butyrate modulates the Akt-mTOR signaling network.....	84
5. Discussion	86
5.1 Multifaceted consequences of SCFAs co-stimulation on the TLR-mediated immune response.....	86
5.2 SCFAs trigger NLRP3 inflammasome-mediated IL-1 β release	87
5.3 LPS + butyrate promote IL-1 β release orchestrated by multiple targets	90
5.3.1 LPS + butyrate induce IL-1 β through a novel NLRP3 inflammasome activation pathway ..	91
5.3.2 TBK1 and STAT3 act as negative regulators of IL-1 β secretion induced by LPS + Butyrate	95
5.3.3 HDAC11 modulates the NLRP3 priming signal.....	96
5.4 Butyrate inhibits the IL-10 downstream signaling pathway	96
5.5 Conclusion.....	99
6. List of Abbreviations.....	100
7. List of Figures and Tables.....	104
8. Appendix	106
Supplementary figure.....	106
9. References	109
10. Acknowledgement.....	132
11. Curriculum Vitae.....	134

1. Abstract

Short-chain fatty acids (SCFAs), which are mainly derived from microbial fermentation of dietary fibres, have been considered to be beneficial to gut health for decades. Recently, a few of studies reported that some patients with inflammatory bowel disease (IBD) showed poor tolerance to diets rich in certain fibres, and that fibre fermentation-derived SCFAs could exacerbate gut inflammation in mouse colitis models. Therefore, intensive efforts are required to further define and characterize the roles of SCFAs under inflammatory state.

Given the mobility (translocation) of microbiota-derived metabolites and recruitment of phagocytes, such as macrophages, in a leaky gut under inflammatory conditions in patients with IBD, I challenged primary human macrophages with the combinations of SCFAs and the TLR-4 agonist LPS. Transcriptomics and proteomics profiling, and measurement of cytokines secretion were performed, which, interestingly, showed that the SCFA butyrate displayed the strongest regulatory effect on the TLR-4-induced genes transcription and translation as well as cytokines production. Furthermore, I found that butyrate could aggravate inflammatory responses by enhancing the TLR-induced pro-inflammatory cytokine interleukin (IL) -1 β and suppressing the anti-inflammatory cytokine IL-10. This was in contrast to the previously reported anti-inflammatory and protective roles of butyrate in intestinal epithelial cells (IECs). In further experiments, working on the mechanisms by which butyrate regulates TLR-mediated IL-1 β and IL-10 production, I discovered that butyrate, together with LPS, induced IL-1 β secretion in an NLRP3 inflammasome-dependent manner, with the engagement of multiple molecules including caspase-8, TBK-1, RIPK1, RIPK3, STAT3 and HDAC11. On the other hand, butyrate strongly inhibited TLR-induced IL-10 signaling with the involvement of STAT1, STAT3, p38 and the Akt-mTOR pathway.

In my thesis, I characterized the effect of SCFAs on the TLR-mediated transcriptional and proteomic responses. Importantly, I showed that SCFAs might be detrimental to gut health in the patients with IBD through regulations of the cytokines IL-1 β and IL-10 in primary human macrophages. I also identified a network of biomolecules engaged in these processes. These findings provide new evidences for a full understanding of how SCFAs impact on gut health and suggest potential novel targets for the treatment of patients with IBD.

2. Introduction

2.1 The immune system: an overview

2.1.1 The functions of the immune system

The immune systems have evolutionarily developed from the beginning of life to maintain the balance between the host and potentially harmful environmental agents, including bacteria, viruses, and fungi (Broecker and Moelling, 2019; Cooper and Alder, 2006). In vertebrates, the immune system is composed of innate immunity and adaptive immunity, which protect the host from pathogenic invaders in a sequential and cooperative manner (Iwasaki and Medzhitov, 2015; Riera Romo et al., 2016). As the first line of defence against pathogens, the innate immune responses are primarily initiated when microbes breach the physical barriers of the body. If the ensuing microbial invasion is not cleared by the innate immune system, the adaptive immune response builds up to specifically target and facilitate the clearance of the pathogens that escaped from the innate immune protection (Raulet, 2004; Vivier and Malissen, 2005).

Innate immunity is a highly complex network comprising organs, tissues and cells. Skin, the gastrointestinal tract, the respiratory tract and the mucosal tissues constitute physical barriers (Hunt, 2011). Physiological fluids such as the mucus, the bile, the gastric acid and the tears provide chemical barriers (Chaplin, 2003; Hunt, 2011). Lastly, immune cells and, to an extent, non-pathogenic commensal bacteria are a biological barrier against potential invaders (Littman and Pamer, 2011). An essential component of the innate immune system are innate immune cells, including phagocytes (macrophages, dendritic cells (DCs) and neutrophils), natural killer (NK) cells, and granulocytes (basophils, eosinophils, neutrophils, and mast cells). These cells function as security guards in the blood and in peripheral tissues to monitor potential threats to the host. Upon detection of the pathogens that breached the surface barriers, innate immune cells may engulf and destroy them (phagocytes) and, meanwhile, secrete cytokines and chemokines, which serve as messengers to alert and recruit other immune cells to the site of infection. Thus, innate immune cells can cooperate to combat pathogens and limit the potential harm to the host (Alfano and Poli, 2005; Lin and Karin, 2007; Striz et al., 2014).

Adaptive immunity has been evolutionarily developed to provide more precise, selective recognition mechanisms that directly target pathogens and collaborate with the innate immune system to fight an established infection (Flajnik and Kasahara, 2010a). The main effector cells of adaptive immunity are lymphocytes, comprising of B cells and T cells.

B cells are subdivided into plasma cells ('antibody factories') producing specific antibodies that help to neutralize and eliminate invading pathogens, and memory B cells, which initiate strong antibody responses after reinfections (Aberle et al., 2013). One vital mechanism for memory B cells to protect the host is the long lifespan of these antibody-mediated immune responses (several decades) (Crotty et al., 2003).

T cells are generally divided into four subtypes, T helper cells ($CD4^+$ T cells), cytotoxic T cells ($CD8^+$ T cells), regulatory T (T_{reg}) cells and memory T cells. Cytotoxic T cells mainly kill host cells infected by viruses and intracellular bacteria through the secretion of cytotoxic granules (Andersen et al., 2006). T helper cells are activated when they recognize and interact with microbe-derived peptide fragments presented in the context of major histocompatibility complex (MHC) class II expressed on the antigen-presenting cells (APCs), such as DCs and macrophages. As the name implies, T helper cells are widely required for the activation of other immune cell types, such as B cells (Ziegler, 2016). Besides T helper cells and cytotoxic T cells, T_{reg} cells are another type of effector T cell, which plays important roles in maintaining tolerance to self-antigens and limiting chronic inflammatory diseases (Vignali et al., 2008). Memory T cells, in analogy to memory B cells, endow the adaptive immune system with the memory to rapidly elicit immune responses to previously encountered antigens (Mueller et al., 2013).

2.1.2 Pathogen recognition machinery

Microbes, including pathogens, commonly share and express a series of structurally conserved molecules, termed pathogen-associated molecular patterns (PAMPs). Cell death and tissue damage also result in the release of abundant endogenous molecules that serve as alarm signals, termed danger-associated molecular patterns (DAMPs) (Mogensen, 2009). The existence of PAMPs and DAMPs enables the innate immune cells to identify and target a wide variety of potentially threatening agents. One of the most well-identified PAMPs is lipopolysaccharide (LPS), a part of the gram-negative bacteria outer membrane. (Foley, 2015). DAMPs can be subdivided into protein DAMPs, such as heat-shock proteins (HSP) and high-mobility group box 1 (HMGB-1) and non-protein DAMPs, including adenosine triphosphate (ATP), mitochondrial DNA (mtDNA) and uric acid (Jounai et al., 2013; Land, 2020). PAMPs and DAMPS can trigger immune responses both individually and in combinations. These molecules are recognized by pattern recognition receptors (PRRs), and PRR activation initiates inflammation to alert further immune system components of the presence of the danger and to protect the host against infections.

PRRs are germline-encoded receptors and sensors mainly expressed on the membranes and in the cytosol of multiple cell types, including innate immune cells. They allow the host to detect and respond to the threats (represented by the emergence of PAMPs and DAMPs) derived from exogenous pathogens and endogenous harmful processes.

PRRs are mainly divided into five classes according to their phylogenetic origin, function and localisation: 1) Toll-like receptors (TLRs); 2) C-type lectin-like receptors (CLRs); 3) Nucleotide-binding oligomerization domain (NOD)-like receptors (NLRs); 4) Retinoic acid-inducible gene-1 (RIG-I)-like receptors (RLRs) and 5) Absent in melanoma 2 (AIM2)-like receptors (ALRs) (Gulati et al., 2018; Nakaya et al., 2017). CLRs and TLRs are integral membrane proteins localized on the cell surface or in the endosomes, while NLRs, RLRs and ALRs are present in the cytosol. Thus, NLRs, RLRs and ALRs are considered to act mostly as sensors, rather than receptors, due to their indirect sensing of DAMPs and PAMPs. In contrast, the localization of CLRs and TLRs predestines them for direct interaction with and recognition of extracellular PAMPs (Kawai and Akira, 2009). The major differences among these PRRs lie in the specificity of ligand recognition (Figure 2.1).

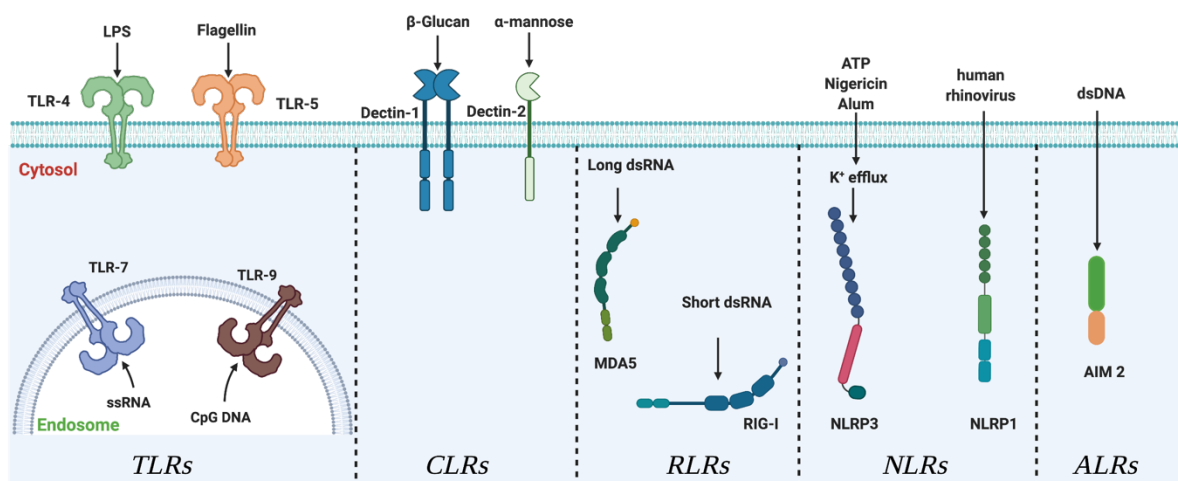


Figure 2.1: Pattern recognition receptors (PRRs) and their ligands.

Schematic and simplistic representation of different PRRs and their ligands. 1) TLRs: TLR-4 and -5 are expressed on the cell surface and their cognate ligands are LPS and Flagellin respectively, while endosomal TLRs, such as TLR-7 and -9 are capable of detecting ssRNA and CpG DNA. 2) CLRs: CLRs are a family of receptors mainly involved in anti-fungal immunity, for example, Dectin-1 could bind to β -glucans, a major component of fungal cell walls, whereas Dectin-2 is able to recognize another component of fungal cell walls such as α -mannose. 3) RLRs: RLRs are cytoplasmic PRRs involved in the recognition of viral infection. MDA5 recognizes long dsRNA (>2000 bp) and RIG-I is able to detect the short dsRNA (<300 bp). 4) NLRs: K^+ efflux triggered by the engagement of ATP, Nigericin and Alum could be sensed by and thereby activate NLRP3. A component of human rhinovirus known as 3C protease could directly cleave and activate NLRP1. 5) ALRs: dsDNA is one of the most well-characterized ligands of AIM2.

ssRNA, single-stranded RNA; CpG DNA, CpG-containing DNA; dsRNA, double-stranded RNA; dsDNA, double-stranded DNA. TLR, Toll-like receptor; CLR, C-type lectin-like receptor; ALR, Absent in melanoma 2 (AIM2)-like receptors; NLR, Nucleotide-binding oligomerization domain (NOD)-like receptor; RLR, Retinoic acid-inducible gene-I (RIG-I)-like receptor; MDA5, melanoma differentiation-associated protein 5; NLRP, NLR family pyrin domain containing.

2.1.3 The NLRP3 inflammasome

The NLR family pyrin domain containing 3 (NLRP3) inflammasome is a cytosolic multimeric protein complex comprising the sensor NLRP3, the adaptor (apoptosis-associated speck-like protein containing a CARD) ASC and the effector caspase-1. The NLRP3 inflammasome activation is a two-step process consisting of the priming step and the activation step. The priming signal can be provided by TLRs activation via their cognate ligands, which promotes transcription and translation of NLRP3 and pro-IL-1 β through activation of the NF- κ B pathway (Guo et al., 2015). An increasing number of structurally diverse chemical, biological and physical triggers have been documented to provide a second, activating signal leading to the assembly of the NLRP3 inflammasome complex. These activators include particulates and crystals, for example, amyloid- β , uric acid, silica, cholesterol, or alum (Braga et al., 2017; Dostert et al., 2008; Ising et al., 2019), pore-forming toxins (pneumolysin and aerolysin) (Gurcel et al., 2006; McNeela et al., 2010), RNA viruses (vesicular stomatitis virus (VSV) and encephalomyocarditis virus (EMCV)) (da Costa et al., 2019; Wang et al., 2014), ATP (Mariathasan et al., 2006a), and the K⁺ ionophore nigericin (Mariathasan et al., 2006a; Pressman, 1976). Given the diversity of these NLRP3 triggers, this protein is generally seen as a sensor of cytosolic alterations rather than a typical receptor activated by a defined ligand (Lamkanfi and Dixit, 2009; Lamkanfi and Kanneganti, 2010). Three common intracellular events have been proposed to activate NLRP3 inflammasome activation: K⁺ efflux, mitochondrial reactive oxygen species (mtROS) production, and lysosomal destabilization and rupture (He et al., 2016; Muñoz-Planillo et al., 2013; Perregaux and Gabel, 1994; Zhou et al., 2010). However, it remains unclear how NLRP3 senses these cellular processes. Upon stimulation of NLRP3 following the priming signal, the NLRP3 inflammasome complex is formed, providing a platform for pro-caspase-1 auto-processing and maturation. Then, active caspase-1 proteolytically cleaves pro-interleukin-1 β (IL-1 β) and pro-interleukin-18 (IL-18) into the active forms of IL-1 β and IL-18. Meanwhile, Gasdermin D (GSDMD) is cleaved as well by active caspase-1 to release the GSDMD N-terminal domain (GSDMD-N), forming pores in the cell membranes and thereby driving an inflammatory type of cell death termed pyroptosis.

In addition to the canonical NLRP3 inflammasome activation pathway described above, non-canonical and alternative NLRP3 inflammasome activation pathways have been reported in different cell types. During Gram-negative bacterial infections, the non-canonical NLRP3 inflammasome pathway represents a cellular strategy to sense an ongoing infection. In general, extracellular LPS can be delivered into the cytosol via TLR4-myeloid differentiation factor 2 (MD2)-cluster of differentiation 14 (CD14) receptor complex-mediated endocytosis or through endocytic uptake of bacterial outer membrane vesicles (OMVs) (Ding and Shao, 2017; Vanaja et al., 2016; Yang et al., 2015). In contrast to TLR4, which senses extracellular LPS, caspase-11 and its human homologs caspases-4 and -5 are engaged in sensing of and activated by cytosolic LPS (Shi et al., 2014). Active caspase-11 (mouse) and caspase-4/5 (human) elicit K^+ efflux through the opening of the pannexin-1 channel and GSDMD cleavage-mediated pyroptosis (Shi et al., 2015), thereby driving K^+ efflux-dependent NLRP3 inflammasome activation and IL-1 β maturation as well as secretion. Finally, different from the two-step activation mechanisms of the canonical and the non-canonical NLRP3 inflammasome pathways, the alternative NLRP3 inflammasome activation only entails one single trigger: extracellular LPS. This pathway is functional in human monocytes and is mediated by TLR4-based LPS recognition and the engagement of the RIPK1/FADD/caspase-8 cascade (Gaidt et al., 2016) (Figure 2.2).

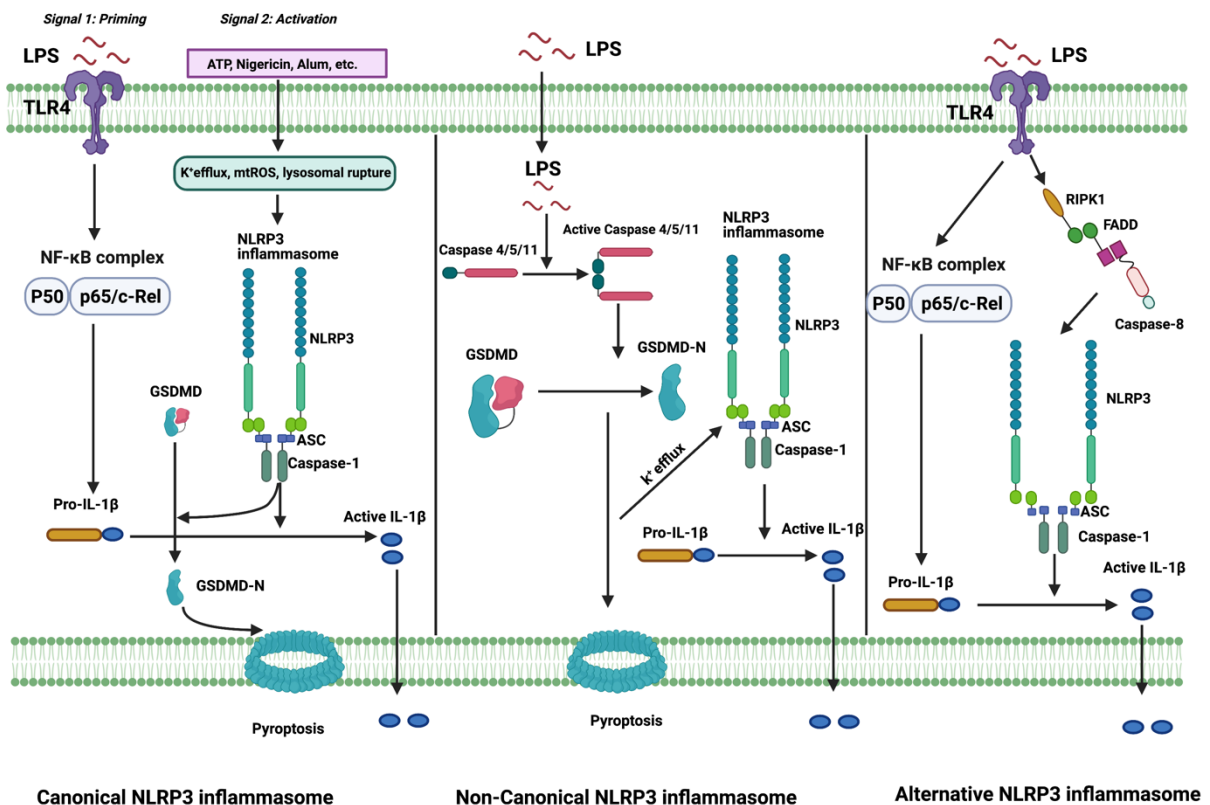


Figure 2.2: NLRP3 inflammasome activation pathways.

Schematic representation of three different NLRP3 inflammasome activation pathways. 1) Canonical NLRP3 inflammasome activation: TLRs, IL-1R and TNFR are involved in the priming step, TLR4 is used as one of the examples in this diagram. LPS binding to TLR4 leads to NF- κ B-mediated transcription of pro-IL-1 β and NLRP3. Following the priming step, the activation signal provided by ATP, Nigericin or Alum elicits K⁺ efflux, mtROS production or lysosomal rupture, which initiates the assembly of the NLRP3 inflammasome complex enabling pro-caspase-1 auto-processing and maturation. Active caspase-1 then cleaves GSDMD and pro-IL-1 β into GSDMD-N and mature IL-1 β , respectively. GSDMD-N is able to form pores in the cell membrane and thereby drive pyroptosis. 2) Non-canonical NLRP3 inflammasome activation: Intracellular LPS could trigger the cleavage of caspase-11 (mouse) and its human homologs caspase-4 and -5 into their active forms, which allows for efflux of K⁺ via GSDMD cleavage-mediated pyroptosis. Subsequently, K⁺ efflux enables the formation of the NLRP3 inflammasome complex, thereby promoting the maturation and secretion of IL-1 β . 3) Alternative NLRP3 inflammasome activation: this pathway is functional in human monocytes in response to extracellular LPS recognition by TLR4, which activates NLRP3 inflammasome-mediated IL-1 β secretion with the engagement of the RIPK1/FADD/caspase-8 cascade, but in the absence of K⁺ efflux and pyroptosis.

NLRP3, NLR family pyrin domain containing 3; TLR, toll-like receptor; IL-1R, interleukin-1 receptor; TNFR, tumour necrosis factor receptor; LPS, lipopolysaccharide; NF- κ B, nuclear factor- κ B; IL-1 β , interleukin-1 β ; mtROS, mitochondrial reactive oxygen species; GSDMD, gasdermin D; GSDMD-N, GSDMD N-terminal domain; RIPK1, receptor-interacting serine/threonine-protein kinase 1; FADD, FAS-associated death domain.

As the core component of the NLRP3 inflammasome complex formation, NLRP3 post-translational modifications have been extensively studied. To date, ubiquitination and phosphorylation of NLRP3 are the most well-described NLRP3 post-translational modifications. Post-translational modifications of NLRP3 license NLRP3 to initiate the interaction with the adaptor ASC and the subsequent recruitment of pro-caspase-1, thereby regulating NLRP3 inflammasome activity (Py et al., 2013; Stutz et al., 2017).

Since the inflammasome was first identified by the Tschopp lab in 2002 (Martinon et al., 2002), its activation has been linked to a number of diseases. Originally, mutations in the NLRP3-encoding gene were discovered in patients with cryopyrin-associated periodic syndrome (CAPS), including familial cold autoinflammatory syndrome (FCAS), Muckle-Wells syndrome (MWS), and neonatal onset multisystem inflammatory disease (NOMID) (Abderrazak et al., 2015; Agostini et al., 2004; Hoffman et al., 2001). With the extensive study on the function of the NLRP3 inflammasome following its discovery, aberrant NLRP3 inflammasome activation has been associated with the pathogenesis of central nervous system disorders (Alzheimer's disease, Parkinson's disease, depression etc.) (Haque et al., 2020; Heneka et al., 2013; Kaufmann et al., 2017), chronic inflammatory diseases (IBD, rheumatoid arthritis, gout etc.) (Guo et al., 2018; Kingsbury et al., 2011; Zhen and Zhang, 2019), metabolic diseases (atherosclerosis, type 2 diabetes, obesity etc.) (Düwell et al., 2010a; Lee et al., 2013; Vandanmagsar et al., 2011), and cancers (colorectal cancer, breast cancer, gastric cancer etc.) (Hamarsheh and Zeiser, 2020). Therefore, significant efforts have been invested in developing strategies to target the NLRP3 inflammasome pathway. These include small

molecule NLRP3 inhibitors (MCC950) (Coll et al., 2015) and OLT1177 (Jansen et al., 2019), a monoclonal antibody against the adaptor ASC (IC100) (Desu et al., 2020a) and a GSDMD inhibitor (disulfiram), which are currently in clinical trials (Chauhan et al., 2020; Hu et al., 2020)

2.1.4 Apoptosis, pyroptosis, necroptosis, and PANoptosis - programmed cell death (PCD) and inflammation

The development and homeostasis of multicellular organisms require a balance between cell proliferation and cell removal throughout the whole life. Regulated cell proliferation is an essential mechanism for the replenishment of dead cells, tissue repair, and growth, while abnormal cell proliferation may result in cancer (Beachy et al., 2004). As a crucial event in the immune response to eliminate cells infected by pathogens or showing signs of neoplastic transformation, PCD has been extensively investigated in the past decades.

Three well-characterized forms of PCD are pyroptosis, apoptosis and necroptosis, their parallel engagement shapes the progression of PANoptosis, a model unifying the different PCD types (Bedoui et al., 2020; Kwaik et al., 2020). All of the PCD types are closely connected by common signaling nodes and functional redundancies, with implications on organismal health and disease.

Apoptosis is a programmed form of 'cellular suicide', leading to the formation of small apoptotic bodies containing fragments of the cytoplasm and the nucleus. Apoptotic cells release or display the so-called 'eat me' signals to phagocytes, such as macrophages (Gregory and Devitt, 2004), for example phosphatidylserine on the outer plasma membrane leaflet of an apoptotic body. When these signals are detected by phagocytes, the apoptotic bodies are engulfed through phagocytosis, enabling clearance of cellular debris from tissues (Gordon and Plüddemann, 2018; Kourtzelis et al., 2020). Apoptosis can be triggered by the intrinsic or the extrinsic pathway, depending on the source of cell death-inducing signals (Khaw-on and Banjerdpongchai, 2012; Matthews et al., 2012).

The intrinsic apoptosis pathway is also known as B-cell lymphoma 2 (BCL-2)-regulated or mitochondria-dependent apoptosis, which is attributed to the critical involvement of BCL-2 family proteins and mitochondria in the regulation of this process. A diverse array of stimuli including nutrient deprivation (Liu et al., 2017), DNA damage (Norbury and Zhivotovsky, 2004) and intracellular oxidative stress (Annunziato et al., 2003) can cause mitochondrial outer membrane permeabilization (MOMP) through modulation of the expression and/or the activation state of BCL-2 family proteins (Bcl-2 homology domain 3 (BH3)-only proteins, BCL-2-associated X protein (BAX), and BCL-2 antagonist or killer (BAK)). MOMP results in the release of a number of mitochondrial proteins from the intermembrane space to the cytosol.

Two of these proteins, cytochrome c and second mitochondria-derived activator of caspases (SMAC), have been shown to initiate the intrinsic apoptotic pathway (Fulda and Debatin, 2006). Cytochrome c recruitment to apoptotic peptidase activating factor 1 (APAF-1) leads to the formation of a multiprotein, ATP-dependent complex called the apoptosome. The apoptosome provides a platform for the catalytic maturation of caspase-9, which is followed by the activation of apoptosis executioner caspases (caspases-3 and -7) (Cai et al., 1998; Jiang and Wang, 2004; Kluck et al., 1997). In addition, once SMAC is released into the cytosol, it can bind to and neutralise X-linked inhibitor of apoptosis protein (XIAP), counteracting the inhibitory effect of XIAP on caspases-3/-7. Thus, caspases-3/-7 become fully functional to mediate apoptosis (Du et al., 2000; Gao et al., 2007).

To date, three extrinsic apoptosis models have been defined, with classical recognition of and interaction between a ligand and a cell surface receptor: FasL (CD95) /Fas, TNF- α /TNF receptor 1 (TNFR1) and TNF-related apoptosis-inducing ligand (TRAIL)/death receptor 5 (DR5). All of these three death receptors, Fas, TNFR1 and DR5, belong to the TNF receptor superfamily and are transmembrane proteins sharing a common cytoplasmic death domain (DD) (Phillips et al., 2001). Following the binding of ligands to their cognate death receptors, adaptors such as Fas-associated death domain (FADD) and TNFR type-1 associated DD protein (TRADD), and pro-caspase-8 or -10 will be recruited to form the death inducing signaling complex (DISC). DISC formation leads to the activation of caspase-8 or -10. The active forms of caspase-8 or -10 then cleave and activate apoptosis executioner pro-caspase-3/-7 (Peter, 2011). However, there is also crosstalk between the intrinsic and the extrinsic apoptosis pathways. For instance, caspase-8 is able to trigger BAX/BAK-mediated MOMP through the cleavage of the BH3-interacting domain death agonist (BID) (Glowacki et al., 2013).

Ultimately, the goal of both the intrinsic and extrinsic apoptotic signaling cascades is to activate pro-caspase-3/7. For that reason, increased amounts of cleaved caspase-3/-7 are used as indicators of apoptosis in scientific research. Caspase-3/7 have a wide range of substrates (more than 100) (Julien and Wells, 2017) essential for the DNA fragmentation, cytoskeleton deformation and nuclear proteins' degradation. These processes explain the typical morphological characteristics of cells undergoing apoptosis: cell shrinkage, chromatin condensation and membrane blebbing (Saraste and Pulkki, 2000).

Pyroptosis is a pro-inflammatory lytic form of PCD, upon which cellular contents are released into the extracellular milieu. Some of these contents act as DAMPs, thereby driving inflammatory immune responses. Pyroptosis modes can be grouped into caspase-1 dependent (canonical inflammasomes) and caspase-1 independent (the non-canonical inflammasome) pathways (Bergsbaken et al., 2009).

The ultimate intracellular event in the process of pyroptosis is the same for both the caspase-1 dependent and independent pathways and consists of cleavage of GSDMD into active GSDMD-N. This is catalyzed by inflammatory caspases: caspase-1, human caspase-4/-5 and murine caspase 11. GSDMD-N can insert into cellular membranes and then forms large oligomeric pores, leading to the formation of pyroptosis.

In contrast to the final outcome, the mechanisms underlying the activation of effector caspases (human caspase-1/4/5 and mouse caspase-11) upstream of GSDMD cleavage are distinct. In the non-canonical inflammasome pathway, the intracellular LPS (from Gram-negative bacteria) can directly bind to and activate human caspase-4/-5 or mouse caspase-11 (Pellegrini et al., 2017). Whereas, the cleavage of pro-caspase-1 in the canonical inflammasome pathway is more complex and requires the formation of a multi-protein complex termed the inflammasome. Most of Inflammasomes are composed of three components, a sensor (NLRP3, NLRC4, AIM2, Pyrin and NLRP1), an adaptor (ASC) and an effector (caspase-1). The adaptor ASC is dispensable for the activation of NLRP1 and NLRC4 inflammasomes (Man et al., 2017). A wide array of PAMPs and DAMPs are sensed by inflammasome sensors, leading to the recruitment of the adaptor ASC and then pro-caspase-1. Thus, an inflammasome complex is assembled, providing a scaffold for dimerization and auto-activation of pro-caspase-1 into mature and enzymatically active caspase-1.

Unlike apoptosis and pyroptosis, necroptosis is a form of PCD that is independent of caspases, which is considered as an alternative cell death modality when the activity of caspases is impaired or blocked by invading bacteria or viruses (Dhuriya and Sharma, 2018). The key molecules driving necroptosis are receptor-interacting serine-threonine kinase 3 (RIPK3) and mixed lineage kinase domain like (MLKL), the latter of which is functionally analogous to GSDMD in pyroptosis. Following the phosphorylation of MLKL by RIPK3, phospho-MLKL undergoes oligomerization and is concomitantly activated. Subsequently, active phospho-MLKL inserts into the plasma membrane to form membrane pores, which allows for the release of cellular contents, including ions and some inflammatory cytokines (Chen et al., 2017; Sai et al., 2019).

Two main activation pathways upstream of RIPK3 have been well-defined based on the dependency on receptor-interacting serine-threonine kinase 1 (RIPK1): 1) the engagement of TNFR1 through its respective ligands binding enables RIPK1 to drive the autophosphorylation of RIPK3; 2) Ligand activation of TLR3/4 activates RIPK3 through the adaptor TIR domain-containing adaptor-inducing interferon- β (TRIF), while the cytosolic RNA sensor DAI (also named ZBP1) could directly bind to and activate RIPK3, both of these RIPK3 activation mechanisms are RIPK1-independent (Weinlich et al., 2017).

PANoptosis (pyroptosis, apoptosis, and necroptosis) is a newly described inflammatory cell death network limiting a broad range of pathogens infections (Place et al., 2021). In theory,

when the PCD executioners GSDMD (pyroptosis), caspase-3/7 (apoptosis), or RIPK3/MLKL (necroptosis) are activated by diverse microbial molecules in combination with inflammatory cytokines (such as TNF- α), all the three types of PCD can be initiated simultaneously in one single cell, termed as PANoptosis. PANoptosis is driven by PANosome, which can be composed of ZBP1, NLRP3, ASC, FADD, caspase-1, caspase-6, caspase-8, RIPK1 and RIPK3 depending on the types of stimuli that induce its formation (Kwaik et al., 2020). One well-characterized model of PANoptosis is mediated by ZBP1 during influenza A virus (IAV) infection. IAV infection activates ZBP1, which drives the assembly of PANosome containing RIPK1/3, caspase-6/8, and the NLRP3 inflammasome that facilitates the cleavage or activation of GSDMD, caspase-3/7, and MLKL in parallel, thereby inducing PANoptosis (Kuriakose et al., 2016).

As one of the most important mechanisms of the host protection against pathogens invasion, of elimination of aberrant and infected immune cells, and of homeostasis maintenance, dysregulated PCD has been involved in the pathogenesis of a number of diseases. It also shows potential as a new therapeutical target for future clinical use.

2.2 Short-chain fatty acids (SCFAs)

2.2.1 Commensal bacteria and metabolites in the gut

The human gut hosts a great number of bacteria (10^{13} - 10^{14}), which, together with viruses, fungi and archaea, forms the gut microbiota. In general, the gut commensal bacteria are nonpathogenic and beneficial to the gut ecosystem through limiting the colonization and invasion of opportunistic pathogens, providing essential nutrients to the host by metabolizing non-digestible food-contained molecules (e.g. dietary fibres) and help in shaping the development of intestinal barriers (Takiishi et al., 2017). In turn, the host provides the microbiota with a stable and nutrient-rich environment enabling their survival and reproduction (Mondot et al., 2013).

However, it has been demonstrated that microbiota is associated with the onset and development of a variety of diseases when the composition and metabolic capacity of the microbiota is disrupted (Wilkins et al., 2019). A reduction in the gut bacteria diversity and load has been frequently reported in the patients with IBD. One of the causes of IBD is proposed to be the deficiency of protective effects from fermentation products, such as SCFAs, vitamin B and vitamin K (Nishida et al., 2018; Russo et al., 2019).

Interestingly, more than 1×10^8 nerve cells embedded in the walls of the digestive system are forming the enteric nervous system (ENS), which is called the “second brain”. The ENS works

independently of the central nervous system (CNS) and mainly controls the digestive processes, such as gastrointestinal motility, absorption of nutrients and gastrointestinal blood flow (Neunlist and Schemann, 2014). It has been demonstrated that the gut microbiota plays crucial roles in the development and functions of the ENS (Heiss and Olofsson, 2019). In addition, the gut-brain axis, a bidirectional network between the gut and the CNS, enables the communication between the intestine, the CNS and the microbiota (Ochoa-Repáraz and Kasper, 2016). Furthermore, gut microbiota has been shown to be involved in the pathogenesis of diverse central nervous system disorders, including anxiety, depression and autism, through gut-brain axis. On the other hand, chronic stress will lead to the transmission of signals from the brain through the gut-brain axis to the ENS, affecting the compositions and functions of the gut microbiota and thereby leading to increased inflammatory responses (Benítez-Burraco et al., 2018).

As the key molecular messengers for the gut commensal bacteria to regulate and maintain gut homeostasis, microbiota-derived metabolites, including SCFAs, retinoic acid and tryptophan have been extensively investigated and highlighted in regulating the immune response. Notably, SCFAs have been shown to be associated with the development of a series of diseases, such as IBD (Round and Palm, 2018; Wang et al., 2019a).

2.2.2 The category and molecular functions of SCFAs

Short-chain fatty acids (SCFAs) are fatty acids with less than 6 carbon atoms (C1 - C5), including formic acid (C1), acetic acid (C2), propionic acid (C3), butyric acid (C4), isobutyric acid (C4), valeric acid (C5), isovaleric acid (C5), and 2-Methylbutanoic acid (C5). Acetate, propionate and butyrate account for around 95% of SCFAs and mainly contribute to gut health (Den Besten et al., 2013; Feng et al., 2018). SCFAs are mainly generated in the large intestine by commensal bacteria such as Bacteroidetes and Firmicutes phylum by the fermentation of non-digestible carbohydrates and soluble dietary fibres. The concentration of SCFAs in the intestinal tract can reach 20 – 140 mM with the molar ratio of 3:1:1 for acetate: propionate: butyrate, respectively (Binder, 2009). Once produced in the gut, SCFAs can be absorbed by intestinal epithelial cells (IECs) and thereby exert their regulatory effects through two distinct ways. One is their translocation into the cytoplasm by passive diffusion or monocarboxylate-transporter 1 (MCT1) and sodium-dependent monocarboxylate transporter-1 (SMCT1) to orchestrate chromosome condensation and thereby gene regulation through modifying the activity of Histone deacetylases (HDACs) and histone acetyltransferases (HATs) (Venegas et al., 2019). The other mechanism involves the activation of G-protein coupled receptors, namely GPR43, GPR41, GPR109A and Olfactory receptor 78 (Olf78), to regulate cell

differentiation and proliferation. In addition, SCFAs, especially butyrate, serves as the primary energy source for colonocytes (Macia et al., 2015a). Recent findings demonstrated that SCFAs could bind to ASC pyrin domain thereby regulating inflammasome activation (Tsugawa et al., 2020). Apart from exerting their local regulatory effect on the gut where they are produced, SCFAs can also be directly absorbed into the peripheral blood circulation to reach different organs, like the liver and the brain. What's more, SCFAs are thought to be neurotransmitters for the connection and communication of the microbiota-gut-brain axis due to their capability to cross blood-brain barrier and therefore modulate neuroimmune responses (Wu et al., 2020).

2.2.3 The role of SCFAs in health and diseases

Due to the importance of SCFAs in health and diseases, the European Commission guidelines of Health Promotion and Disease Prevention recommends adults to have a dietary fibre intake ranging from 25 – 38 g/day as a pre-emptive measure against the development of non-communicable diseases (NCDs) including cardiovascular disease, type 2 diabetes, and colorectal cancer. One of the mechanisms by which dietary fibres lower the risk of cardiovascular disease is through reducing the production of cholesterol and regulating blood pressure (Gunness and Gidley, 2010). Several mouse models indicated that SCFAs could improve blood sugar control and insulin sensitivity and increase lipolysis, affecting the development of adiposity and type 2 diabetes (Canfora et al., 2015; Puddu et al., 2014).

In addition, SCFAs show a wide array of benefits to maintain gut homeostasis and health, such as promoting epithelial cells to secrete mucus to enhance gut barrier function (Bilotta and Cong, 2019) and B cells production of IgA to coordinate the balance between commensal bacteria and the host (Wu et al., 2017), and inducing the production of IL-17 and IL-18, which are responsible for tissue repair and epithelial integrity respectively (Asarat et al., 2016; Kalina et al., 2002).

However, the alterations in the levels of SCFAs and compositions of SCFAs-producing bacteria have been associated with the pathogenesis of Alzheimer's Disease (AD) and mood disorders (Liu et al., 2020; Marizzoni et al., 2020; Nishiwaki et al., 2020). Clinical studies have observed the decreased concentrations of faecal SCFAs in the patients with depression than in healthy subjects (Caspani et al., 2019), while, interestingly, administration of sodium butyrate has shown the capabilities to reverse several cognitive dysregulations, such as mania and depression, in rat models (Sarkar et al., 2016). The most well-documented involvement of SCFAs on the chronic inflammatory diseases is represented by its engagement in IBD

(Gonçalves et al., 2018; Huda-Faujan et al., 2010), including Crohn's disease and ulcerative colitis, which will be introduced in more details in the next section.

2.3 Inflammatory bowel disease (IBD)

2.3.1 The pathogenesis of IBD

Due to the rapid development of globalisation and changing of dietary habits, Inflammatory bowel disease (IBD) is becoming a global challenge and threat to public health with progressively increasing incidence and prevalence worldwide. Based on epidemiological research, more than 6.8 million people globally are suffering from IBD (Alatab et al., 2020). IBD is a type of chronic inflammatory disease characterized by inflammation of the gastrointestinal tract. The two main types of IBD are classified into Crohn's disease (CD) and ulcerative colitis (UC) according to the clinical manifestation and site of inflammation in the gastrointestinal tract. CD can occur at any part of the digestive system, of which the most common organ affected is the distal portion of the end of small intestine connecting to the colon. The inflamed areas in CD appear discontinuously or in patches adjacent to normal tissue and the inflammation could expand to the whole layers of the bowel wall (Hendrickson et al., 2002). In contrast, UC generally affects rectum and large intestine continuously and only cause inflammation in the innermost layer of the lining of the colon and rectum (Lee et al., 2018). The clinical symptoms between CD and UC are similar and include persistent diarrhea, bloody stool, cramping pain in the abdomen, fatigue and weight loss.

Even though IBD has already been described several decades ago, the pathogenesis for its initiation and development is still not entirely understood. With the development of genome-wide association studies (GWAS) and extensive epidemiological research on the cause of IBD, four different etiological models with high interplay have been proposed to be implicated in the pathogenesis of IBD:

1) Genetic factors

Epidemiological research indicates that children of IBD patients are more susceptible to develop into IBD themselves, suggesting that IBD development might have an inheritable component (Santos et al., 2018). Around 30 commonly shared genetic risk loci have been identified in both CD and UC through GWAS. Nucleotide-binding oligomerization domain 2 (*NOD2*) is the first gene discovered that is associated with CD, and approximately 30% of patients with Crohn's disease have been found mutations in *NOD2* (Guan, 2019). Furthermore, monogenic mutations in *IL10*, *IL10RA* and *IL10RB* have been frequently observed and described in the very early onset inflammatory bowel disease (VEO-IBD), and mouse models

with loss-of-function mutations in the genes encoding IL-10R will spontaneously develop into colitis (Shouval et al., 2016; Zhu et al., 2017).

2) Environmental factors

Given that only a quarter of IBD patients are associated with genetic factors and, on the other hand, with the incidence of IBD surging in the gradually industrialized developing countries, emerging evidences indicate that environmental factors, such as air pollution, diet and food additives, might be contributing to the pathogenesis of IBD (Abegunde et al., 2016). A series of reports demonstrated that fibre-rich diets, such as those rich in fruits and vegetables, are associated with a lower risk of Crohn's diseases. The potential connection resides in the fact that dietary fibres could be fermented into SCFAs by commensal bacteria in the gut, which protects the gut from dysbiosis and enhances the integrity of the gut mucosa (Limdi, 2018; Mentella et al., 2020). In addition, lack of fibre in westernized diets that in turn are rich in fat, sugar and animal proteins is considered as one of the main factors for the prevalence of IBD in the developed countries in the past decades (Statovci et al., 2017). Antibiotics use is another risk factor associated with IBD, the underlying mechanism of which lies in the compositional change of the gut microbiome (Nguyen et al., 2020). The alteration of gut microbiota is associated with the development of IBD as shown in several clinical studies and mouse models (Casén et al., 2015; Lupp et al., 2007; Zuo and Ng, 2018).

3) Immune response dysregulation

The intestinal mucosa functions as a natural barrier maintaining the homeostasis between luminal contents, including microbiota, bacterial products and innate immune cells. The damage to the mucosal barrier resulting from genetic factors, environmental factors and dysbiosis could lead to abnormal intestinal permeability, initiating immune responses through the activation of intestinal epithelial cells (IECs). Furthermore, Impaired intestinal permeability and barrier function allows for the translocation of commensal bacteria and microbial metabolites to encounter with and activate the recruited innate immune cells, such as macrophages, DCs and neutrophils. In response to immune recognition of commensal bacteria and microbial metabolites, several cytokines and chemokines, including IL-1 β , IL-12, IL-6, IL-23, TNF- α and transforming growth factor- β (TGF- β), are secreted by these innate immune cells thereby mediating a chronic inflammation of the gastrointestinal tract. Additionally, these cytokines are able to promote the differentiation and activation of T cells (T_H1, T_H2, T_H17 and T_{Reg}), which in turn amplify the immune response by producing IFN- γ , IL-17 and TNF- α (Neurath, 2014). Collectively, the aberrant mucosal immune responses cause tissue destruction and chronic intestinal inflammation, thereby driving the development of IBD and manifesting its symptoms (Ramos and Papadakis, 2019).

2.3.2 Clinical treatment and therapeutic targets of IBD

Due to the complexity and unclear pathogenesis of IBD, there is still no specific medication and treatment to cure IBD. All the clinical treatments are targeted towards the reduction of the underlying inflammation, control symptoms and achieve long-term remission (Pithadia and Jain, 2011). Four main categories of drug therapies have been recommended for the clinical treatment of IBD, including anti-inflammatory drugs, immune system suppressors, biologics and antibiotics (Misselwitz et al., 2020). Surgery will be another option for the treatment of IBD if all the drug therapies are still not able to alleviate the clinical symptoms and improve quality of life. However, to cope with the rising incidence of IBD worldwide, a wide array of scientific researches and novel drugs focusing on current and potential therapeutic targets of IBD are being extensively investigated, some of which are showing promising results for future clinical use. The promising drug targets of IBD therapy are:

1) TNF- α : Due to the increased concentrations of TNF- α in IBD patients, it has become the preferred target for the treatment of IBD. To date, four main drugs, adalimumab, certolizumab pegol, golimumab and infliximab, targeting TNF- α have been approved for treating IBD patients. Furthermore, AVX-470, an orally administered antibody targeting TNF- α , is under phase 3 clinical trial and showing an alternative to the traditional intravenous infusions of anti-TNF- α drugs (Hartman et al., 2016). However, around 10 – 40% of IBD patients failed to respond to the anti-TNF- α therapy. Therefore, alternatives need to be developed and used for those IBD patients who do not respond well to anti-TNF- α therapy.

2) IL-12/IL23: Th1 and Th17 cells have been shown to be associated with the pathogenesis of IBD. The cytokines IL-12 and IL-23, both mainly produced by macrophages and DC, are essential for the differentiation of Th1 and Th17. Thus, blocking the function or secretion of IL-12p40 and IL-23 is emerging as a new approach for the treatment of IBD. Ustekinemab is the first IL12/23 inhibitor approved for the treatment of Crohn's disease, providing an alternative option for IBD patients non-respondent to anti-TNF- α agents (Simon et al., 2016). In addition, another two monoclonal antibodies, risankizumab and mirikizumab, targeting against IL-23p19 subunit are undergoing phase 2 clinical trials as well (Feagan et al., 2017; Sandborn et al., 2020).

3) IL-6 and OSM: Accumulating evidences demonstrate that the serum level of IL-6 is correlated with the severity of CD. IL-6 has regulatory effect on the expression of antiapoptotic proteins Bcl-2 and Bcl-xl. Therefore, IL-6 is a promising therapeutic target for the treatment of IBD (Atreya and Neurath, 2005; Atreya et al., 2000). Concomitantly, the humanized monoclonal antibody targeting IL-6 developed by pfizer, PF-04236921, showed promising results towards the treatment of CD in clinical phase 2 trial (Danese et al., 2019).

Oncostatin M (OSM) is another member of IL-6 family. A new report found that the expression of OSM and its receptor OSMR are highly increased in the patients with IBD and to drive gut inflammation. Blockade of OSM *in vivo* alleviated the severity of pathology in mouse models with colitis (West et al., 2017). Furthermore, the expression level of OSM is considered as an indicator to predict to which extent the IBD patients respond to anti-TNF- α therapy. Therefore, targeting OSM could be a new strategic approach for the treatment of patients with IBD who failed to respond to anti-TNF- α therapy in the future.

4)IL-1 β : It has been reported that the expression of IL-1 β is highly increased in the biopsies from patients with UC and CD and the elevated levels of IL-1 β in the serum of IBD patients is associated with the disease severity (Bordon, 2017; Mao et al., 2018). On the other hand, the active status of the NLRP3 inflammasome, the main source of IL-1 β , is positively correlated with the development of intestinal inflammation in IBD. In accordance, treatment with the IL-1 β receptor antagonist (anakinra) could ameliorate gut inflammation in some patients with IBD (Neudecker et al., 2017; Shouval et al., 2016). In addition, the pharmacological inhibitor of NLRP3, MCC950, displayed therapeutic potential for the treatment of IBD as oral administration of MCC950 at 40 mg/kg attenuated the inflammatory response in a murine colitis model (Perera et al., 2018). Taken together, all of the studies described above indicate that targeting the NLRP3 inflammasome-IL-1 β signaling hold great potential as a new therapeutic strategy for the treatment of IBD (Chen et al., 2021).

2.4 Objective of this study

As one of the main microbiota-derived metabolites, SCFAs have been associated with the pathogenesis and development of diverse diseases, such as type 2 diabetes, peritonitis and IBD (Jennings-almeida et al., 2021; Schroeder and Bäckhed, 2016). However, due to the complicated pathogenesis of IBD, the roles of SCFAs in the development of IBD are still debatable. Recently, it was reported that certain dietary fibres displayed detrimental effects to the gut health in patients with IBD and in mouse colitis models. Therefore, intensive investigations are required to further define and characterize the roles of SCFAs under inflammatory state on the IBD development.

The initiation and amplification of inflammatory response during the development of IBD are mostly mediated by cytokines secreted by immune cells, such as macrophages. Thus, screening of the functions of SCFAs on the regulation of cytokines might shed some light on the mechanisms by which SCFAs mediate their detrimental effects in IBD.

Even though a number of drugs targeting cytokines involved in the pathophysiology of IBD (TNF- α , IL-6, IL-10 etc.) have been developed for the treatment of IBD, none of them is able

to fully revert the IBD phenotype. The NLRP3 inflammasome has emerged as a new target for a plethora of chronic inflammatory diseases. Importantly, it has been demonstrated that NLRP3 inflammasome activation correlates with the severity of IBD. Additionally, SCFAs have been shown to have profound roles in macrophages through various mechanisms, e.g. via ligand interaction with GPCRs such as GPR43 or by modulating the epigenetic landscape through the inhibition of HDACs. Moreover, most of the studies about the roles of SCFAs in IBD conducted so far used mouse models, but there are still open questions towards the translational capability of these results to the human system. Therefore, it is of great importance to explore the impact of SCFAs on NLRP3 inflammasome activation in primary human macrophages, the underlying mechanisms behind which could provide potential therapeutic targets for the treatment of IBD.

Finally, given the indispensable anti-inflammatory role of IL-10 in the protection against IBD, it is particularly meaningful to investigate how SCFAs shape the IL-10 signaling pathway.

In details, four specific aims were determined:

- 1: To characterize the roles of SCFAs, in combination with LPS, on the profiles of mRNA and protein expression in primary human macrophages
- 2: To investigate the impact of SCFAs, together with LPS, on the NLRP3 inflammasome-mediated IL-1 β signaling pathway.
- 3: To further screen for the potential molecules involved in the mechanisms by which SCFAs plus LPS regulate the NLRP3 inflammasome-mediated IL-1 β signaling pathway.
- 4: To test the effects of SCFAs on the TLR-mediated IL-10 signaling pathway.

3 Materials and Methods

3.1 Materials

3.1.1 Devices

Name	Supplier
Cell incubator	SANYO Biomedical
Sterile tissue culture hood	Fischer Scientific
Centrifuges	Eppendorf
Pipettes (0.1 µl – 1 ml)	Mettler-Toledo
Pipetboy acu	Integra Biosciences
Multichannel pipettes	Mettler Toledo
4°C fridge	Liebherr
- 20°C freezers	Liebherr
- 80°C freezers	ThermoScientific
- 150°C freezers	SANYO Biomedical
Plate reader SpectraMax i3	Molecular Devices
Western Blot reader Odyssey	LICOR Biosciences
Blotting system Xcell II Blot Module	Invitrogen
WES	Protein simple
Thermocycler T3000	Analytica Jena
MAGPIX [®] system	Luminex
Thermocycler Tadvanced (96-well)	Biometra
Heatblock Thermomixer	Eppendorf
Microplate Washer	BioTek
Counting chamber Neubauer	Brand
Cell counter TALI	Life Technologies
Tissue culture microscope	Leica
Electroporator	Invitrogen
Scale	Sartorius
Plater Shaker	neolab
MACS multiStand	Miltenyi Biotec

3.1.2 Consumables

Name	Supplier
Pipet tips (0.1 – 1 ml)	Mettler Toledo
15 ml, 50 ml tubes	Greiner bio-one
5 ml, 10 ml, 25 ml pipettes	Greiner bio-one
Tissue culture flasks	Greiner bio-one
6-well plate Nunc delta surface (for hMDMs)	ThermoFisher
6-well plates for cell culture	Greiner bio-one
12-well plates for cell culture	Greiner bio-one
24-well plates for cell culture	Greiner bio-one
96-well plates for cell culture	Greiner bio-one
96-well plates for ELISA	Nunc
384-well qPCR plate	Applied Biosystems
384-well plates for HTRF	Labomedic
NuPAGE® Novex 4 -12% Bis-Tris Gel 1.5 mm, 10 Well	Novex Life Technologies
NuPAGE® Novex 4 -12% Bis-Tris Gel 1.5 mm, 15 Well	Novex Life Technologies
PVDF membrane (Immobilon-FL, 0.45 µm)	Merck
Cell scrapers	Sarstedt
Column hMDMs purification	Miltenyi Biotech
Filter for hMDMs purification	Miltenyi Biotech
Needles	B. Braun
Syringes	BD Biosciences

3.1.3 Chemical and Reagents

Name	Supplier
2-Mercaptoethanol	Sigma-Aldrich
Benzonase® Nuclease	Sigma-Aldrich
Bovine serum albumin (BSA)	Sigma-Aldrich
CD14 MicroBeads UltraPure (human)	Miltenyi Biotecnology
cOmplete EDTA-free Protease-Inhibitor	Roche Life Science
Cocktail Tablets	

CRID3	Pfizer
Dimethyl sulfoxide (DMSO)	AppliChem
DMEM	GIBCO
dNTP mix (10 mM)	ThermoFisher
DPBS	GIBCO
EDTA solution 0.5 M, pH 8.0	GIBCO
Ethanol	AppliChem
Ficoll-Paque PLUS	GE Healthcare Life Sciences
Ebselen	Torcis
Flagellin	Invitrogen
LPS ultrapure EB	Invitrogen
Methanol	Roth
Nigericin, free acid	Invitrogen
Necrostatin-1s	Torcis
NuPAGE 10 x Sample reducing agent	Invitrogen
NuPAGE 20 x MES buffer	Invitrogen
NuPAGE 4 x LDS loading buffer (8% LDS, 40% glycerol, 2.04 mM EDTA, 0.88 mM SERVA Blue G, 0.7 mM phenol red, 564 mM Tris, pH 8.5)	Invitrogen
NuPAGE Precast Bis-Tris PAGE gels	Invitrogen
Pam3CSK4	Invitrogen
PageRuler Plus prestained protein ladder	ThermoFisher
PBS 10 x (2 g potassium chloride, 2 g potassium dihydrogen phosphate, 80 g sodium chloride, 11.5 g/l di-sodium hydrogen phosphate anhydrous)	Pan Biotech
Chloroform	Merck
Penicillin/streptomycin	ThermoFisher
PMA	Sigma
PMSF	Applichem
PVDF membrane Immobilon-FL	Millipore
R848	Invivogen
Reducing agent 10 x (500 mM DTT)	Life Technologies
rhGM-CSF	Immunotools
rhM-CSF	Immunotools

rhIL-10	Immunotools
RPMI1640	GIBCO
Sodium Acetate	Sigma Aldrich
Sodium Propionate	Sigma Aldrich
Sodium Butyrate	Sigma Aldrich
Sodium Chloride	Merck
Sodium Potassium	Sigma Aldrich
Sodium dodecyl sulfate (SDS)	Sigma Aldrich
Sodium pyruvate	Life Technologies
Superscript III reverse transcriptase	Thermo Fisher
TBS 20 x (400 mM Tris, 3 M NaCl, pH 7.4)	Santa Cruz
TrisGlycine Buffer 10 x (0.025 M Tris, 0.192 M glycine, pH 8.5)	ThermoScientific
Tris HCl Buffer 1 M, pH 7.4	AppliChem
Triton X-100	Roth
TRizol Reagent	Life Technologies
Trypan blue	Sigma-Aldrich
Trypsin-EDTA 0.05%	GIBCO
Tween 20	Roth
VX-765	Selleckchem
Z-IETD-FMK	R&D systems
PDTC	Torcis

3.1.4 Kits

Kit	Supplier
Bichoninic acid (BCA) assay	ThermoScientific
Human IL-1 β HTRF kit	Cisbio
Human TNF α HTRF kit	Cisbio
Human IL-10 HTRF kit	Cisbio
Pierce BCA Protein Assay Kit	ThermoFisher
Pierce LDH Cytotoxicity Assay Kit	Life Technologies
Caspase-8 activity assay kit	Promega
Cellular ROS Assay Kit (DCFDA/H2DCFDA)	abcam

Akt/mTOR Phosphoprotein 11-Plex	Merck
Magnetic Bead Kit	
Mouse IL-1 β HTRF kit	Cisbio
Mouse TNF- α HTRF kit	Cisbio
Mouse IL-10 Elisa Kit	R&D Systems
RNeasy Mini Kit	Qiagen
RNase-free NDase set	Qiagen
Maxima TM SYBR Green/ROX qPCR	ThermoFisher Scientific
Master Mix	

3.1.5 Antibodies

Table 1: List of antibodies used for Western blot and WES

Antibody	Clone	Dilution	Company
NLRP3	D4D8T	1:1000	CST
Pro-IL-1 β	Ab2105	1:500	abcam
STAT1	9172	1:1000	CST
STAT3	9132	1:1000	CST
P38MAPK	9212	1:1000	CST
Phospho-STAT1(Y701)	9171	1:1000	CST
Phospho-STAT3(Y705)	9145	1:1000	CST
Phospho-P38MAPK(Thr180/Tyr182)	9211	1:1000	CST
HDAC11	58442	1:1000	CST
cFLIP _L	5634	1:1000	CST
cFLIP _S	5634	1:1000	CST
Caspase-1	4199	1:1000	CST
Caspase-8	9746	1:1000	CST
β -Tubulin	2128	1:1000	CST
TBK-1	3013	1:1000	CST
Phospho-TBK-1	5483	1:1000	CST
RIPK1	94C12	1:1000	CST
NF- κ B	6956	1:1000	CST
Phospho-NF- κ B	4764	1:1000	CST

β -Actin	926-42210	1:1000	Li-cor
XIAP	2042	1:1000	CST
cIAP1	7065	1:1000	CST
cIAP2	3130	1:1000	CST
RIPK3	13526	1:1000	CST
Human IL-1 β /IL-1F2	-	1:500	R&D
ASC	HASC-71	-	Biolegend
Anti-mouse IRDye 800CW	-	1:20000	Li-Cor
Anti-mouse IRDye 680RD	-	1:20000	Li-Cor
Anti-rabbit IRDye 800CW	-	1:20000	Li-Cor
Anti-rabbit IRDye 680RD	-	1:20000	Li-Cor
Streptavidin IRDye 680RD	-	1:20000	Li-Cor

3.1.6 siRNAs for electroporation

All the siRNAs used in this project were purchased from ThermoFisher Scientific.

Table 2: List of siRNAs used for electroporation

Target gene	Identifier
Negative Control #1	4390843
Negative Control #2	4390844
NLRP3 #1	s41554
NLRP3 #2	s41556
Caspase-8 #1	s2426
Caspase-8 #2	s2427
RIPK1 #1	137228
RIPK1 #2	137229
RIPK3 #1	s21740
RIPK3 #2	s21742
RIPK3 #3	s21741
STAT3 #1	s743
STAT3 #2	s744
TBK-1 #1	s761
TBK-1 #2	s763
cFLIP #1	s16864

cFLIP #2	s16864
HDAC11 #1	130749
HDAC11 #2	130750

3.1.7 qPCR primers

Table 3: List of qPCR primers used for amplification of human genes

Target	Sequence
hHPRT-F	TCAGGCAGTATAATCCAAAGATGGT
hHPRT-R	AGTCTGGCTTATATCCAACACTTCG
hIL1B-F	CTGTACCTGTCCTGCGTGTTGA
hIL1B-R	TGGGCAGACTCAAATTCCAGCT
hNLRP3-F	TCGGAGACAAGGGGATCAAA
hNLRP3-R	AGCAGCAGTGTGACGTGAGG
hCASP1-F	ACAACCCAGCTATGCCCACA
hCASP1-R	GTGCGGCTTGACTTGTCCAT
hPYCARD-F	GAGCTCACCGCTAACGTGCT
hPYCARD-R	ACTGAGGAGGGGCCTGGAT
hIL-10-F	GCCGTGGAGCAGGTGAAGA
hIL-10-R	AGTCGCCACCCTGATGTCTC

3.1.8 Cell culture media

Table 4: List of cell culture medium

Medium	Composition	
Complete RPMI	RPMI	
	FCS	10%
	penicillin/streptomycin	1%
	Sodium pyruvate	1 x
	GlutaMAX	1 x
RPMI (LDH assay)	RPMI	
	FCS	0.1%
	penicillin/streptomycin	1%

	Sodium pyruvate GlutaMAX	1 x 1 x
RPMI (Electroporation)	RPMI FCS Sodium pyruvate GlutaMAX	 10% 1 x 1 x
Complete DMEM	DMEM FCS penicillin/streptomycin Sodium pyruvate GlutaMAX	 10% 1% 1 x 1 x
FreeStyle™ 293 Expression Medium	-	-

3.1.9 Buffers and Solutions

Table 5: List of buffers and solutions

Application	Buffer name	Composition	
Tissue Culture	Cell freezing solution	FCS	80%
		DMSO	10%
		Medium	10%
hPBMC isolation	MACs buffer	PBS	1 x
		BSA	0.5%
		EDTA	2 mM
Western blot	Transfer Buffer	TrisGlycine Buffer	1 x
		Methanol	20%
	Blocking Buffer	TBS	1 x
		BSA	3%
TBST	TBS	1 x	
	Tween 20	0.05%	
TBS	TBS	1 x	
Cell lysis	RIPA lysis buffer	Tris-HCl (pH 7.4)	20 mM

		NaCl	150 mM
		EDTA	1 mM
		Triton X-100	1%
		Glycerol	10%
		SDS	0.1%
		Sodium deoxycholate	1 mM
		cOmplete EDTA-free	1 x
		Protease-Inhibitor	
		PMSF	0.2 mM
	NP-40 lysis buffer	Tris-HCl (pH 7.4)	20 mM
		NaCl	150 mM
		EDTA	1 mM
		Nonidet P-40	1%
		Glycerol	10%
		cOmplete EDTA-free	1 x
		Protease-Inhibitor	
	SDS lysis buffer	SDS	4%
		DTT	10 mM
		Tris-HCl (pH 8.0)	50 mM

3.1.10 Primary cells and Cell lines

All the buffy coats used in this thesis are provided by the blood donation service of the University Hospital Bonn (UKB)

Table 6: List of primary cells and cell lines

Name	Supplement	Source
hPBMC	-	Buffy coat
hMDMs (GM-CSF)	GM-CSF	Buffy coat
hMDMs (M-CSF)	M-CSF	Buffy coat
THP-1-monocyte	-	ATCC
THP-1-Macrophage	PMA	ATCC

WT BMDM	L929	C57BL/6
<i>Nlrp3</i> ^{-/-} BMDM	L929	C57BL/6
<i>Pycard</i> ^{-/-} BMDM	L929	C57BL/6
<i>Casp1/11</i> ^{-/-} BMDM	L929	C57BL/6
<i>Aim2</i> ^{-/-} BMDM	L929	C57BL/6
<i>Ripk3</i> ^{-/-} BMDM	L929	C57BL/6

3.1.11 Mice

Wild-type (WT) C57BL/6 mice, *Nlrp3*^{-/-}, *Pycard*^{-/-}, *Casp1/11*^{-/-}, *Aim2*^{-/-} and *Ripk3*^{-/-} mice were purchased from The Jackson Laboratory (Bar Harbor, ME, USA).

3.2 Methods

3.2.1 Cell culture and counting

The general cell culture conditions are 37°C with 5% CO₂ in a humidified atmosphere. THP-1 cells were cultured in tissue culture suspension flasks (25 – 75 cm²) in complete RPMI 1640 medium. Primary human monocytes and monocytes-derived macrophages (hMDMs) were cultured in tissue culture plates (96-, 12- and 6- wells) at the concentration of 1.0 – 2.0x10⁶ cells/ml in complete RPMI 1640 medium. Bone marrow derived macrophages (BMDMs) were cultured in 15 cm² cell culture dishes in complete DMEM medium supplemented with 20% L929.

Two methods were used in this project to count the cells depending on the number of cell lines or donors. Cells were stained for viability with trypan blue and subsequently either counted with a hemocytometer (Neubauer) or with the automated TALI cell counter (Thermo Fisher Scientific).

3.2.2 Cultivation and stimulation of THP-1 monocytes

THP-1 cells cultured in suspension flasks were passaged regularly to maintain a cell density of 3.0 x 10⁵ – 1.0 x 10⁶ cells/ml. When doing experiments, 8.0 x 10⁴ cells/well in 100 µl complete RPMI 1640 medium were seeded into 96-well plate. 50 µl of 4x working concentration of LPS (1 ng/ml) and 50 µl of 4x working concentration of butyrate (0.5 – 20 mM) were added on top of the cells simultaneously to incubate for 16 hours. After 16 hours, 100 µl of cells-free

supernatant were harvested for the cytokines measurement after the plates were centrifuged for 5 minutes at 340 x g.

3.2.3 Cultivation, differentiation and stimulation of THP-1 macrophages

THP-1 monocytes cultured in suspension flasks were incubated with PMA (100 nM) for 16 hours to differentiate into adherent THP-1 macrophages. After differentiation, THP-1 macrophages were washed twice with PBS to wash out the remaining PMA, then pre-warmed fresh complete RPMI 1640 medium were added to the cells for 6 – 8 hours. 5 mM EDTA in PBS was used to detach and harvest the cells.

After cell counting, 8.0×10^4 cells/well in 100 μ l medium were seeded in 96-well plate, in which 50 μ l of 4x working concentration of LPS (1 ng/ml) and 50 μ l of 4x working concentration of butyrate (0.5 – 20 mM) were added on top of the cells simultaneously to incubate for 16 hours. Then, 100 μ l of cells-free supernatant were harvested for the cytokine measurement by Elisa or HTRF after the plates were centrifuged for 5 minutes at 340 x g.

3.2.4 Purification and stimulation of human PBMCs

Prior to the purification of PBMCs, waste bottles and scissors were sterilized with 75% ethanol and put in the hood. The blood was diluted with PBS at the ratio of 1:1, then 35 ml of blood/PBS mixture was gently pipetted on top of 15 ml Ficoll. 3 layers were generated in the falcon after the samples were centrifuged for 20 minutes at 700 x g without brake. The middle layer, containing human peripheral blood mononuclear cell (PBMC), were transferred to a new falcon, washed twice with PBS and counted as described in section 3.2.1. Then 1.0×10^5 /100 μ l of PBMCs were seeded in 96-well plate. Subsequently, 50 μ l 4 ng/ml LPS (4x) and 50 μ l 40 mM butyrate (4x) were added to the cells simultaneously to incubate for 16 hours. Then, to remove cell debris in the supernatants, the plates were centrifuged for 5 mins at 340 x g and 100 μ l of cell-free supernatants were harvested for the cytokines measurement by HTRF.

3.2.5 Purification, differentiation and stimulation of primary human monocyte-derived macrophages (hMDMs)

Following the purification of PBMCs described in section 3.2.3, 250 μ l CD14 magnetic microbeads were incubated with PBMCs at 4°C for 15 minutes. Prior to filtering and transferring the cells to pre-separation filters on top of LS columns placed in a magnetic field, PBMCs were washed once with MACS buffer to remove the extra CD14 beads for the CD14⁺

monocytes selection. Subsequently, CD14⁺ monocytes were isolated after 3 times washing and final elution with 3 – 5 ml MACS buffer. In order to differentiate CD14⁺ monocyte into human macrophages, cells were resuspended and diluted by Complete RPMI containing 3.1 µl/ml rhGM-CSF to 2.0 x 10⁶ cells/ml, and then 5 ml cells were seeded in 6-well plate to culture for 3 days at 37°C, 5% CO₂. At day 3, hMDMs were harvested and plated for experimental use. In 96-, 12- or 6- well plates, 1.0 x 10⁵, 1.0 x 10⁶ or 2.0 x 10⁶ cells were seeded respectively and 100 µl stimuli were added on top of the cells to incubate for 16 hours. Subsequently, supernatants and cell lysates were harvested to perform HTRF, Western blot or WES for cytokines measurement and proteins detection.

3.2.6 Homogeneous Time Resolved Fluorescence (HTRF)

In this project, human and murine cytokines were quantified by HTRF (Cisbio). Briefly, 12 µl cell-free supernatants were transferred into 384-well HTRF plates (white). Subsequently, 3 µl pre-mixed solution containing respective donor antibody and acceptor antibody at the ratio of 1:1 were added to the samples. Then plates were sealed and incubated either at 4°C overnight or at room temperature for 3 hours. Afterwards, the fluorescence of both donor antibodies and acceptor antibodies were measured at 620 nm and 688 nm with a measurement delay of 50 ms by a SpectraMax i3 system.

3.2.7 Western blot

To analyse the protein expression in cell lysates and supernatants, Western blot and WES (section 3.2.8) were used in this thesis.

3.2.7.1 Samples preparation

After washing the cells twice with 1 ml cold PBS, 50 µl/1 x10⁶ cells fresh RIPA lysis buffer were added to lyse the cells. Then, cell lysates were scraped and transferred into 1.5 ml Eppendorf tubes for further centrifugation at 10,000 x g for 15 minutes at 4°C to remove DNA. Finally, fresh cell lysates were transferred into new 1.5 ml Eppendorf tubes for the protein quantification and denaturation.

To precipitate proteins in the supernatants for the detection of cleaved IL-1β and cleaved caspase-1, 500 µl methanol and 125 µl chloroform were mixed with 500 µl cell-free supernatants. Subsequently, the mixtures were vortexed and then centrifugated at 13,000 x g for 2 minutes. To get the precipitated proteins, the first layer containing methanol and water

were discarded and another 500 µl methanol were laid on top of the second layer. Afterwards, the mixtures were vortexed and centrifugated again at 13,000 x g for 2 minutes. Then, all the supernatants were discarded and the pellet at the bottom of Eppendorf tubes was left to dry for 10 – 15 minutes at room temperature. In the end, 25 µl mixtures of LDS buffer (1x) and reducing agent (1x) were used to resuspend the dried pellet.

3.2.7.2 Protein quantification

Protein quantification was performed using bicinchoninic acid (BCA). In brief, 10 µl of cell lysates samples were diluted 5x by addition of ddH₂O and transferred to 96-well plate. A serial dilution of BSA were prepared according to the instructions in the BCA protein assay kit and used as standard for protein quantification. Afterwards, 200 µl premixed solution containing Reagent A and B at the ration of 50:1 were laid on top of samples and standards to incubate 30 minutes at 37°C. Then the absorbance at 562 nm was read by a SpectraMax i3 system.

3.2.7.3 SDS-PAGE

After the cell lysates diluted in LDS buffer and reducing agent were heated for 10 minutes at 95°C to allow for proteins denaturation, 40 µg of proteins per sample and 5 µl pre-stained protein ladder were loaded into the Bis-Tris gels (4 –12%). Proteins of cell lysates were separated using MOPS buffer for 80 – 90 minutes at 120 V, while the precipitated proteins were separated using MES buffer for 45 minutes at 120V.

3.2.7.4 Western blot

After all the proteins in the gel were transferred to PVDF membrane using a semi-wet transfer system, 5 ml TBS buffer were used to block the membrane for 1 hour at room temperature. Then, the membrane was incubated with 5 ml TBST buffer containing primary antibody overnight at 4°C. Next day, to wash out extra and unstained primary antibody on the membrane, the membrane was washed 3 times with 5 ml TBST buffer. Subsequently, 5 ml secondary antibodies diluted by TBST buffer were incubated with the membrane for 1 hour at room temperature in the dark. Prior to scanning fluorescent signals on the membrane by Odyssey imager, the membrane was washed twice with TBST and once with TBS.

3.2.8 WES

To prepare the loading samples for WES, 1 part 5x fluorescent Master Mix was combined with 4 parts cell lysates samples to the final concentration of 0.1 mg/ml. Then the samples were heated at 95°C for 5 minutes. All the samples were loaded to the separation plate according to the manufacturer's instructions. Subsequently, the separation plate was centrifuged for 5 minutes at 800 x g. The samples were electrophoretically separated by a 25-capillary cartridge (12 – 230 kDa) with the settings as follows:

Loading time of the separation matrix	200 s
Loading time of the stacking matrix	15 s
Loading time of the samples	9 s
Separation time of the samples at 375 V	25 min
Incubation time with the primary antibody	90 min
Incubation time with the secondary antibody	30 min

All the results were processed and analysed with the Compass for WES.

3.2.9 Small interfering RNA (siRNA) electroporation in primary human macrophages

All the siRNA-mediated knockdown experiments in primary human macrophages were performed by electroporation using a Neon Transfection System (MPK5000; Invitrogen). Each reaction used $1.2 - 1.5 \times 10^6$ hMDMs, which were mixed with 10 μ l buffer R and 75 pmol (1.5 μ l) siRNA. Subsequently, the samples were taken up using a 10- μ l Neon Pipette Tip and electroporated with the following protocol: 1400 V, 20 ms, 2 pulses. The electroporated cells were cultured in 10% FCS RPMI medium without antibiotics for 3 days. For some of the siRNAs with low knockdown efficiency, cells need to be electroporated again at day 3 after the first electroporation and cultured in 10% FCS RPMI medium without antibiotics for another 2 days. $0.5 - 1 \times 10^6$ cells were lysed by 30 μ l RIPA buffer containing cOmplete™ EDTA-free protease inhibitor and phosphatase inhibitor to prepare the samples for the validation of siRNA-mediated knockdown efficiency by either Western blot or WES.

3.2.10 Caspase-8 activity assay

1.5×10^5 cells /well were seeded into white 96-well plate in 100 μ l. 100 μ l of the indicated stimuli were added to the cells. Cells were incubated for 16 hours. Afterwards, the plate was centrifuged for 5 minutes at 340 x g and supernatants were collected for the measurement of cytokines. The cells were washed once with PBS. Then 25 μ l caspase-8 Glo assay buffer containing MG-312 were added to the cells immediately. After the samples were incubated for 30 – 60 minutes in dark, the luminescent signal was measured at 470 nm by a SpectraMax i3 system.

3.2.11 Intracellular ROS production assay

1.0×10^5 cells/well were seeded into white 96-well plate in 100 μ l RPMI1640 phenol red free medium. After overnight incubation at 37°C and 5% CO₂, cells were washed once with 100 μ l 1x filtered buffer provided by the kit (ab113851; abcam). 100 μ l pre-warmed 20 μ M DCFDA were added to and incubated with the cells for 45 minutes at 37°C and 5% CO₂, following which cells were washed twice with 100 μ l PBS or 1 x filtered buffer to remove the remaining DCFDA in the wells. Then, another 100 μ l indicated stimuli or positive control (2 mM H₂O₂) were added to the cells to elicit intracellular ROS production. After The samples were incubated for 1 – 4 hours at 37°C and 5% CO₂, the fluorescence was measured at Ex/Em = 485/535 nm by a SpectraMax i3 system.

3.2.12 Lactate dehydrogenase (LDH) assay

To determine the cell viability of hMDMs in response to the treatment with LPS and butyrate, the activity of released LDH in the supernatants were measured and quantified as an indicator of cell death. 1.0×10^5 hMDMs were seeded into 96-well plates in 100 μ l RPMI 1640 medium containing 0.1% FCS. Another 100 μ l indicated stimuli were added to and cultured with the cells for 16 hours, after which the plate was centrifugated for 5 minutes at 340 x g to remove non-adherent cells from the supernatants. Meanwhile, 200 μ l 1 x lysis buffer provided by the kit (Pierce LDH cytotoxicity Assay) were used to lyse the control cells as positive control. Afterwards, 25 μ l supernatants and 25 μ l LDH assay buffer were transferred and mixed in a transparent 384-well plate and incubate for 30 minutes in the dark. Then the absorbance was measured at 490 nm and 680 nm by a SpectraMax i3 system.

3.2.13 Live cell imaging for cell death analysis by IncuCyte

This experiment was performed in collaboration with Neil Stair (Institute for Genetics, University of Cologne). hMDMs were used to determine cell viability by live cell imaging. 3.5×10^4 cells /well were seeded into a 96-well plate in RPMI 1640 medium containing rhGM-CSF (3.1 μ l/ml). The following live cell imaging dyes were also added where indicated: Diyo-1 (1:10,000), Caspase-3/7 green detection reagent (1:2,000), pSIVA (1:500), DRAQ7 (1:3,000). DRAQ7 was added to the medium containing either pSIVA or Caspase-3/7 dye. Cells were allowed to reattach for 4 hours before addition of any compounds. LPS (10 ng/ml) was added 3 hours prior to addition of nigericin (10 μ M) as a positive control. Inhibitors were added directly to the appropriate wells 30 minutes prior to addition of LPS and butyrate for the following final concentrations: Emricasan (2.5 μ M), Necrostatin-1s (30 μ M), CRID3 (2 μ M). Cell death analysis was performed using the IncuCyte bioimaging platform which is housed in a high humidity, 37°C, 5% CO₂ incubator. Four images were captured per well in the appropriate fluorescent channels and phase contrast every one or two hours for 24 hours. These images were analyzed using the IncuCyte analysis software. The fluorescent count/image was averaged between four images/well. This was used to yield the average cell count/image/well, demonstrating membrane-permeabilized cells in the case of Diyo-1 or DRAQ7 and apoptotic cells for pSIVA or Caspase-3/7. Each condition was measured in technical duplicates for each donor.

3.2.14 Reverse transcription quantitative real-time PCR

3.2.14.1 RNA isolation

1.0×10^6 hMDMs per well were seeded in 12-well plate and incubated with indicated stimuli for 16 hours, after which 350 μ l RLT lysis buffer containing 1% (v/v) β -mercaptoethanol were used to lyse the cells at room temperature. Cell lysates were harvested and transferred into new Eppendorf tubes for further RNA isolation according to the manufacturer's instructions (RNeasy Mini Kit, Qiagen). 25 μ l nuclease-free water were used to elute RNA from the columns and the resulting RNA concentrations and purities were quantified using the NanoDrop™ 2000 spectrophotometer.

3.2.14.2 cDNA synthesis

In all the experiments I performed in this project, 500 ng-1000 ng RNA of each sample were synthesized into cDNA by reverse transcription PCR (RT-PCR). 1 μ l of oligo dT were mixed with the same amount of RNA per condition and adjusted to 12.9 μ l with RNase-free water and then heated for 5 minutes at 65°C. After 1 minute incubation on ice, the samples were mixed with 6.1 μ l of a pre-mixture containing 4 μ l 5x reaction buffer, 1 μ l 10 mM dNTPs, 1 μ l 0.1 M DTT and 0.1 μ l superscript III reverse transcriptase. Finally, cDNA was generated by incubating the samples for 50 minutes at 50°C followed by another 5 minutes at 85 °C.

3.2.14.3 Quantitative real-time PCR (qPCR)

cDNA was normally diluted 1:10 by nuclease-free water. After the cDNA were diluted by nuclease-free water, 10 μ l mastermix composed of 2 μ l cDNA, 5 μ l SYBR Green, 1 μ l H₂O and 2 μ l of a mix containing both reverse primer (2 μ M) and forward primer (2 μ M) were prepared and pipetted into 384-well qPCR plate. The qPCR was performed on the QuantStudio 6 Flex real time-PCR system, and the relative expression of the target mRNA was analysed using the $\Delta\Delta C_T$ method with HPRT as the reference mRNA.

3.2.15 ASC specks imaging

200 μ l of 1×10^6 /ml hMDMs per well were seeded in 8-well ibidi slides. The cells were treated with medium, LPS (1 ng/ml) or butyrate (10 mM), alone or in combination, for 16 hours, or primed with LPS (10 ng/ml, 3 hours) prior to the addition of NLRP3 inflammasome activator Nigericin (10 μ M, 1.5 hours). Then, the cells were fixed with 200 μ l 4% formaldehyde in PBS after 30 minutes incubation at room temperature, followed by two washes with 200 μ l PBS. 100 μ l of mixtures containing 10 μ l human FcR blocking reagent and 90 μ l permeabilization buffer were incubated with the cells for 10 minutes at 37°C. Afterwards, the cells were stained with 4 μ l of directly labelled anti-ASC-647 (1:25) and incubated overnight at 4°C in the dark. To wash out the extra antibodies, the cells were washed twice with 200 μ l permeabilization buffer. Subsequently, 100 μ l DNA dye Hoechst diluted by PBS (1:3,000) were incubated with the cells for 10 minutes at room temperature in the dark, which is followed by two washes with 200 μ l PBS to remove the remaining Hoechst solution. Finally, the cells were filled with 200 μ l PBS and imaged by Observer Z1 epifluorescence microscope (ZEISS). The analysis of ASC specks was processed by counting the number of cells using Hoechst as a nuclear marker as well as the ASC 647 signal to count the specks to ultimately calculate the number of ASC

specks per cell. This analysis was performed by using the image analyser software Cell profiler 3.0 with the help of Dr. Tomasz Próchnicki.

3.2.16 Multiple immunoassay by Luminex

The multiple cytokines immunoassay in the cell-free supernatants were performed by Dr. Bianca Martin (Institute of Innate Immunity, University of Bonn) using the Bio-Plex Pro™ Human Cytokine 27-plex Assay kit according to the manufacturer's instructions.

The measurement of intracellular phosphorylation of the Akt/mTOR pathway was performed using the MILLIPLEX MAP Akt/mTOR phosphoprotein Magnetic Bead11-plex Kit. 1.0×10^6 cells/ml were seeded in 12-well plate and then challenged by the indicated stimuli for 16 hours. After the incubation time, the plate was centrifugated for 5 minutes at $340 \times g$ and cell-free supernatants were then collected for the cytokine measurement. Subsequently, 50 μ l cell lysis buffer provided by the kit were added to the cells to incubate for 15 minutes at 4°C. The proteins concentration in the cell lysates were quantified by BCA assay and adjusted to the same concentration with cell lysis buffer. Following the protocol provided by the manufacturer, 25 μ l of each sample were used for the measurement of phosphoproteins. The plate was read by MAGPIX instrument (Merck). This experiment was performed with the help of Carl Christian Kolbe.

3.2.17 RNA-sequencing (RNA-Seq)

The experiment was performed by Dr. Bianca Martin (Institute of Innate Immunity, University of Bonn) and the resulting data was processed and analysed by Dr. Christina Budden (Institute of Innate Immunity, University of Bonn).

3.2.17.1 RNA isolation

1.0×10^6 GM-MDMs were treated NaCl (10 mM), SCFAs (acetate, propionate or butyrate; 10 mM) or TSA (0.5 μ M) in the presence or absence of LPS (1 ng/ml) for 16 hours and subsequently lysed in TRIZOL (Invitrogen) and total RNA was extracted using the RNeasy Mini Kit (Qiagen) according to the manufacturer's protocol. RNA was eluted in RNase-free water. The quality of the RNA was assessed by measuring the ratio of absorbance at 260 nm and 280 nm using a Nanodrop 2000 Spectrometer (Thermo Scientific) and by visualization of 28S and 18S band integrity on a TapeStation 2200 (Agilent).

3.2.17.2 Generation of cDNA libraries and sequencing

Total RNA was converted into libraries of double-stranded cDNA molecules as a template for high-throughput sequencing using the Illumina TruSeq RNA Sample Preparation Kit v2. Briefly, mRNA was purified from 100 – 500 ng of total RNA using poly-T oligo-attached magnetic beads. Fragmentation was carried out using divalent cations under elevated temperature in Illumina proprietary fragmentation buffer. First strand cDNA was synthesized using random oligonucleotides and SuperScript II. Second strand cDNA synthesis was subsequently performed using DNA Polymerase I and RNase H. Remaining overhangs were converted into blunt ends via exonuclease/polymerase activities and enzymes were removed. After adenylation of 3'ends of DNA fragments, Illumina adaptor oligonucleotides were ligated to prepare for hybridization. DNA fragments with ligated adaptor molecules were selectively enriched using Illumina PCR primers in a 15 cycles PCR reaction. Size-selection and purification of cDNA fragments with preferentially 200 bp in insert length was performed using SPRIbeads (Beckman-Coulter). Size distribution of cDNA libraries was measured using the Agilent high sensitivity DNA assay on a TapeStation 2200 (Agilent). cDNA libraries were quantified using KAPA Library Quantification Kits (Kapa Biosystems). After cluster generation on a cBot, 75 bp single read sequencing was performed on a HiSeq1500 and de-multiplexed using CASAVA v1.8.2.

3.2.17.3 RNA-Seq data analysis

Pre-processing of RNA-Seq data was performed by a standardized and reproducible pipeline based on the Docker system (Docker image is available via docker hub, limesbonn/hisat2). Briefly, alignment to the human reference genome hg19 from UCSC was conducted by Hisat2 (Hisat2, 2.0.6) (Kim et al., 2015) using standard settings. The external gene names and Entrez gene IDs matching the original Ensembl gene IDs were obtained using The biomaRt package (v2.38.0) (Kinsella et al., 2011) and a DGEList object was created using the raw counts and gene annotation using the edgeR package (v3.24.0) (Robinson et al., 2009). Since genes with very low counts are not useful, only genes that had at least 10 reads in a worthwhile number of samples determined by the design matrix were kept. In addition, each kept gene is required to have at least 15 reads across all the samples. Filtering was performed using the filterByExpr function. Afterwards, counts were normalised. The aim of normalisation is to remove systematic technical effects that occur in the data to ensure that technical bias has minimal impact on the results. Normalisation was done by using TMM method (Robinson and Oshlack, 2010) (weighted, trimmed mean of M-values) with the application of edgeR calcNormFactors function. In contrast to other procedures, where the proportion of each gene's reads is

computed relative to the total number of reads and compared across all samples, here it is taken into account that different experimental conditions might express a diverse RNA repertoire and therefore might lead to not directly comparable proportions. To put it simply, normalisation is supposed to level the median of gene expression values across samples, assuming that the majority of genes are expressed at an equal level. After data normalisation and with the edgeR package v3.24.0, estimateDisp was used to estimate common dispersion and tagwise dispersion and transform the data for linear modelling. Multidimensional scaling (MDS) plot visualising the relationship between the samples were displayed with the batch-corrected data according to all the donors. For each comparison, differentially expressed genes (DEGs) were identified with a false discovery rate (FDR)-adjusted p-value < 0.05. Gene set enrichment analysis was performed using the camera function of the limma package v3.38 (Wu and Smyth, 2012) with the hallmark gene set collections from the Molecular Signatures Database v5.2 (Liberzon et al., 2015; Subramanian et al., 2005).

3.2.18 Mass Spectrometry (MS)

3.2.18.1 Samples preparation and LC-MS/MS

This experiment was performed in collaboration with Meera Phulphagar (Max Planck Institute of Biochemistry, Martinsried), and the resulting data was processed and analysed by Meera Phulphagar and Dr. Christina Budden (Institute of Innate Immunity, University of Bonn).

1.5×10^6 GM-MDMs were cultured in 1 ml RPMI 1640 medium in 12-well plates and challenged by indicated stimuli for 16 hours. The cells were washed twice with PBS before lysing the cells with 200 μ l SDS lysis buffer containing freshly added DTT. Cell lysates were collected into new Eppendorf tubes and boiled for 10 minutes. 800 μ l pre-cooled acetone were mixed with the samples and then incubated overnight at -20°C . Subsequently, the samples were washed twice with 80% acetone after centrifugation (19,000 \times g, 20 minutes, 4°C). The pellets at the bottom of tubes were dried for 15 minutes at room temperature and stored at -80°C .

Frozen samples were resuspended in 50 μ l of digestion buffer containing 1% SDC, 10 mM TCEP, 55 mM CAA, 25 mM Tris (pH = 8) and boiled for 10 minutes to denature proteins. After sonication using a Bioruptor (Diagenode), protein concentration was measured via BCA assay. 50 μ g of proteins were digested with 1 μ g Lys-C and Trypsin overnight at 37°C and 1500 rpm. Peptides were desalted and purified using 2 discs of SDB-RPS material and re-suspended in 2% acetonitrile/0.1% TFA for LC-MS.

Reverse phase chromatographic separation of peptides was performed by loading approximately 200 – 500 ng of peptides on a 50-cm HPLC-column (75- μ m inner diameter; in-house packed using ReproSil-Pur C18-AQ 1.9- μ m silica beads; Dr Maisch GmbH, Germany) coupled to an EASYnLC 1200 ultra-high-pressure system. Peptides were separated with a buffer system consisting of 0.1% formic acid (buffer A) and 80% acetonitrile in 0.1% formic acid (buffer B) using a linear gradient from 5 to 30% B in 110 minutes. The column temperature was set to 60°C.

The LC was coupled to a quadrupole Orbitrap mass spectrometer (Q Exactive HFX, Thermo Fisher Scientific, Rockford, IL, USA) via a nano-electrospray ion source. The mass spectrometer was operated in a data-dependent acquisition mode, collecting MS1 spectra (60,000 resolution, 300 – 1650 m/z range) with an automatic gain control (AGC) target of 3E6 and a maximum ion injection time of 20 ms. The top-15 most intense ions from the MS1 scan were isolated with an isolation width of 1.4 m/z. Following higher-energy collisional dissociation (HCD) with a normalized collision energy (NCE) of 27%, MS2 spectra were collected (15,000 resolution) with an AGC target of 5E4 and a maximum ion injection time of 28 ms. Dynamic precursor exclusion was enabled with a duration of 30 s.

3.2.18.2 MS data processing and analysis

Mass spectra were searched against the 2019 Uniprot mouse databases using MaxQuant version 1.5.5.2 with a 1% FDR at the peptide and protein level. Peptides required a minimum length of seven amino acids with carbamidomethylation as a fixed modification, and N-terminal acetylation and methionine oxidations as variable modifications. Enzyme specificity was set as C-terminal to arginine and lysine using trypsin as protease and a maximum of two missed cleavages were allowed in the database search. The maximum mass tolerance for precursor and fragment ions was 4.5 ppm and 20 ppm, respectively. 'Match between runs' was enabled to transfer peptide identifications between individual measurements with a 0.7-min window after retention time alignment. Label-free quantification was performed with the MaxLFQ algorithm using a minimum ratio count of 2. Protein identifications were filtered by removing matches to the reverse database, matches only identified by site, and common contaminants. Data filtering and Statistical analysis was performed with Perseus v1.5.5.5, GraphPad Prism v7.03, Microsoft Excel, and R Studio v3.4.0. Data was filtered further such that only proteins with identifications in all replicates of one cell type were retained. Missing values were imputed from a normal distribution of intensity values at the detection limit of the mass spectrometer. Statistical analysis was performed as indicated in the figure legends with a constant permutation based FDR correction at 5%. Further analyses are same as those in section 3.2.17.

4. Results

4.1 Characterization of the effects of short-chain fatty acids (SCFAs) on TLR-induced cellular responses through transcriptomic and proteomic analysis

SCFAs, the major metabolic products of commensal microbes, have been initially identified as inhibitors of histone deacetylases (HDACi) (Waldecker et al., 2008). Thus, SCFAs extensively modulate gene transcription by suppressing the removal of acetyl groups from the lysine residues of histones, resulting in relaxed and opened chromatin. Furthermore, several groups demonstrated the involvement of SCFAs in multiple cellular events, including apoptosis, cell proliferation and differentiation. These effects are mediated by the SCFAs' gene transcription modulatory functions (Fu et al., 2004; Tang et al., 2011)

How SCFAs in combination with other bacterial components, such as LPS, shape cellular responses and fate and what kind of cellular processes are engaged remained elusive. To specifically characterize the impact of SCFAs on TLR-induced cellular responses, transcriptomic and proteomic analyses of primary human macrophages were performed in the presence of SCFAs and TLR ligands.

4.1.1 Transcriptomic analysis reveals regulatory functions of SCFAs on the TLR-induced gene expression profile

To obtain a comprehensive picture of the broad effects of SCFAs on gene transcription, RNA-sequencing was performed to examine the transcriptomes of primary human macrophages that were unstimulated or treated with acetate, propionate, butyrate, NaCl, or trichostatin (TSA), alone or in co-stimulation with LPS. In this experiment, NaCl served as a negative control and the inhibitor of class I and II mammalian HDACs TSA was used to mimic the inhibitory role of SCFAs on HDACs.

To visualise the level of similarity between all the samples in response to the treatments of interest, a multidimensional scaling (MDS) plot was generated (Figure 4.1.1A). The plot shows a clear separation of the samples according to the LPS co-stimulation (Figure 4.1.1A). Additionally, butyrate- and TSA-treated samples clustered far apart from NaCl or acetate-treated samples, whereas propionate-treated samples clustered half-way between the previous two groups (Figure 4.1.1 A). Accordingly, butyrate- and TSA-treated samples showed similar numbers of differentially expressed transcripts upon LPS challenge and this number

was lower in the case of propionate-treated samples (Figure 4.1.1 B). Of note, the stimulation with acetate did merely affect the LPS-induced changes in gene expression (Figure 4.1.1 B). To further compare the LPS-induced differentially expressed (DE) genes selectively modulated by butyrate, TSA and propionate, the fold changes (FC) of genes within the LPS + butyrate vs LPS comparison were compared against those within LPS + propionate vs LPS comparison (Figure 4.1.1 C) or LPS + TSA vs LPS comparison (Figure 4.1.1 D), respectively. In line with the sample clustering in Figure 4.1.1 A, the distribution of both up- and down-regulated genes in the comparison of butyrate vs TSA showed a higher similarity compared to butyrate vs propionate. A heat map depicting the clustered expression of DE genes of the analysed samples (Figure 4.1.1 D) demonstrates a vast overlap of DE genes regulated by butyrate and TSA. Propionate showed a moderate similarity to butyrate (Figure 4.1.1 E). Taken together, propionate and butyrate, but not acetate, robustly modified the LPS-induced gene expression profile in primary human macrophages. Moreover, the highly similar effect on the gene expression of butyrate and TSA upon LPS treatment suggests that butyrate possibly modifies gene transcription through the inhibition of HDACs.

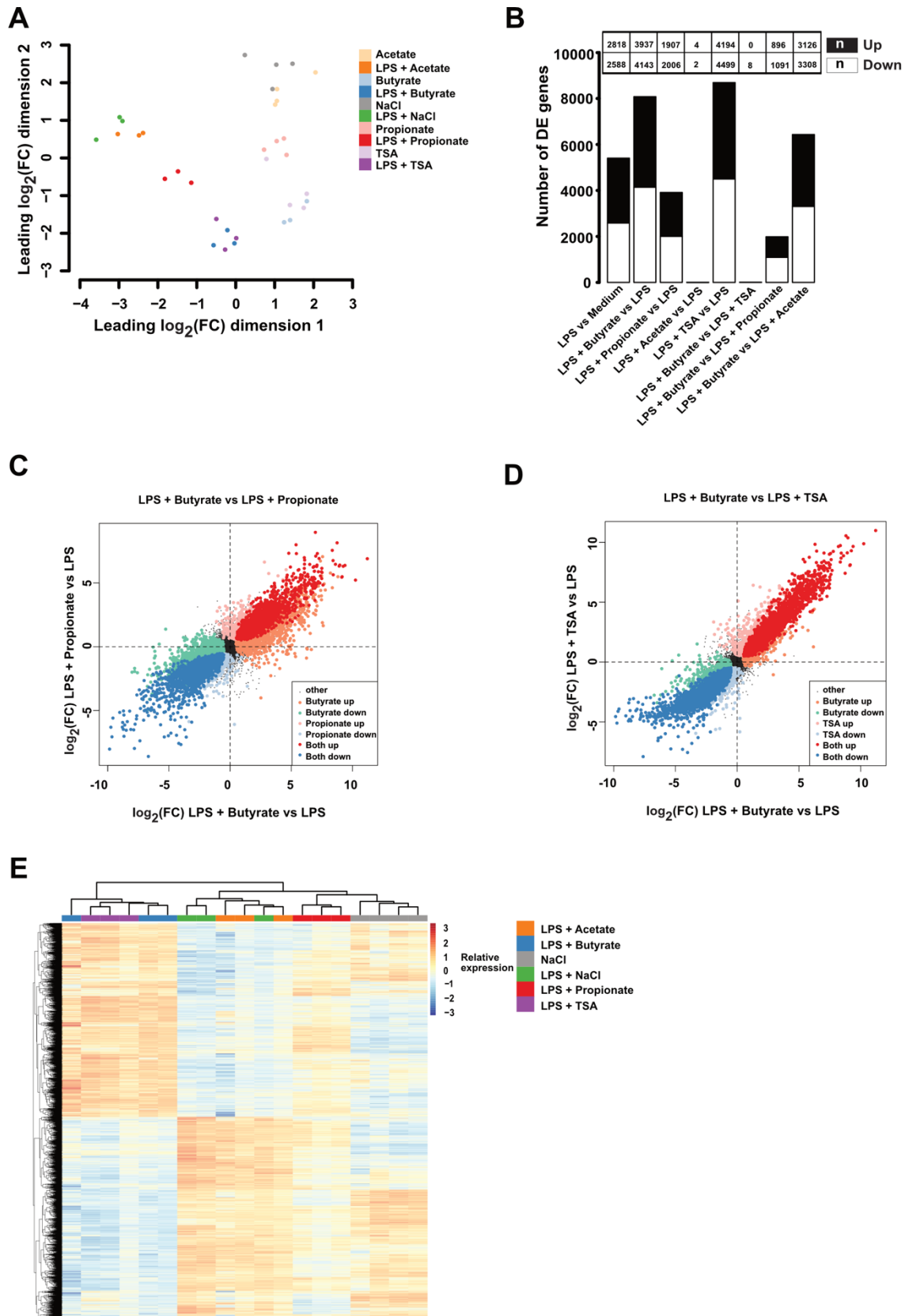


Figure 4.1.1: SCFAs regulate TLR-induced gene transcriptional profile

GM-MDMs were treated with either NaCl (10 mM), acetate (10 mM), propionate (10 mM), butyrate (10 mM) or TSA (0.5 μM) in the absence or presence of LPS (1 ng/ml) for 16 hours. Isolated mRNA was processed using the Illumina TruSeq RNA Sample Preparation Kit v2 and subjected to transcriptomic analysis. **(A)**: Multidimensional

scaling (MDS) plot visualising the relationship between the samples, $n = 3$ or 4 . **(B)**: Barplot depicting the number of differentially expressed genes (DEGs) that significantly changed more than 1.2 fold in the comparisons between groups of interest. **(C-D)**: Comparison of **(C)** $\log_2(\text{FC})$ LPS + Butyrate to $\log_2(\text{FC})$ LPS + Propionate and **(D)** $\log_2(\text{FC})$ LPS + Butyrate to $\log_2(\text{FC})$ LPS + TSA. Significantly up- and down-regulated transcripts are highlighted by colour. **(E)**: Heat map depicting relative expression values of transcripts that were significantly changed in LPS + butyrate vs LPS + NaCl comparison, scaled by row.

The experiment was performed by Dr. Bianca Martin (Institute of Innate Immunity, University of Bonn).

Transcriptomic data were analyzed and raw figures were generated by Dr. Christina Budden (Institute of Innate Immunity, University of Bonn).

4.1.2 DE Genes regulated by SCFAs are associated with diverse cellular processes

Following the identification of the broad effects of SCFAs on the LPS-induced gene expression changes, I proceeded to investigate the pathways that were enriched within the DE genes in the comparison of interest. To this end, gene set enrichment analysis (GSEA) was performed using the hallmark gene set of the Molecular Signatures Database (MSigDB).

Interestingly, stimulation with LPS + acetate led to an enrichment of genes within the Myc Targets V1 and Myc Targets V2 gene sets (Figure 4.1.2 A), while stimulation with LPS + propionate led to an enrichment of genes within the interferon- (IFN-) α response and IFN- γ response gene sets (Figure 4.1.2 B). It is noteworthy that stimulation with LPS + butyrate and LPS + TSA were associated with the very similar enriched gene sets, including the IFN- α response gene set, IFN- γ response gene set, inflammatory response gene set, allograft rejection gene set, IL-6-Jak-Stat3 signaling gene set, and complement gene set (Figure 4.1.2 C and D).

In summary, butyrate stimulation induces the enrichment of gene sets associated with diverse cellular processes related to inflammation and immunity in LPS-treated primary human macrophages, presumably through its role on HDAC inhibition.

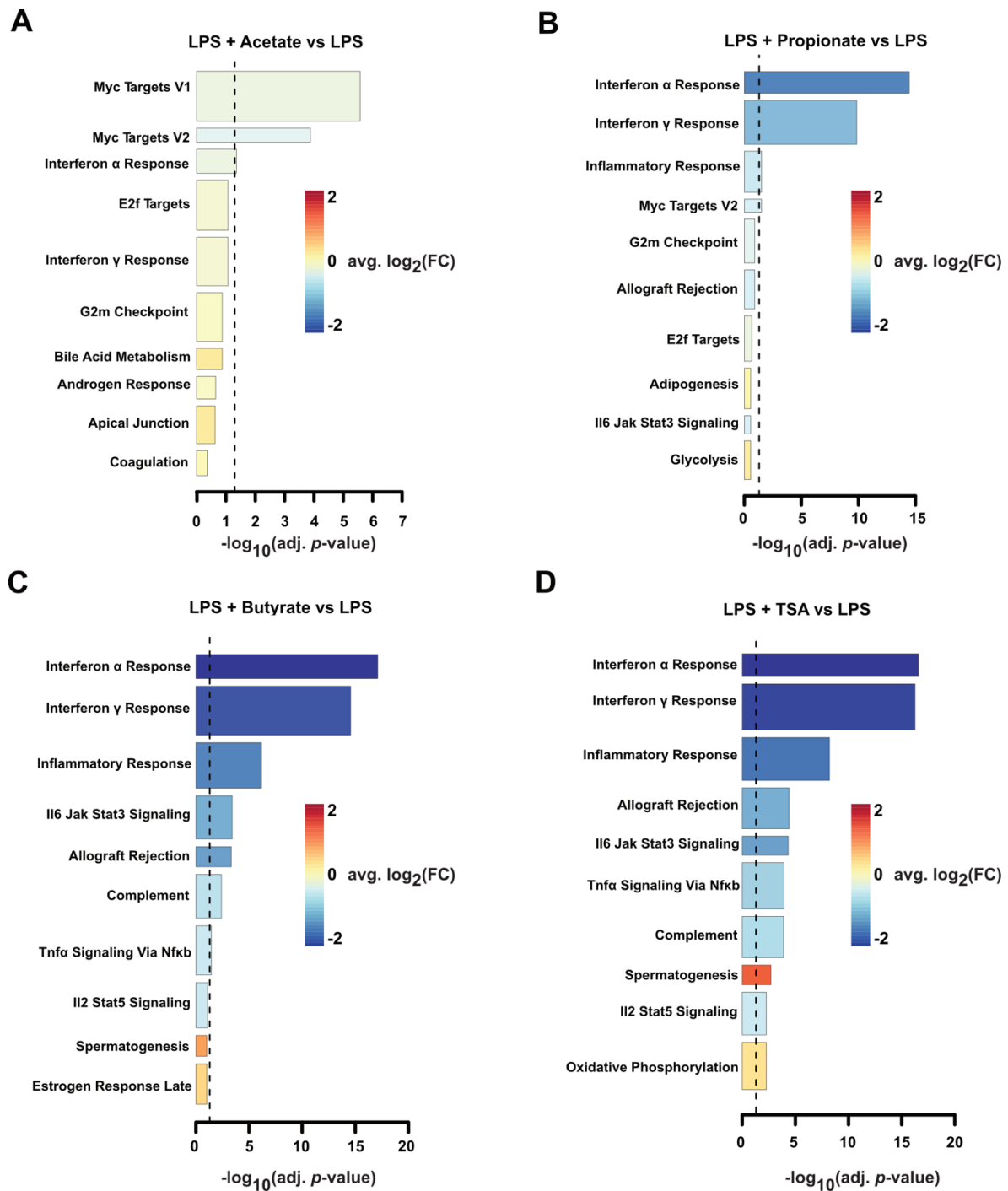


Figure 4.1.2: LPS + butyrate and LPS + TSA have a similar effect on the cellular processes based on hallmark gene sets enrichment

(A-D): Gene set enrichment analysis (GSEA) was performed based on the Molecular Signatures Database (MSigDB), using the hallmark gene sets. Plots show the top 10 hallmark gene sets in the following comparisons: (A) LPS + acetate vs LPS, (B) LPS + propionate vs LPS, (C) LPS + butyrate vs LPS and (D) LPS + TSA vs LPS. Bars are coloured by average $\log_2(\text{FC})$. Bar width represents the number of genes in the respective gene set. Dashed line indicates adjusted p -value threshold.

The experiment was performed by Dr. Bianca Martin (Institute of Innate Immunity, University of Bonn).

Data were analysed and raw figures were generated by Dr. Christina Budden (Institute of Innate Immunity, University of Bonn).

4.1.3 Dissecting the influence of SCFAs on TLR-mediated cellular responses through proteomic analysis

Given the poor correlations between mRNA transcripts abundance and protein expression resulting from posttranscriptional modifications, mRNA stability, or protein stability (Liu et al., 2016b; Maier et al., 2009), mass spectrometry was performed to study how SCFAs, and potentially other HDACi, modify the proteome of TLR-stimulated macrophages. These experiments provided insights into how the butyrate-mediated HDAC inhibition impacts the protein expression levels on a global scale.

I stimulated primary human macrophages with LPS in the absence or presence of butyrate or TSA for 16 hours and collected whole-cell lysates. Approximately 3500 proteins were detected in each sample by mass spectrometry.

To minimise the batch effect of different donors, batch correction was performed according to the four or five donors. Batch-corrected data were graphed in an MDS plot, which displayed a clear clustering of the samples according to their treatment group, with good separation between the different treatments (Figure 4.1.3 A). I observed that both butyrate and TSA modulated the LPS-induced changes in protein expression. Interestingly, the number of detected DE proteins regulated by butyrate (156) was 4 times higher than the number of those regulated by TSA (39) (Figure 4.1.3 B), of which 113 or 31 proteins were down-regulated, accounting for respectively 72% and 79% of the identified DE proteins. This result suggests that butyrate might regulate the LPS-induced changes in protein expression through a mechanism distinct from targeting HDACs.

To compare the expression levels of the DE proteins between butyrate and TSA, a FC/FC plot (Figure 4.1.3 C) and a heat map (Figure 4.1.3 D) were generated. Intriguingly, the FCs between both the LPS + butyrate vs LPS comparison and the LPS + TSA vs LPS comparison are similar for the DE proteins. Moreover, most of the DE proteins regulated by TSA are covered by those modulated by butyrate (Figure 4.1.3 C), indicating that butyrate had a stronger regulatory effect than TSA on LPS-induced changes in protein expression. In addition, the proteins expression profiles upon stimulation with LPS + butyrate and LPS + TSA were not as similar as the respective gene expression profiles (Figures 4.1.1D and 4.1.3 D).

Lastly, GSEA was performed based on the hallmark gene sets of the MSigDB to characterize the potential signaling networks to which the identified DE proteins belong and the biological processes in which they may play a role. Butyrate had similar effects on the enrichment of gene sets at the mRNA and protein levels (Figures 4.1.2 C and 4.1.3 F). However, at the protein level, TSA did not have the strong effect on the inflammatory response gene set and

the TNF- α signaling via NF- κ B gene set that had been observed on the transcriptome level (Figures 4.1.2 D and 4.1.3 G).

Taken together, in primary human macrophages, butyrate has a broader modulatory effect on LPS-induced changes in protein expression than TSA. On the protein level, butyrate stimulation led to the enrichment of several gene sets, including the inflammatory response gene set, the IFN- α response gene set, and the IFN- γ response gene set.

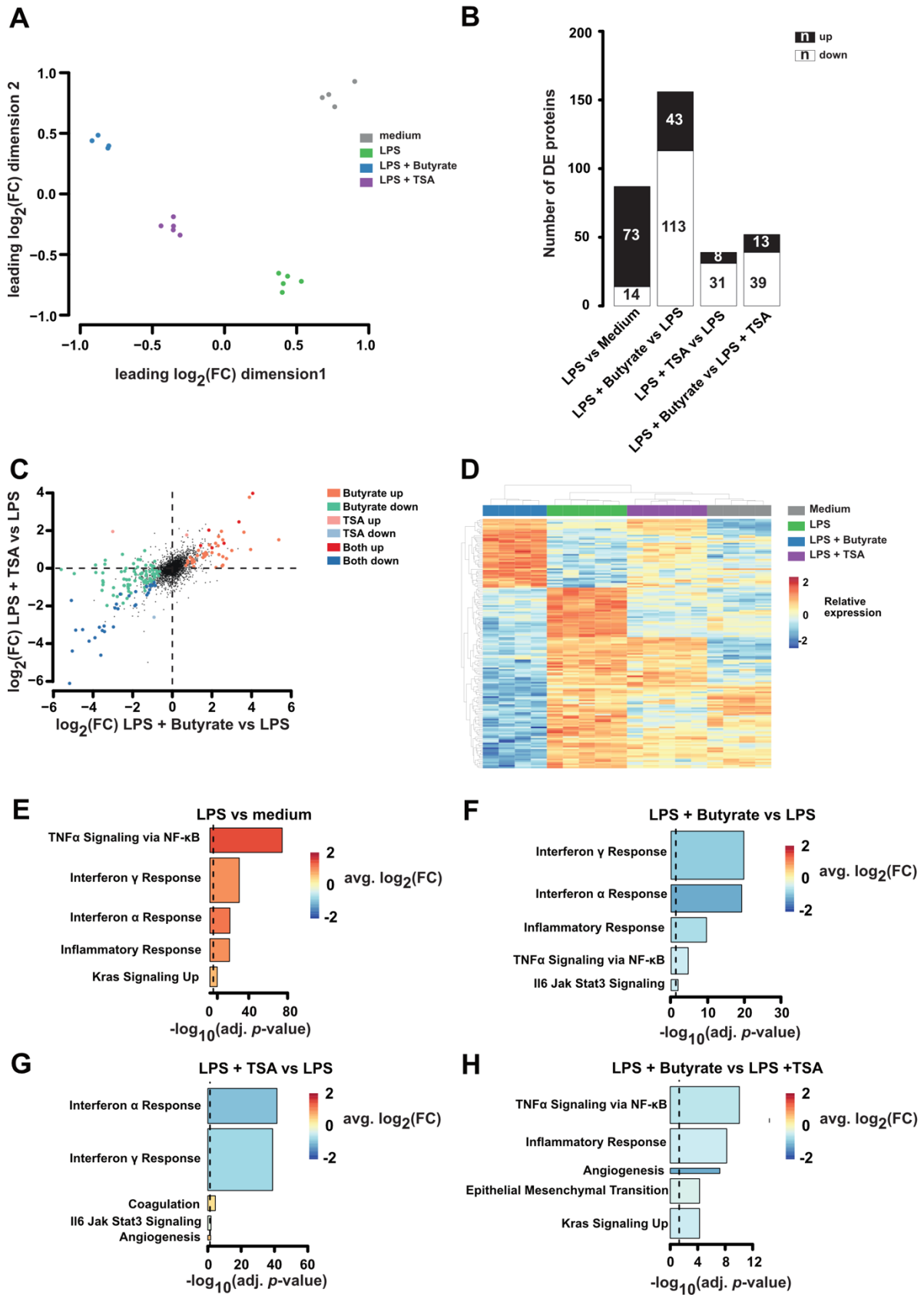


Figure 4.1.3: SCFAs regulate TLR-induced proteomics profile

GM-MDMs were treated with either LPS, LPS + butyrate, LPS +TSA or left untreated for 16 hours. Extracted protein was subjected to mass spectrometry. **(A)**: Multidimensional scaling (MDS) plot visualising the relationship between

the samples, $n = 4$ or 5 . **(B)**: Barplot depicting the number of differentially expressed (DE) proteins that significantly changed more than 1.2 fold across different comparisons. **(C)**: Comparison of $\log_2(\text{FC})$ LPS + butyrate to $\log_2(\text{FC})$ LPS + TSA. Significantly up- and down-regulated proteins are highlighted by colour. **(D)**: Heat map depicting relative expression values of proteins that were significantly changed in LPS + butyrate vs LPS comparison, scaled by row. **(E-H)**: Gene set enrichment analysis (GSEA) was performed based on the Molecular Signatures Database (MSigDB), using the hallmark gene sets. Plots show the top 5 hallmark gene sets in the following comparisons: **(E)** LPS vs medium, **(F)** LPS + butyrate vs LPS, **(G)** LPS + TSA vs LPS and **(H)** LPS + butyrate vs LPS + TSA. Bars are coloured by average $\log_2(\text{FC})$. Bar width represents the number of genes in the respective gene set. Dashed line indicates adjusted p -value threshold.

The experiment was performed in collaboration with Meera Phulphagar (Max Planck Institute of Biochemistry, Martinsried).

Data were analysed and all the figures were generated by Dr. Christina Budden (Institute of Innate Immunity, University of Bonn).

4.2 SCFAs regulate the LPS-induced cytokine secretion profile in primary human macrophages

The intestinal permeability barrier is the most important factor maintaining gut homeostasis and health. A defective mucosal barrier in inflammatory bowel disease (IBD) patients results in an increased intestinal permeability, enabling the translocation and exposition of luminal microbial products to trigger an immune response by phagocytes (Michielan and D'Incà, 2015). Previous studies have found increased concentrations of IL-1 β , IL-2, TNF- α and IL-6 in the patients with IBD, and anti-TNF- α therapy has been approved for use in Crohn's disease for almost 20 years (Brynskov et al., 1992; Neurath, 2017). In addition, The development of IBD also involves other dysregulated cytokine signaling, including IL-18, IL-10, IL-15, IL-17 and IL-23 (Sanchez-Muñoz et al., 2008). When immune cells are invaded by pathogens, cytokines, as the soluble regulatory signal, are generated and released by these cells to orchestrate the inflammatory responses (Lacy and Stow, 2011). As a major contributor to the development of the IBD, cytokines play the crucial roles in the pathogenesis of Crohn's disease and ulcerative colitis (Neurath, 2014). Among the immune cell populations mediating inflammatory responses and cytokine production, monocyte-derived macrophages (MDMs) are highly enriched in the intestine under inflammatory conditions (Italiani and Boraschi, 2014).

In my study, I focused on the effects of SCFAs on the LPS-induced cytokine profile in primary human macrophages to determine whether SCFAs play a role in the inflammatory responses through regulation of cytokine secretion.

4.2.1 SCFAs modulate the production of multiple LPS-induced cytokines

To partially mimic the leaky gut microenvironment *in vitro* and explore the effects of SCFAs on cytokines production under inflammatory conditions, rhGM-CSF-differentiated primary human MDMs (GM-MDMs) were challenged with LPS in the presence or absence of acetate,

propionate, or butyrate for 16 hours. After stimulation, a set of cytokines was then measured in the tissue culture supernatants using bead-based Luminex[®] assays.

Propionate and butyrate displayed similar and strong effects on the LPS-induced cytokines production, while the effects of acetate on the LPS-induced cytokines were mild (Figure 4.2.1). Among all the LPS-induced cytokines, the levels of the pro-inflammatory cytokines IL-1 β and interferon-inducible protein 10 (IP-10) were increased, and those of IL-7, IL-12p70, TNF- α , monocyte chemoattractant protein (MCP) and vascular endothelial growth factor (VEGF) were decreased in the propionate- and butyrate-treated samples. The concentration of the anti-inflammatory cytokine granulocyte-colony stimulating factor (G-CSF) was increased, and the levels of Interleukin 1 receptor antagonist (IL-1Ra) and IL-10 were decreased by propionate and butyrate in a dose-dependent fashion (Figure 4.2.1).

Collectively, these results demonstrate that the SCFAs propionate and butyrate have a regulatory effect on the LPS-induced cytokine secretion, indicating that SCFAs could be involved in the inflammatory response through the regulation of cytokine signaling.

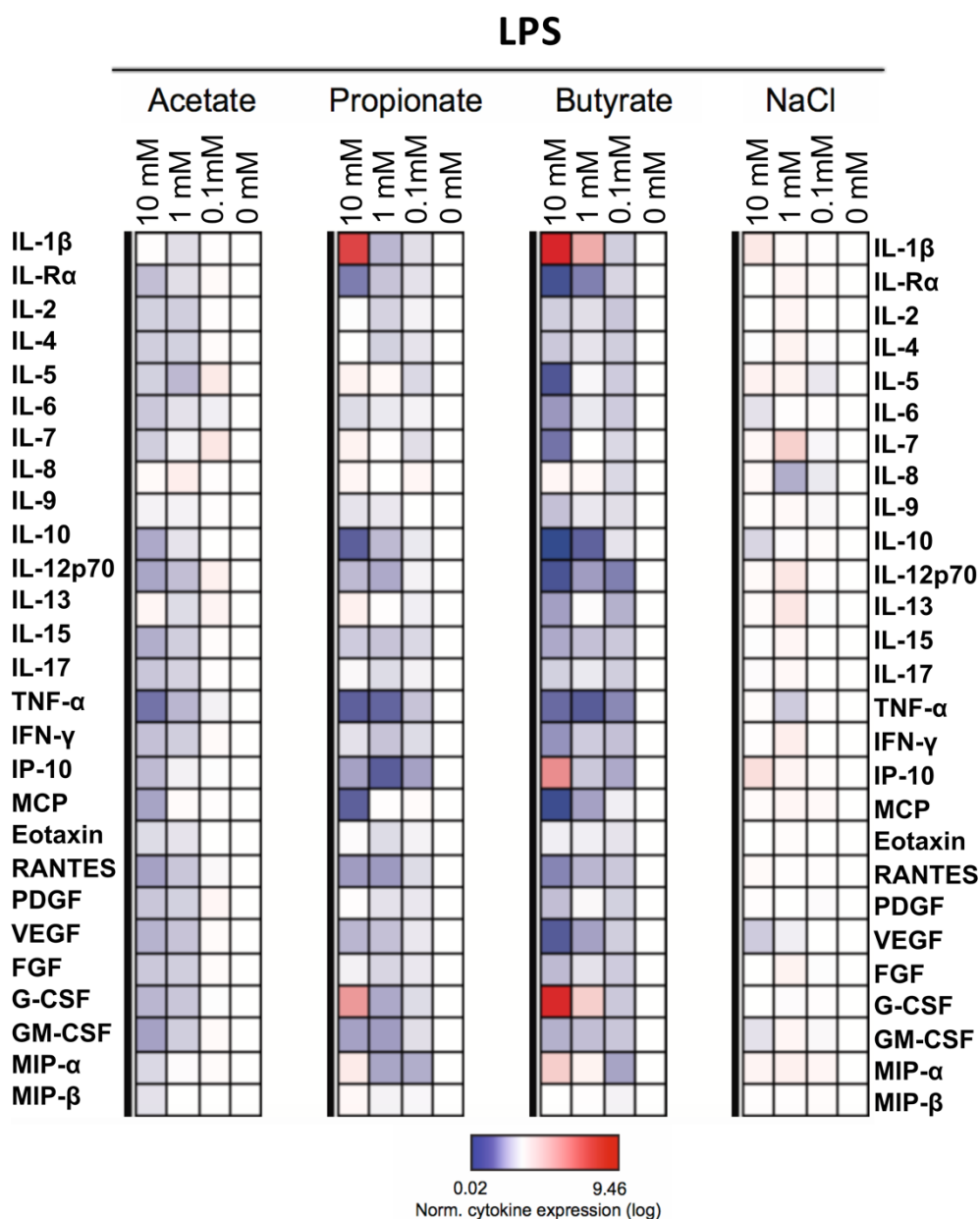


Figure 4.2.1: SCFAs regulate LPS-induced cytokines production in primary human macrophages.

GM-CSF-differentiated primary human monocytes-derived macrophages (GM-MDMs) were challenged with increasing concentrations of SCFAs or NaCl (0 mM, 0.1 mM, 1 mM, or 10 mM) in the presence of LPS (1 ng/ml) for 16 hours. Cytokines were measured from cell-free supernatants by MILLIPLEX[®] Multiplex Assay and the results were normalized to LPS only treatment. Mean value of 6 different donors are shown in logarithmic scale.

The experiment was performed and analysed by Dr. Bianca Martin. (Institute of Innate Immunity, University of Bonn).

4.2.2 Butyrate in combination with LPS induce IL-1 β secretion in macrophages but not in monocytes

As one of the most prominent cytokines in the pathogenesis of IBD, IL-1 β signaling has been extensively investigated in multiple cell types, including macrophages, intestinal epithelial cells (IECs), dendritic cells (DCs), monocytes, and neutrophils. To explore and compare the effects of SCFAs on IL-1 β secretion between different cell types, I challenged GM-MDMs and M-CSF-differentiated primary human monocyte-derived macrophages (M-MDMs), peripheral blood mononuclear cells (PBMCs), THP-1 cells ('monocyte-like'), and PMA-differentiated THP-1 cells (PMA-THP-1; 'macrophage-like') with LPS and butyrate. As a positive control, LPS-stimulated cells were treated with Nigericin, a known and widely-used NLRP3 inflammasome activator.

Interestingly, I found that butyrate triggered IL-1 β secretion in the presence of LPS in a time- and dose-dependent manner in GM-MDMs (Figure 4.2.2 A, B). Furthermore, butyrate in the presence of LPS induced IL-1 β secretion from M-MDMs in a time-dependent manner (Figure 4.2.2 C). Butyrate also elicited IL-1 β secretion from PMA-THP-1 cells both in the presence and in the absence of LPS (Figure 4.2.2 D). In contrast, butyrate had no effect on IL-1 β release in PBMCs (Figure 4.2.2 E) and THP-1 cells without the PMA differentiation (Figure 4.2.2 F). Taken together, these results demonstrate that butyrate can induce IL-1 β secretion from macrophages in the presence of LPS, but this phenotype was not observed in PBMCs and in monocyte-like cells.

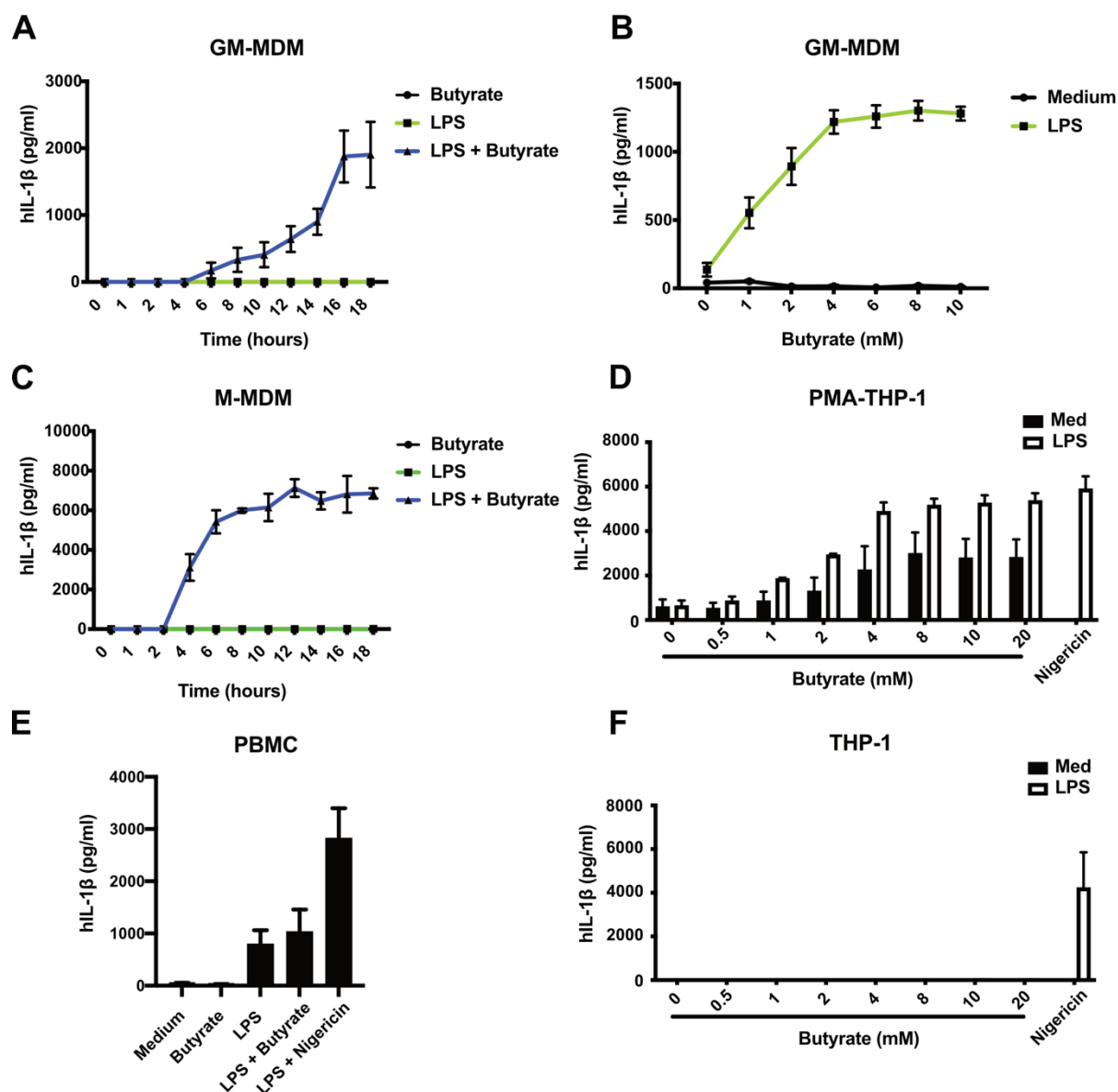


Figure 4.2.2: LPS plus butyrate elicit human macrophages, but not monocytes, to secrete IL-1 β .

(A): GM-MDMs were treated with LPS (1 ng/ml) in the presence or absence of butyrate (10 mM) for the indicated time. The levels of IL-1 β in the cell-free supernatants were measured by HTRF. (B): GM-MDMs were treated with medium or LPS (1 ng/ml) in the presence of increasing concentration of butyrate for 16 hours. The levels of IL-1 β in the cell-free supernatants were measured by HTRF. (C): M-CSF-differentiated primary human monocyte-derived macrophages (M-MDMs) were treated with LPS (1 ng/ml) in the presence or absence of butyrate (10 mM) for the indicated time. The levels of IL-1 β in the cell-free supernatants were measured by HTRF. (D): PMA-differentiated THP-1 cells were cocultured with LPS (1 ng/ml) and increasing concentration of butyrate for 16 hours, or pre-treated with LPS (1 ng/ml) for 3 hours before subsequent addition of Nigericin (10 μ M, 1.5 hours) serving as positive control. The levels of IL-1 β in the cell-free supernatants were measured by HTRF. (E): Peripheral blood mononuclear cells (PBMCs) were treated with LPS (1 ng/ml) or butyrate, alone or in combination, for 16 hours, or pre-treated with LPS (1 ng/ml) for 3 hours before subsequent addition of Nigericin (10 μ M, 1.5 hours) serving as positive control. The levels of IL-1 β in the cell-free supernatants were measured by HTRF. (F): THP-1 cells were treated with LPS (1 ng/ml) and increasing concentration of butyrate for 16 hours, or pre-treated with LPS (1 ng/ml) for 3 hours before subsequent addition of Nigericin (10 μ M, 1.5 hours) serving as positive control. The levels of IL-1 β in the cell-free supernatants were measured by HTRF. Pooled data from $n = 3$ (A, C, D, F) or 4 (B, E), each in technical duplicates, mean + SEM.

4.2.3 Butyrate induces IL-1 β release in concert with TLR activation

Having observed that butyrate could induce IL-1 β secretion in primary human macrophages in the presence of LPS, a TLR-4 ligand (Figure 4.2.2), I went on to test whether this effect is TLR-4-specific. To this end, I used the agonists of TLR1/2/6 (Pam3CSK4), TLR5 (Flagellin), and TLR7/8 (R848), to stimulate GM-MDMs in the presence or absence of butyrate. Nigericin served as positive control triggering IL-1 β release through activation of the NLRP3 inflammasome. IL-1 β was assessed in the supernatants by HTRF and western blot, respectively (Figure 4.2.3 A and B).

Butyrate dramatically increased IL-1 β secretion when co-incubated with the TLR1/2/6 agonist Pam3CSK4, the TLR4 agonist LPS, the TLR5 agonist flagellin or TLR7/8 agonist R848 (Figure 4.2.3 A, B), indicating that butyrate broadly induces IL-1 β secretion in primary human macrophages treated with various TLR ligands.

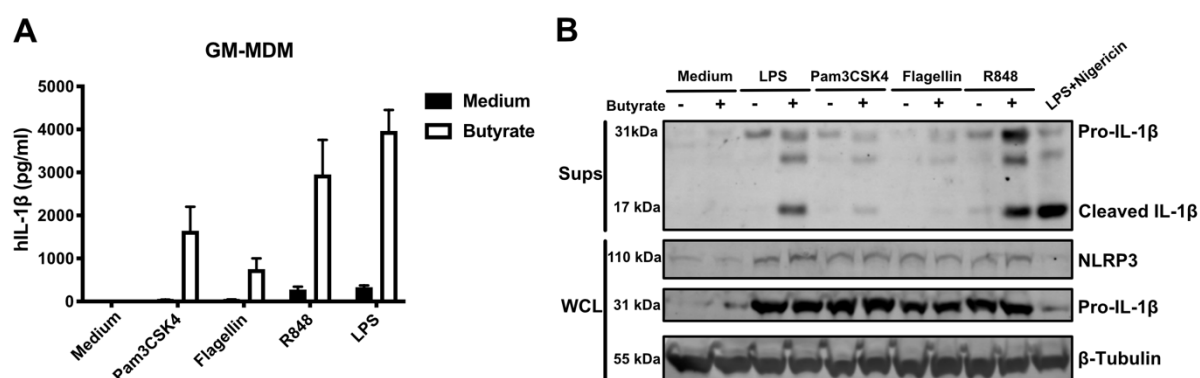


Figure 4.2.3: Butyrate in combination with TLR agonists induce IL-1 β secretion

(A-B): GM-MDMs were treated with medium or butyrate (10 mM) in the presence of agonists of TLR1/2/6 (Pam3CSK4, 10 ng/ml), TLR4 (LPS, 1 ng/ml), TLR5 (Flagellin, 500 ng/ml), and TLR7/8 (R848, 250 ng/ml) for 16 hours, or pre-treated with LPS (1 ng/ml) for 3 hours before subsequent addition of Nigericin (10 μ M, 1.5 hours) serving as positive control. **(A)** The levels of IL-1 β in the cell-free supernatants were measured by HTRF. **(B)** The levels of cleaved IL-1 β and NLRP3, pro-IL-1 β and β -Tubulin, serving as loading control, were evaluated by Western blot in the supernatants (Sups) and whole cell lysates (WCL), respectively. Pooled data from $n = 6$ (A), each in technical duplicates, mean + SEM. Blots are representative of three independent experiments.

4.2.4 LPS + butyrate induce IL-1 β secretion in a NLRP3 inflammasome-dependent manner

To date, much attention has been given to IL-1 β processing and secretion, as it is a prominent pro-inflammatory cytokine in acute and chronic inflammatory diseases (Dinarello, 2011; Lukens et al., 2012). Based on the published reports, activation of NLRP3 results in the assembly of the NLRP3 inflammasome complex, which ultimately induces caspase-1-

mediated IL-1 β processing and subsequent secretion. This response may be induced by bacterial infections and cellular damage (Próchnicki and Latz, 2017). To address whether IL-1 β release in response to LPS + butyrate is NLRP3-dependent, I pre-treated GM-MDMs with CRID3, a pharmacological inhibitor of NLRP3, or VX-765, a caspase-1 inhibitor (McKenzie et al., 2018; Wannamaker et al., 2007a), and assessed IL-1 β secretion. Pharmacological inhibition of NLRP3 and caspase-1 by CRID3 and VX-765, respectively, robustly decreased the IL-1 β secretion in response to LPS and butyrate in human GM-MDMs (Figure 4.2.4 A, B, C).

To exclude the off-target effect of these commercial inhibitors, I silenced the expression of NLRP3 with siRNA in GM-MDMs. Scrambled siRNA was used as negative control. NLRP3 siRNA efficiently silenced the expression of NLRP3 in primary human GM-MDMs (Figure 4.2.4 D), and IL-1 β secretion was completely abolished in the siRNA treated cells upon treatment with LPS + butyrate (Figure 4.2.4 E), while TNF- α secretion remained unaffected (Figure 4.2.4 F). In addition, the knockdown of NLRP3 by siRNA had no impact on the NLRC4 inflammasome-mediated IL-1 β secretion in response to NLRC4 inflammasome activator prgl, excluding the off-target effect of the NLRP3 siRNA.

The effect of SCFAs promoting the secretion of IL-1 β was previously tested in different human cell types within this work. However, whether LPS and butyrate treatment of murine bone marrow-derived macrophages (BMDMs) also promotes IL-1 β secretion was still not known. On the other hand, recapitulating the experiments in BMDMs allows for the utilisation of gene knockout mouse models, which could further provide more solid results with respect to the dependency of IL-1 β secretion triggered by LPS + butyrate on the NLRP3 inflammasome. To test this, BMDMs generated from wild type (WT), *Nlrp3*^{-/-}, *Pycard*^{-/-}, *Casp1/11*^{-/-} and *AIM2*^{-/-} were challenged with LPS and butyrate and their supernatants were analysed for the secretion of IL-1 β . Nigericin, Prgl and PolydA:dT here served as NLRP3, NLRC4 and AIM2 inflammasome mediated IL-1 β positive control, respectively. Intriguingly, I observed that LPS + butyrate strongly induced IL-1 β secretion in WT BMDMs (Figure 4.2.4 G). In the absence of NLRP3, ASC or Caspase-1/11, IL-1 β release upon treatment with LPS + butyrate was significantly reduced compared to the control WT BMDMs (Figure 4.2.4 G). However, the deficiency of AIM2 had no effect on the IL-1 β release in response to LPS plus butyrate. In all these cells TNF- α secretion was not significantly changed (Figure 4.2.4 H).

Collectively, these results demonstrated that IL-1 β induction in response to LPS + butyrate is NLRP3 inflammasome-dependent.

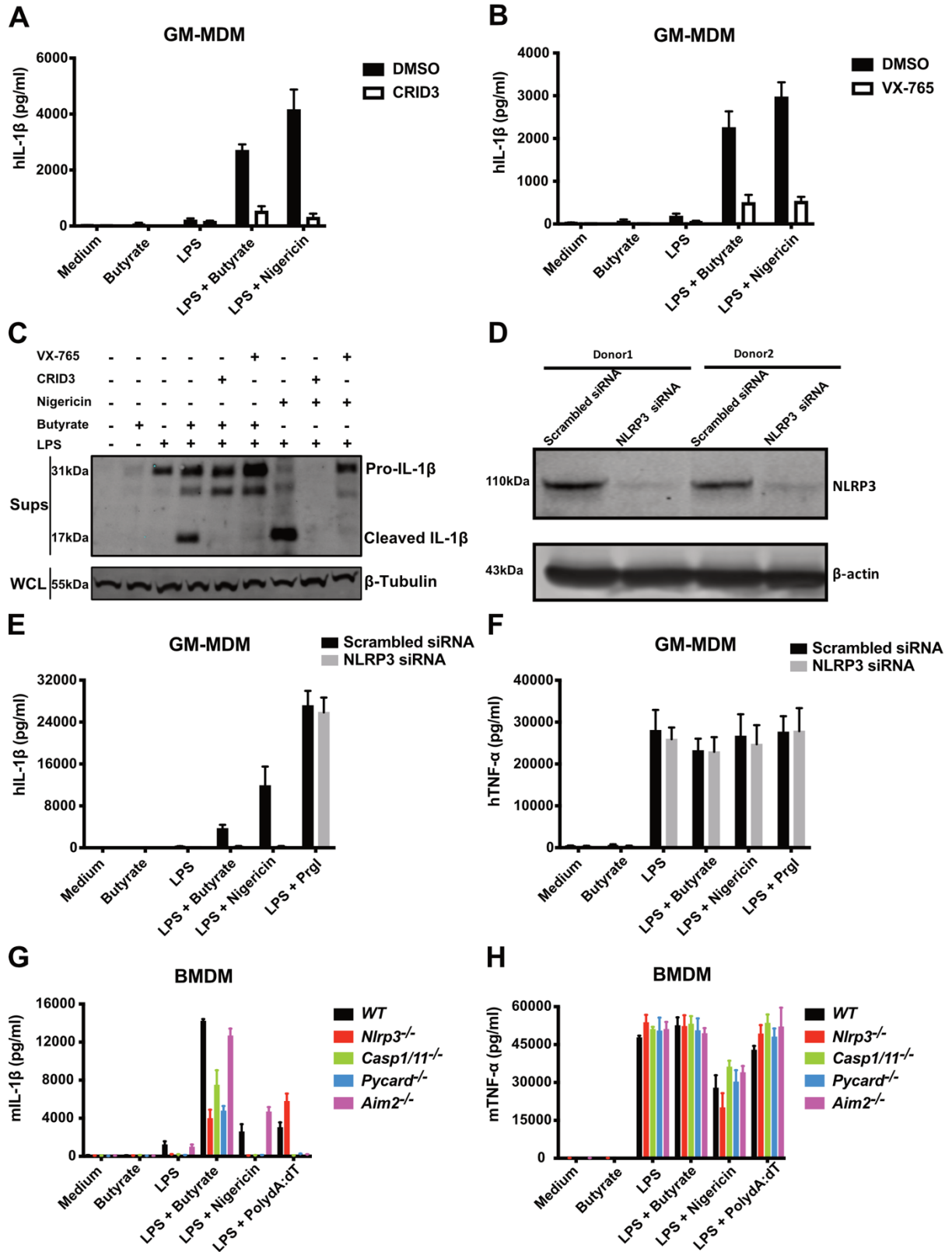


Figure 4.2.4: The IL-1 β secretion driven by LPS + butyrate is NLRP3 inflammasome-dependent.

(A-B): GM-MDMs were pre-treated with either DMSO or (A) CRID3 (2 μ M) or (B) VX-765 (40 μ M) for 0.5 hour before stimulation with medium, LPS (1 ng/ml) or butyrate (10 mM), alone or in combination, for 16 hours, or primed with LPS (1ng/ml, 3 hours) and then stimulated with CRID3 (2 μ M, 0.5 hour) or VX-765 (40 μ M, 0.5 hour) prior to the addition of the NLRP3 inflammasome activator Nigericin (10 μ M, 1.5 hours). The levels of IL-1 β in the cell-free

supernatants were measured by HTRF. **(C)**: GM-MDMs were treated as in **A** and **B**, the levels of cleaved IL-1 β and β -Tubulin, serving as loading control, were evaluated by Western blot in the supernatants (Sups) and whole cell lysates (WCL), respectively. **(D)**: GM-MDMs were electroporated with either scrambled siRNA or NLRP3 siRNA, Knock-down efficiency was quantified by the detection of NLRP3 by Western blot. **(E-F)**: GM-MDMs were electroporated with either scrambled siRNA or NLRP3 siRNA before the stimulation with medium, LPS (1 ng/ml) or butyrate (10 mM), alone or in combination, for 16 hours, or LPS (1 ng/ml, 3 hours) followed by administration of NLRP3 inflammasome activator Nigericin (10 μ M, 1.5 hours) or NLRC4 inflammasome activator PrgI (500 ng/ml) complexed with protective antigen (PA, 250 ng/ml). The levels of **(E)** IL-1 β and **(F)** TNF- α in the cell-free supernatants were measured by HTRF. **(G-H)**: BMDMs generated from WT, *Nlrp3*^{-/-}, *Pycard*^{-/-}, *Casp1/11*^{-/-} and *Aim2*^{-/-} were treated with medium, LPS (200 ng/ml) or butyrate (10 mM), alone or in combination, for 16 hours, or primed with LPS (200 ng/ml, 3 hours) prior to administration of the NLRP3 inflammasome activator Nigericin (10 μ M, 1.5 hours) or the AIM2 inflammasome activator PolydA:dT (2 μ g/ml) complexed with 0.5 μ l lipofectamine. The levels of **(G)** IL-1 β and **(H)** TNF- α in the cell-free supernatants were measured by HTRF. Pooled data from n = 3 (A, G, H) or 6 (B) or 7 (E, F), each in technical duplicates, mean + SEM. Blots are representative of three (C) or two (D) independent experiments.

4.2.5 Butyrate does not impair the priming of primary human macrophages in response to TLR activation

In macrophages, the NLRP3 inflammasome activation requires two signals, the priming signal (signal 1) and the activation signal (signal 2) (Bauernfeind et al., 2009; Duewell et al., 2010b). Priming signals can be provided by TLR activation through their respective ligands to activate the transcription factor NF- κ B, thereby leading to the expression of NLRP3 and pro-IL-1 β . A wide range of stimuli and cellular events can provide activation signals for the assembly of the NLRP3 inflammasome following the priming step, including bacterial toxins, particulate matter such as cholesterol crystals, ROS production, ATP, and K⁺ ionophores (Kelley et al., 2019). In the process of NLRP3 inflammasome activation and IL-1 β secretion driven by LPS + butyrate, LPS is expected to activate the NF- κ B pathway, leading to the expression of NLRP3 and pro-IL-1 β , but it was unclear whether butyrate acts at the level of the priming or the activating signal. To address this question, I evaluated the expression of components of the NLRP3 inflammasome at the mRNA and protein levels and the phosphorylation status of NF- κ B in human GM-MDMs treated with TLR agonists and butyrate. Butyrate treatment strongly reduced the LPS-induced expression of NLRP3 and pro-IL-1 β at mRNA level (Figure 4.2.5 A, B), whereas it did not modify the mRNA levels of caspase-1 or ASC (encoded by the gene *PYCARD*) (Figure 4.2.5 C, D). Consistently with this observation, NF- κ B phosphorylation upon activation of different TLRs was robustly decreased in the presence of butyrate (Figure 4.2.5 E). Strikingly, the inhibitory effect of butyrate on the TLR-induced NF- κ B phosphorylation and LPS-mediated upregulation of NLRP3 and pro-IL-1 β transcripts did not translate into differences at the protein levels of NLRP3 and pro-IL-1 β (Figure 4.2.5 F). Altogether, the

priming signal of NLRP3 inflammasome was not affected by butyrate in primary human macrophages.

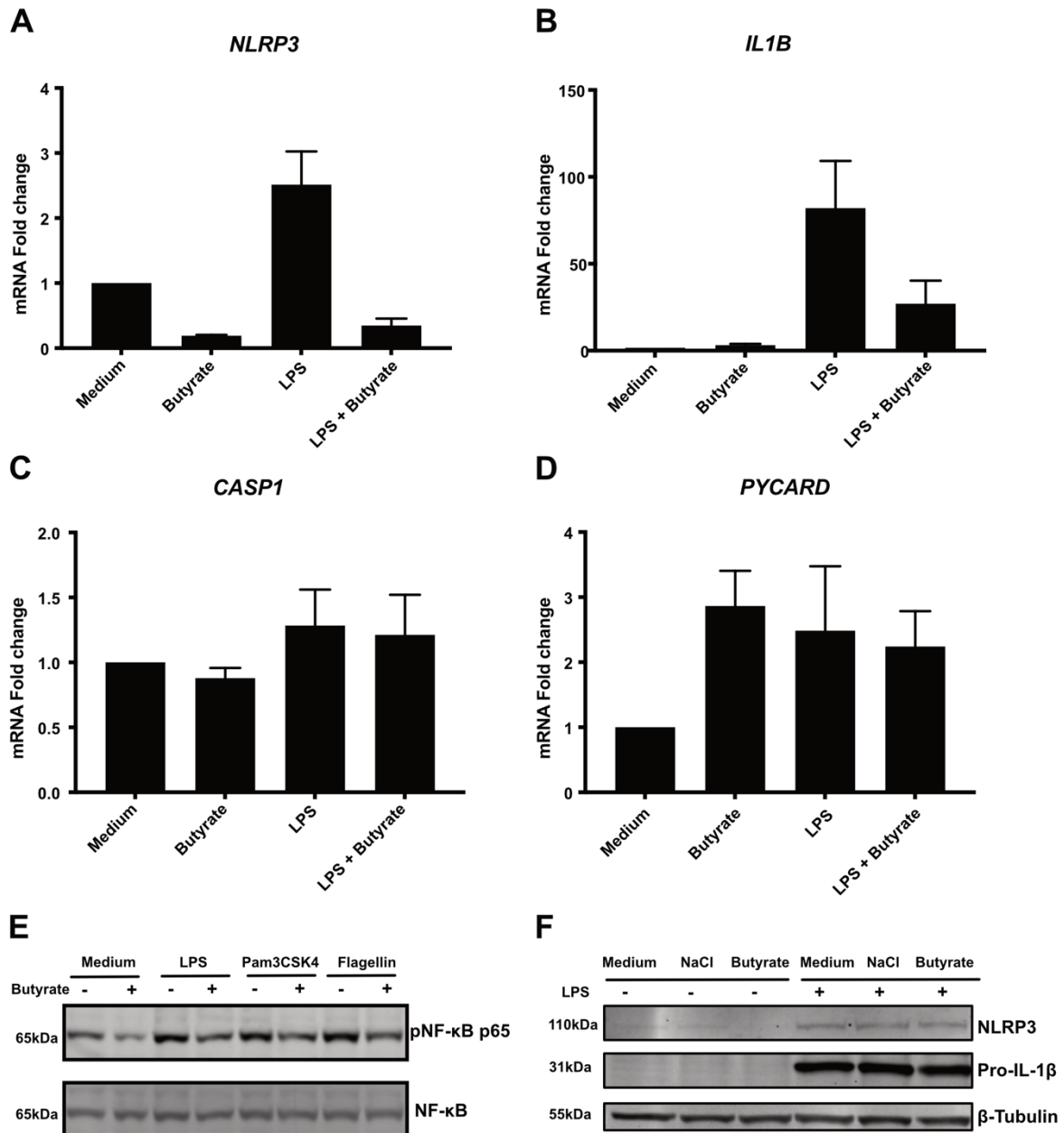


Figure 4.2.5: Butyrate has no effect on the priming signal of NLRP3 inflammasome

(A-D): GM-MDMs were treated with medium, LPS (1 ng/ml) or butyrate (10 mM), alone or in combination, for 16 hours. The mRNA levels of (A) *NLRP3*, (B) *IL1B*, (C) *CASP1*, (D) *PYCARD* were assessed by qPCR. (E): GM-MDMs were treated with Pam3CSK4 (10 ng/ml), LPS (1 ng/ml), Flagellin (500 ng/ml) with or without butyrate (10 mM) for 16 hours. The levels of phosphorylated NF-κB p65 and total NF-κB p65 were evaluated by Western blot. (F): GM-MDMs were treated with medium, NaCl (10 mM) and butyrate (10 mM) with or without LPS (1 ng/ml) for 16 hours. The levels of NLRP3, pro-IL-1β and β-Tubulin, serving as loading control, were evaluated by Western blot. Pooled data from n = 7 (A, B, C, D), each in technical duplicates, mean + SEM. Blots are representative of two (E) or three (F) independent experiments

4.2.6 LPS + butyrate drive NLRP3 inflammasome activation dependently on potassium efflux

Since butyrate did not affect the protein expression of the NLRP3 inflammasome components, I next contemplated whether butyrate could contribute to the second step of NLRP3 inflammasome activation. To test this hypothesis, I studied the role of butyrate on the production of cytosolic ROS, which has been demonstrated to be associated with the activation of NLRP3 inflammasome. Cytosolic ROS production was quantitatively assessed by the fluorogenic dye dichlorofluorescein diacetate (DCFDA) kinetically in GM-MDMs treated with increasing concentrations of butyrate. I found that butyrate treatment induced ROS production in a time- and dose-dependent manner (Figure 4.2.6 A, B). Moreover, the combination of LPS and butyrate produced higher amounts of ROS than butyrate alone, though LPS had no effect on ROS production (Figure 4.2.6 C).

To further test the involvement of butyrate-induced ROS production on the secretion of IL-1 β upon the treatment of LPS + butyrate. Cells were treated with LPS + butyrate in the presence of the ROS scavengers PDTC or Ebselen and IL-1 β levels were measured to evaluate NLRP3 inflammasome activation. The presence of PDTC and Ebselen showed no effect on the butyrate-driven IL-1 β secretion in GM-MDMs (Figure 4.2.6 D, E), suggesting that the butyrate-induced ROS are not the mediator responsible for inflammasome activation. Additionally, this result adds evidence to the controversial notion that ROS production may be dispensable for activation of the NLRP3 inflammasome (Abais et al., 2015; Cirillo et al., 2019; Li et al., 2020; Shio et al., 2015).

With accumulating reports on the mechanisms of NLRP3 inflammasome activation, a consensus has been reached that K⁺ efflux is the common event upstream of the NLRP3 inflammasome assembly in response to a number of NLRP3 agonists (Muñoz-Planillo et al., 2013). Therefore, I stimulated GM-MDMs with LPS + butyrate in culture medium containing increasing concentrations of KCl, and observed a dose-dependent reduction of IL-1 β release by increased extracellular KCl concentrations (Figure 4.2.6 F). This result indicated, similar to many other NLRP3 agonists, that the butyrate-driven NLRP3 inflammasome activation is K⁺ efflux-dependent.

Taken together, two conclusions can be drawn from the results shown in Figure 4.2.6: (1) the butyrate-induced ROS production is dispensable for the NLRP3 inflammasome activation in primary human macrophages; (2) IL-1 β secretion induced by LPS + Butyrate is K⁺ efflux-dependent.

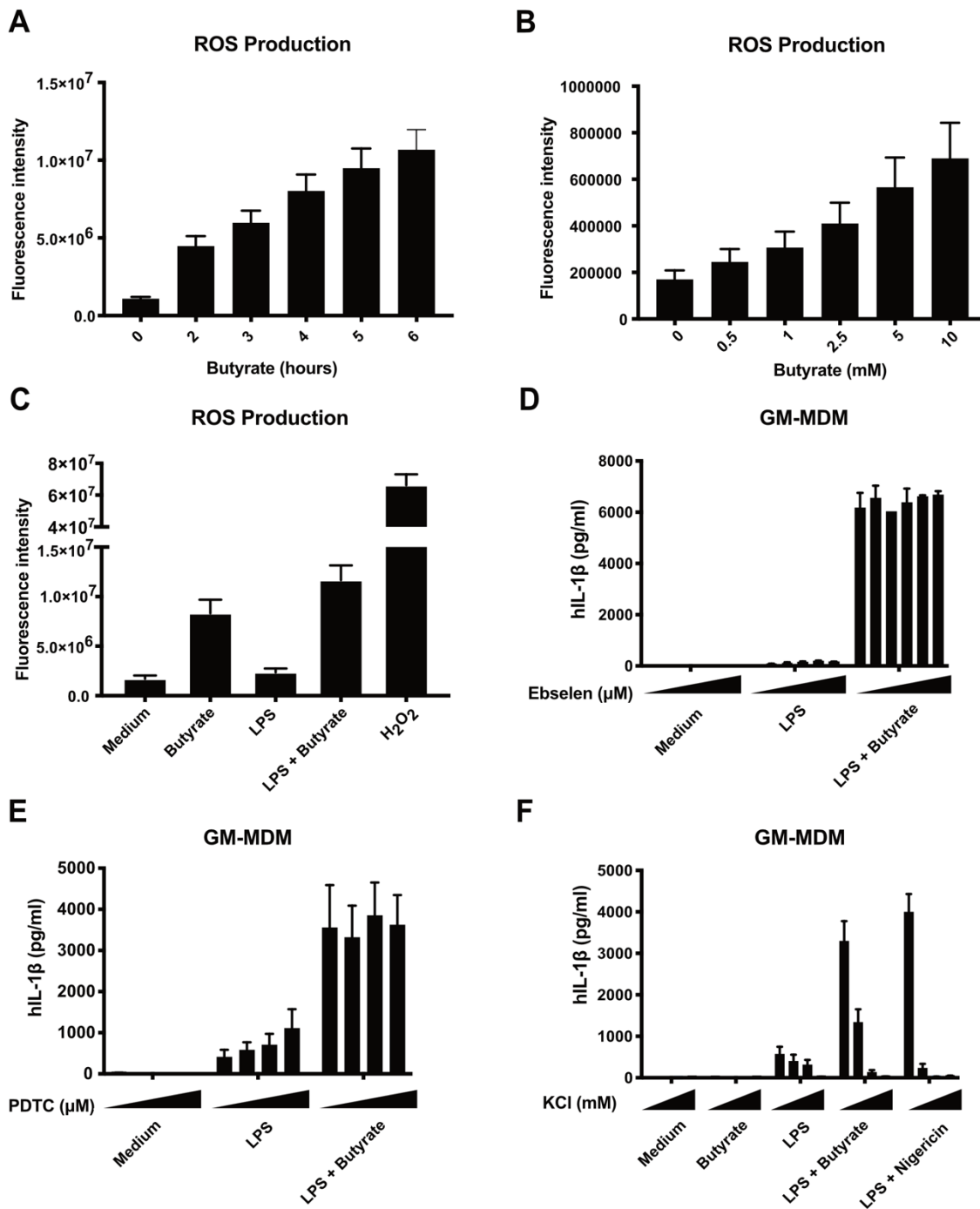


Figure 4.2.6: Butyrate drives NLRP3 inflammasome activation through potassium efflux

(A-B): GM-MDMs were incubated with the dye DCFDA (40 μ M, 45 minutes) and then washed with PBS twice prior to treatment with either (A) butyrate (10 mM) for the indicated time, or with (B) increasing concentrations of butyrate for 4 hours. The level of ROS production was quantified by the fluorescence intensity of the DCFDA dye. (C): GM-MDMs were incubated with the dye DCFDA (40 μ M, 45 minutes) and then washed with PBS twice prior to treatment with medium, LPS (1 ng/ml) or butyrate (10 mM), alone or in combination, or H₂O₂ (2 mM), serving as positive control, for 4 hours. The level of ROS production was quantified by the fluorescence intensity of the DCFDA dye. (D-E): GM-MDMs were pre-incubated with increasing concentrations of the ROS scavengers (D) Ebselen (2.5, 5, 10, 20, or 40 μ M) or (E) PDTC (5, 10, or 20 μ M) for 30 minutes before subsequent stimulation with medium, LPS (1 ng/ml) or LPS (1 ng/ml) + butyrate (10 mM) for 16 hours. The levels of IL-1 β in the cell-free supernatants were measured by HTRF. (F): GM-MDMs were treated with increasing concentrations of KCl (5, 30, 60, or 90 mM) as

indicated for 30 minutes before treatments with medium, LPS (1 ng/ml) or butyrate (10 mM), alone or in combination, for 16 hours, or with LPS (1 ng/ml, 3 hours) prior to administration of the NLRP3 inflammasome activator Nigericin (10 μ M, 1.5 hours). The levels of IL-1 β in the cell-free supernatants were measured by HTRF. Pooled data from n = 3 (A) or 4 (B, E) or 8 (F) or 9 (C), each in technical duplicates, mean + SEM, or n = 2 (D), each in technical duplicates, mean + SD.

4.2.7 LPS + butyrate trigger NLRP3 inflammasome activation but not pyroptosis and ASC speck formation

Upon NLRP3 inflammasome activation by diverse stimuli, the adaptor ASC, containing a pyrin domain (PYD) and a caspase activation and recruitment domain (CARD), can interact with NLRP3 and then assemble into helically structured filaments that forms a high-molecular weight complex termed pyroptosome. Pyroptosome provide scaffolds for the recruitment of pro-caspase-1 to form the NLRP3 inflammasome complex. In this complex, ASC oligomerization results in the formation of ASC specks, which is considered as a hallmark of the canonical inflammasome activation (Dick et al., 2016; Gaidt et al., 2016). In addition, with the formation of NLRP3 inflammasome complex, the inflammasome effector protease, pro-caspase-1, undergoes dimerization and autocatalytic processing to become converted to its active form. Active caspase-1 cleaves pro-IL-1 β into mature IL-1 β and activates the pore-forming cell death effector GSDMD, initiating a highly inflammatory lytic form of cell death named pyroptosis (Liu et al., 2016a; Shi et al., 2015; Wang et al., 2019b).

To test whether the activation of the NLRP3 inflammasome in response to LPS + butyrate could induce pyroptosis, I measured the release of LDH through a colorimetric assay and assessed the amount of the cleaved form of GSDMD in GM-MDMs by Western blot. Nigericin served as positive control for the NLRP3 inflammasome-driven LDH release and GSDMD cleavage. Surprisingly, compared to the medium alone control, no significant LDH release from LPS + butyrate-treated GM-MDMs was observed at different timepoints (0 – 18 hours), indicating the treatment with LPS + butyrate did not induce pyroptosis (Figure 4.2.7 A). Furthermore, in cells treated with LPS + butyrate I detected the 43-kDa (p43) fragment of GSDMD, but not the 30-kDa (p30) fragment of GSDMD, even though it is the p30 fragment that mediates pyroptosis in cells stimulated with LPS + nigericin (Figure 4.2.7 B) (Aglietti et al., 2016; Taabazuing et al., 2017). In contrast, the p43 GSDMD fragment is a downstream product of the activity of apoptotic caspases-3 and -7 and incapable of mediating pyroptosis (Figure 4.2.7 B) (Taabazuing et al., 2017). This observation could partially explain why there is no pyroptosis observed in GM-MDMs in response to LPS + butyrate.

Importantly, the observation that the p43 fragment of GSDMD is generated in LPS + butyrate-treated cells suggests that LPS + butyrate could induce apoptosis instead of pyroptosis. To

gain further insight into the fate of GM-MDMs treated with LPS + butyrate, cell viability was monitored kinetically for 24 hours using the Incucyte live-cell imaging system.

Unexpectedly, no significant induction of cell death was observed under any of the tested conditions, even after 24 hours, except for the positive control (nigericin-induced pyroptosis; Figure 4.2.7 C).

In addition, to determine whether the observed NLRP3 inflammasome activation induced by LPS + butyrate in human GM-MDMs co-occurred with the formation of ASC specks, I imaged and quantified the number of ASC specks in treated cells using an antibody against ASC conjugated to a fluorophore. Treatment of LPS + butyrate did not promote the formation of ASC specks (Figure 4.2.7 D), indicating that the secretion of IL-1 β in GM-MDMs occurs without pyroptosome formation (Figure 4.2.7 D).

In summary, I demonstrated that, in GM-MDMs, LPS + butyrate could activate the NLRP3 inflammasome in the absence of ASC speck formation, leading to IL-1 β secretion but not to GSDMD-driven pyroptosis or any other type of cell death.

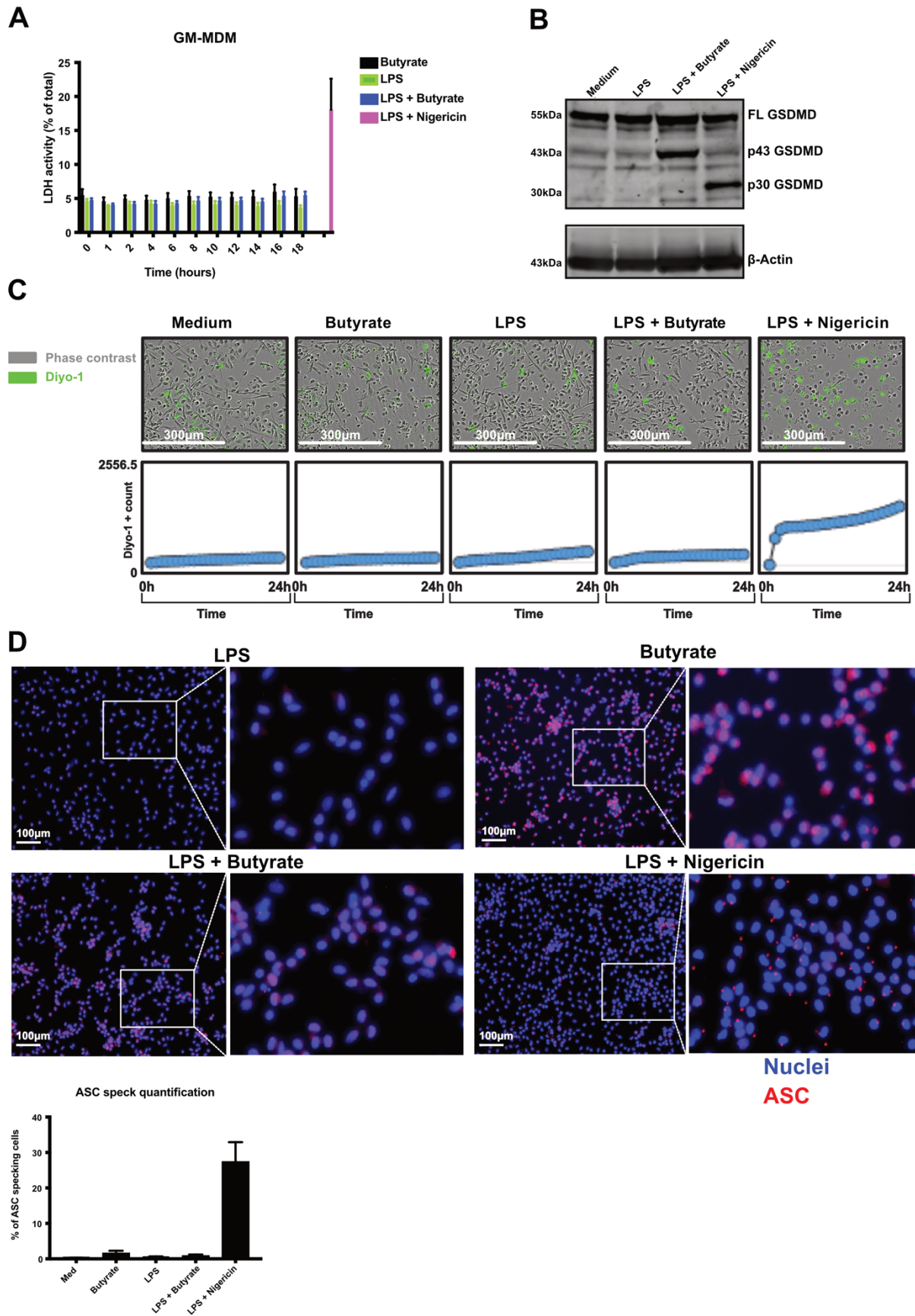


Figure 4.2.7: LPS + butyrate induce no cell death and ASC specks formation

(A): GM-MDMs were treated with butyrate (10 mM) or LPS (1 ng/ml), alone or in combination, for the indicated period of time, or primed with LPS (1 ng/ml, 3 hours) followed by the administration of the NLRP3 inflammasome activator Nigericin (10 μ M, 1.5 hours). The levels of cell death were determined by measuring LDH release. Pooled data from $n = 3$, each in technical duplicates, mean + SEM. **(B):** GM-MDMs were treated medium, LPS (1 ng/ml) or LPS (1 ng/ml) + butyrate (10 mM) for 16 hours, or primed with LPS (1 ng/ml, 3 hours) prior to subsequent administration of the NLRP3 inflammasome activator Nigericin (10 μ M, 1.5 hours). The levels of full length, cleaved form of GSDMD and β -actin, serving as loading control, were evaluated by Western blot. Blots are representative of three independent experiments. The experiments were performed by Alesja Dernst (Institute of Innate Immunity, University of Bonn). **(C):** GM-MDMs were loaded with live cell imaging dye Diyo-1 (1:10,000) before treatments with medium, LPS (1 ng/ml) or butyrate (10 mM), alone or in combination, for 24 hours, or with LPS (10 ng/ml, 3 hours) prior to the administration of Nigericin (10 μ M) serving as positive control. Cell death analysis was performed using the IncuCyte bioimaging platform, in which four images were captured per well in the appropriate fluorescent channels and phase contrast every one or two hours for 24 hours. The images shown in upper panel of (C) were captured and displayed at the time point of 24 hours. Fluorescent dye Diyo-1 count/image in 24 hours shown in the lower panel of (C) was averaged between four images/well. This was used to give average cell count/image/well, demonstrating membrane-permeabilized cells. Shown is one representative experiment out of $n = 4$ with technical duplicates. These experiments were performed in collaboration with Neil Stair (Institute for Genetics, University of Cologne). **(D):** GM-MDMs were treated with LPS (1 ng/ml) or butyrate (10 mM), alone or in combination, for 16 hours, or primed with LPS (1 ng/ml, 3 hours) followed by the administration of the NLRP3 inflammasome activator Nigericin (10 μ M, 1.5 hours). ASC specks were imaged by the Zeiss Observer.Z1 widefield fluorescence microscope and quantified by Cell Profiler 3.1.8 software, respectively. Pooled data from $n = 2$, each in technical duplicates, mean + SD. This experiment was performed with the help of Dr. Tomasz Prochnicki (Institute of Innate Immunity, University of Bonn).

4.3 Multiple mediators are involved in the induction of IL-1 β in response to LPS + butyrate in primary human macrophages

To date, SCFAs have been extensively reported to have anti-inflammatory effects in different cell types and mouse models (Ang et al., 2016; Corrêa-Oliveira et al., 2016; Kaisar et al., 2017; Silva et al., 2018; Wang et al., 2015). In contrast, few investigations suggested that SCFAs could promote inflammation through regulation of cytokine release (Jennings-Almeida et al., 2021; Singh et al., 2019). In section 4.2, I have for the first time demonstrated that butyrate co-administered with TLR ligands promotes NLRP3 inflammasome activation and IL-1 β secretion in primary human macrophages and other cell types. These results support the notion that SCFAs could also enhance inflammatory responses, possibly in a context-dependent manner.

Therefore, in this section, I would like to investigate the mechanisms controlling IL-1 β secretion driven by LPS + butyrate in primary human macrophages.

4.3.1 Butyrate inhibits the expression of cFLIP, an endogenous inhibitor of caspase-8

Cellular FLICE-inhibitory protein (cFLIP), an endogenous inhibitor of caspase-8, is essential for macrophage survival (Gordy et al., 2011; Huang et al., 2010). Several studies demonstrated that cFLIP is required for the optimal NLRP3 inflammasome activation and IL-

1 β release (Feoktistova et al., 2011; Muendlein et al., 2020). Thus, I tested the effect of butyrate on the expression of cFLIP at the mRNA and protein levels in human GM-MDMs. I observed a strong inhibitory effect of butyrate on the mRNA and protein levels of the long and short isoforms of cFLIP (encoded by *CFLAR*), cFLIP_L and cFLIP_S, both in the presence and absence of LPS (Figure 4.3.1 A-C). This suggests that cFLIP downregulation could be associated with the LPS + butyrate-driven IL-1 β secretion.

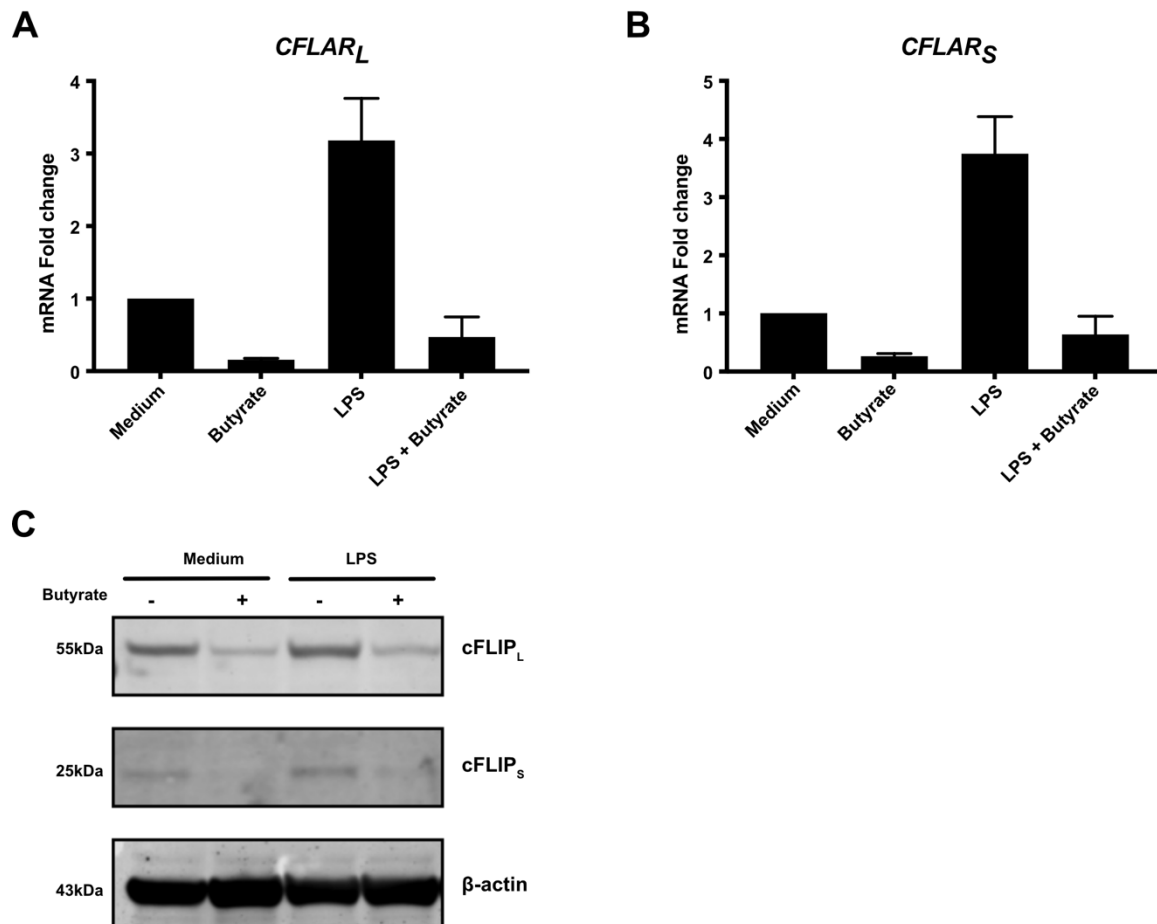


Figure 4.3.1: Butyrate inhibits the expression of cFLIP at gene and protein level

(A-C): GM-MDMs were treated with medium, butyrate (10 mM) or LPS (1 ng/ml), alone or in combination, for 16 hours. The mRNA levels of (A) *CFLAR_L*, (B) *CFLAR_S* were assessed by qPCR. The protein levels of (C) cFLIP_L, cFLIP_S and β -actin, serving as loading control, were evaluated by Western blot. (A, B) Pooled data from n = 7, each in technical duplicates, mean + SEM. (C) Blots are representative of four independent experiments. The experiments were performed with the help of Alesja Dernst (Institute of Innate Immunity, University of Bonn) and Romina Kaiser (Institute of Innate Immunity, University of Bonn).

4.3.2 LPS + butyrate induce IL-1 β secretion in a caspase-8-dependent manner

As butyrate robustly inhibited the expression of cFLIP in human GM-MDMs, I proceeded to test whether butyrate could fuel the NLRP3 inflammasome activation and the consequential IL-1 β release through caspase-8 activation by downregulating cFLIP.

So far, caspase-8 has been shown to regulate IL-1 β release through various pathways in different cell types: 1) caspase-8 modulates the expression of pro-IL-1 β via NF- κ B and is required for post-translational activation of the NLRP3 inflammasome through the interaction with caspase-1 and ASC in BMDMs. (Gurung et al., 2014; Sagulenko et al., 2013); 2) caspase-8 can directly cleave pro-IL-1 β into the mature and active form of IL-1 β in HEK293T cells infected by fungal pathogens such as *Candida albicans* and certain bacteria, for example *Mycobacterium bovis* (Moriwaki et al., 2015); 3) caspase-8 negatively regulates the NLRP3 inflammasome activation mediated by the RIPK1/RIPK3/MLKL complex in dendritic cells (DCs) (Antonopoulos et al., 2015); 4) the TRIF-RIPK1-FADD-caspase-8 axis is pivotal in the LPS-induced 'alternative' NLRP3 inflammasome activation in human monocytes (Gaidt et al., 2016). Due to the diverse and sometimes contradictory roles suggested for caspase-8 in IL-1 β release regulation, I assessed the effect of butyrate on caspase-8 activity as well as the reliance of the LPS + butyrate-driven IL-1 β release on caspase-8.

In a luminescence assay, butyrate increased caspase-8 activity when administered both alone and in combination with LPS (Figure 4.3.2 A), which is consistent with and might be resulting from the decreased expression of cFLIP (Figure 4.3.1). Moreover, pharmacological inhibition of caspase-8 by Z-IETD-FMK dramatically reduced IL-1 β release in response to LPS + butyrate in GM-MDMs (Figure 4.3.2 B, C), even though the protein expression of NLRP3 and pro-IL-1 β was not affected by Z-IETD-FMK (Figure 4.3.2 C).

To further validate the involvement of caspase-8 in the secretion of IL-1 β , I employed caspase-8-targeting siRNA to knock down caspase-8 expression in human GM-MDMs. Caspase-8 siRNA efficiently decreased the expression of caspase-8, while the scrambled and RIPK1-targeting siRNAs served as negative controls (Figure 4.3.2 D). Importantly, caspase-8 siRNA knockdown reduced the IL-1 β secretion induced by LPS + butyrate, but it did not affect the expression of NLRP3 and pro-IL-1 β or the release of TNF- α (Figure 4.3.2 D-F). In summary, I demonstrated that the induction of IL-1 β elicited by LPS + butyrate is caspase-8-dependent, but the mechanism does not rely on its proposed effect on the expression of the NLRP3 inflammasome components.

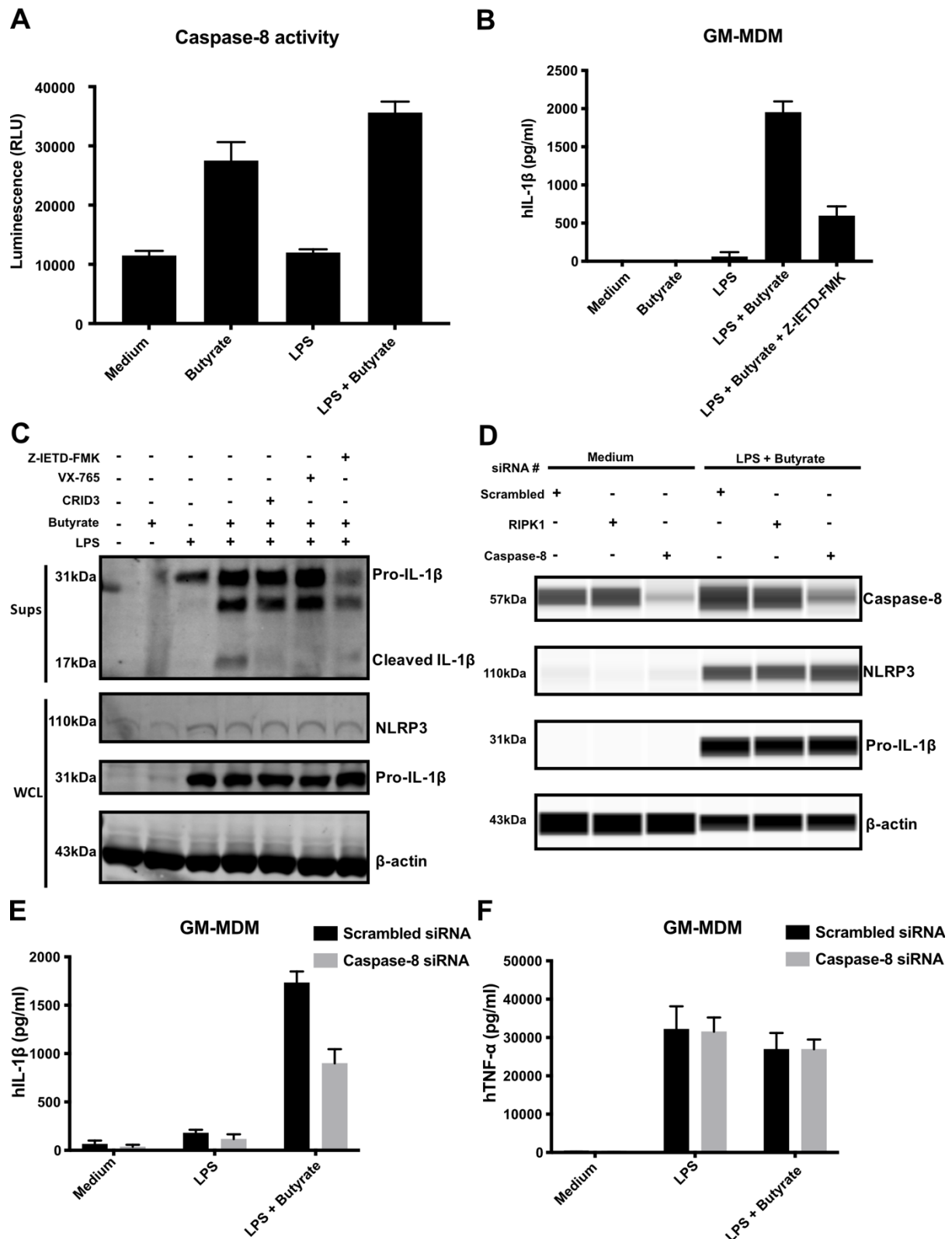


Figure 4.3.2: Caspase-8 is involved in the IL-1 β production driven by LPS + butyrate

(A): GM-MDMs were treated with medium, butyrate (10 mM) or LPS (1 ng/ml), alone or in combination, for 16 hours. The activity of the intracellular caspase-8 was assessed by using Caspase-Glo[®] assay kit. The luminescence is proportional to caspase-8 activity. (B): GM-MDMs were treated with medium, LPS (1 ng/ml) or butyrate (10 mM), alone or in combination, for 16 hours in the presence or absence of Z-IETD-FMK (5 μ M) 0.5 hour before treatment with activators. The levels of IL-1 β in the cell-free supernatants were measured by HTRF. (C): GM-MDMs were

treated with medium, LPS (1 ng/ml) or butyrate (10 mM), alone or in combination, for 16 hours in the presence or absence of CRID3 (2 μ M), VX-765 (40 μ M) or Z-IETD-FMK (5 μ M) 0.5 hour before treatment with activators. The levels of pro-IL-1 β and cleaved IL-1 β in the supernatants (Sups), and NLRP3, pro-IL-1 β and β -actin, serving as loading control, in the whole cell lysates (WCL) were evaluated by Western blot. **(D)**: GM-MDMs were electroporated with either scrambled siRNA, RIPK1 siRNA or caspase-8 siRNA before the stimulation with medium, LPS (1 ng/ml) or LPS (1 ng/ml) + butyrate (10 mM) for 16 hours. The levels of caspase-8, NLRP3, pro-IL-1 β and β -actin, serving as loading control, were evaluated by WES. **(E-F)**: GM-MDMs were electroporated with either scrambled siRNA or caspase-8 siRNA before the stimulation with medium, LPS (1 ng/ml) or LPS (1 ng/ml) + butyrate (10 mM) for 16 hours. The levels of **(E)** IL-1 β and **(F)** TNF- α in the cell-free supernatants were measured by HTRF. Pooled data from n = 2 (A), each in technical duplicates, mean + SD, or n = 3 (B) or 5 (E, F), each in technical duplicates, mean + SEM. (C, D) Blots are representative of two independent experiments.

4.3.3 RIPK3 is involved in the IL-1 β secretion induced by LPS + butyrate

RIPK3 is a serine/threonine kinase that is critical for the necroptosis-mediated inflammation. In addition, several reports demonstrated that RIPK3 is required for the NLRP3 inflammasome activation and IL-1 β secretion independent of necroptosis (Chen et al., 2018; Humphries et al., 2015; Newton, 2015). RIPK3 has also been shown to be crucial for the caspase-1- and caspase-8-mediated IL-1 β maturation in response to stimulation with LPS (Moriwaki et al., 2015).

Based on the observation that LPS + butyrate induced IL-1 β secretion without necroptosis but with the involvement of caspase-8, I examined whether the butyrate-driven IL-1 β release relies on RIPK3. siRNA knockdown of RIPK3 in primary human macrophages and RIPK3-deficient mice were employed to investigate the effect of RIPK3 ablation on the butyrate-driven IL-1 β release.

Unfortunately, all the tested RIPK3-targeting siRNAs failed to inhibit the expression of RIPK3 in human GM-MDMs (Supplementary figure 1). To circumvent this problem, BMDMs were generated from *Ripk3*^{-/-} and WT mice and, similar to the experimental setup for human cells, stimulated with LPS and/or butyrate for 16 hours. Intriguingly, the deficiency of RIPK3 drastically abolished IL-1 β secretion induced by LPS + butyrate (Figure 4.4.3 A), but the TNF- α levels were unaffected in RIPK3-deficient cells (Figure 4.4.3 B). Taken together, I concluded that RIPK3 is involved in the IL-1 β release driven by LPS + butyrate in primary murine macrophages.

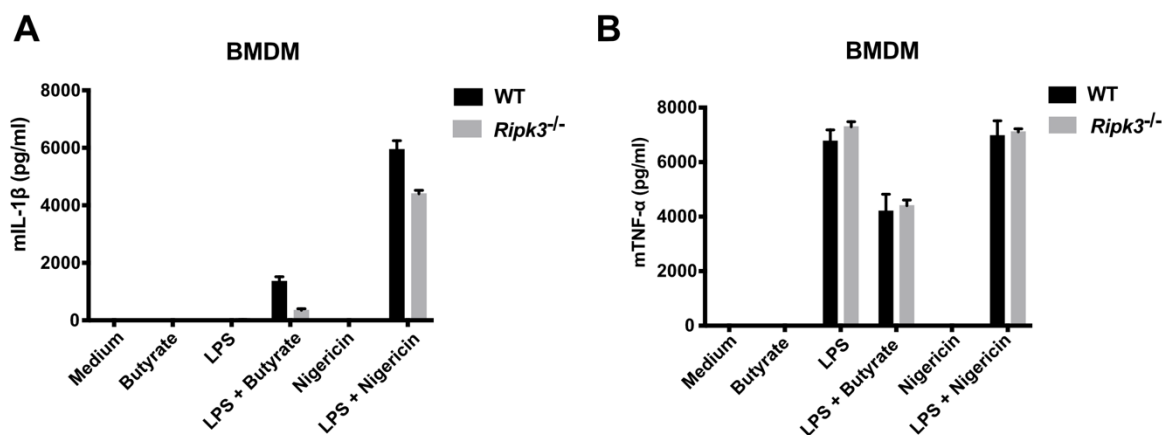


Figure 4.3.3: The IL-1 β secretion elicited by LPS + butyrate is RIPK3-dependent

(A-B): BMDMs generated from WT and *Ripk3*^{-/-} mice were treated with medium, butyrate (10 mM) or LPS (200 ng/ml), alone or in combination, for 16 hours, or left unprimed or primed with LPS (200 ng/ml, 3 hours) prior to the addition of NLRP3 inflammasome activator Nigericin (10 μ M, 1.5 hours). The levels of (A) IL-1 β and (B) TNF- α in the cell-free supernatants were measured by HTRF. Pooled data from n = 3, each in technical duplicates, mean + SEM. This experiment was performed by Debjani Biswas (Department of Medicine, University of Massachusetts Medical school) and Dr. Peter Düwell (Institute of Innate Immunity, University of Bonn).

4.3.4 RIPK1 negatively regulates IL-1 β secretion driven by LPS + butyrate

RIPK1 is an essential component of the ripoptosome (complex II) and the necrosome (see section 2.1.4). Formation of these complexes results in apoptosis or necroptosis, respectively, upon engagement of the TNF receptor 1 by TNF- α (Humphries et al., 2015). Additionally, RIPK1 was also demonstrated to drive NF- κ B-mediated cell survival and inflammatory responses (Bertrand and Vandenabeele, 2010; Kim et al., 2011). Takahashi et al. (2014) found that RIPK1 has a protective effect on intestinal epithelial cells survival by suppressing caspase-8-mediated apoptosis independently of its kinase activity (Takahashi et al., 2014a). To follow up on my previous observation that LPS + butyrate-driven IL-1 β secretion is caspase-8- and RIPK3-dependent, I further investigated the involvement of RIPK1 in this process. First, I evaluated the effect of butyrate on the protein expression of RIPK1. Secondly, I targeted RIPK1 in human GM-MDMs by siRNA as well as the RIPK1 inhibitor necrostatin1 (Nec1) to explore the function of RIPK1 in the LPS + butyrate-driven IL-1 β release.

As a result, I observed that butyrate increased the LPS-induced expression of RIPK1 at the protein level (Figure 4.3.4 A). In addition, pharmacological inhibition of RIPK1 kinase activity by Nec1 did not affect the IL-1 β or TNF- α release induced by LPS + butyrate (Figure 4.3.4 B, C). Consistent with this, RIPK1 siRNA almost completely ablated the protein expression of RIPK1 but had no effect on the protein expression of NLRP3 and pro-IL-1 β induced by LPS + butyrate (Figure 4.3.4 D), excluding the potential effect of RIPK1 on the NF- κ B signaling pathway. However, RIPK1 deficiency increased IL-1 β secretion driven by LPS alone or LPS

+ butyrate (Figure 4.3.4 E) without any apparent effect on TNF- α secretion (Figure 4.3.4 F). These observations suggested that RIPK1 could be a negative regulator of the inflammasome response to LPS + butyrate, possibly in a manner independent of its kinase activity.

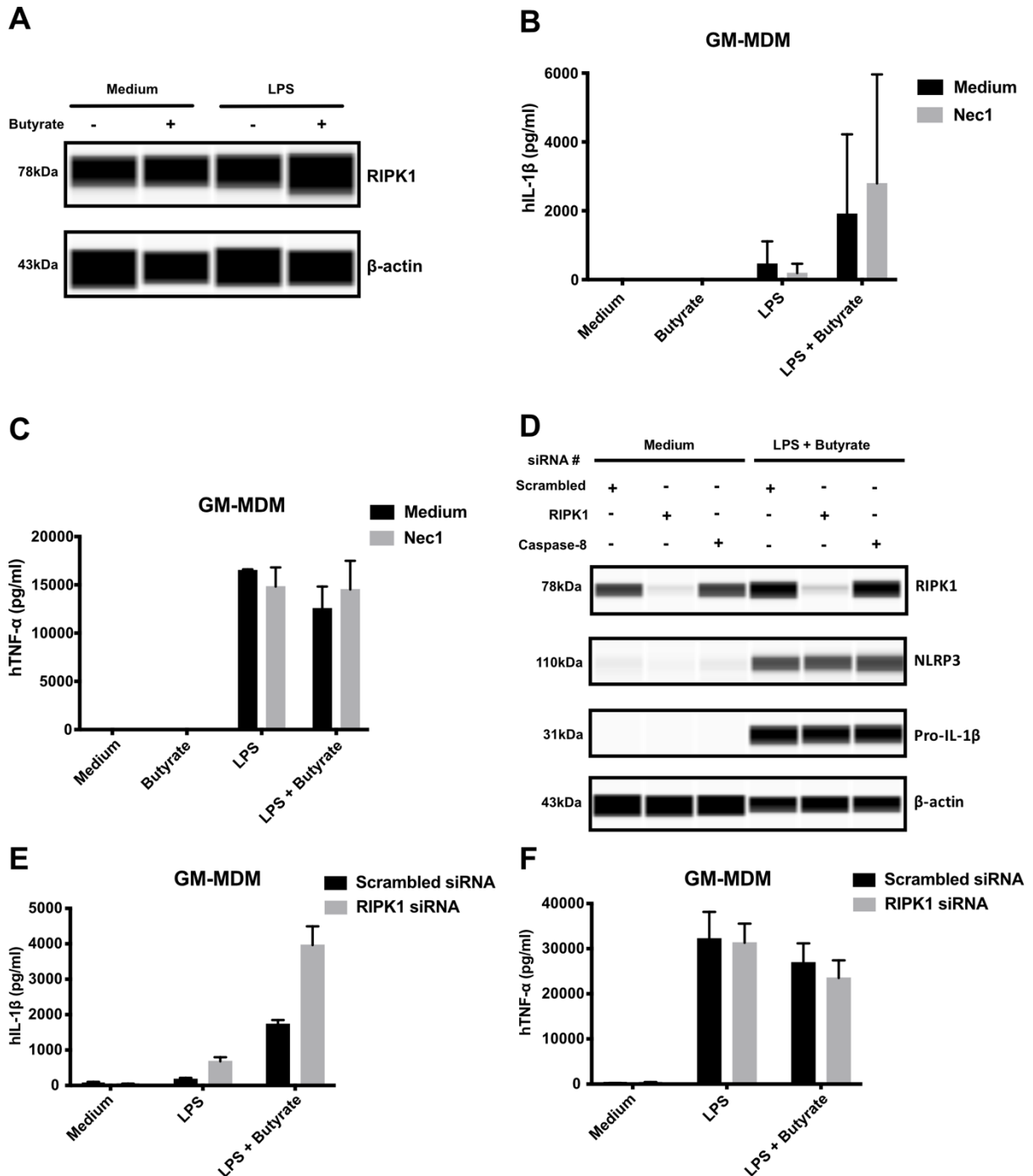


Figure 4.3.4: RIPK1 is involved in the IL-1 β induction in response to LPS + butyrate

(A): GM-MDMs were treated with medium, butyrate (10 mM) or LPS (1 ng/ml), alone or in combination, for 16 hours. The intracellular protein levels of RIPK1 and β -actin, serving as loading control, were evaluated by Western blot. (B-C): GM-MDMs were pre-incubated with medium or necrostatin1 (Nec1, 1 μ M) for 0.5 hour before treatments with medium, butyrate (10 mM) or LPS (1 ng/ml), alone or in combination, for 16 hours. The levels of (B) IL-1 β and (C) TNF- α in the cell-free supernatants were measured by HTRF. (D): GM-MDMs were electroporated with either

scrambled siRNA, RIPK1 siRNA or caspase-8 siRNA before the stimulation with medium or LPS (1 ng/ml) + butyrate (10 mM) for 16 hours. The levels of RIPK1, NLRP3, pro-IL-1 β and β -actin, serving as loading control, were evaluated by WES. **(E-F)**: GM-MDMs were electroporated with either scrambled siRNA or caspase-8 siRNA before the stimulation with medium, LPS (1 ng/ml) or LPS (1 ng/ml) + butyrate (10 mM) for 16 hours. The levels of **(E)** IL-1 β and **(F)** TNF- α in the cell-free supernatants were measured by HTRF. Pooled data from n = 3 (B, C) or 5 (E, F), each in technical duplicates, mean + SEM. (A, D) Blots are representative of two independent experiments.

4.3.5 STAT3 is a negative regulator of the IL-1 β response to LPS + butyrate

NF- κ B is considered as the central transcription factor initiating the transcription of NLRP3 and pro-IL-1 β in cells treated with TLR agonists such as LPS. In addition, members of the STAT family, such as STAT1 and STAT3, have emerged as another group of crucial transcription factors involved in NLRP3 and pro-IL-1 β regulation (Kopitar-Jerala, 2017; Labzin et al., 2016). Moreover, a growing body of evidence also shows that STAT3 could control the NLRP3 inflammasome-dependent release of IL-1 β by its regulatory effect on mitochondrial activity (Balic et al., 2020a).

To explore the involvement of STAT3 in LPS + butyrate-induced IL-1 β release, I used STAT3-targeting siRNAs to knock down STAT3 expression in human GM-MDMs. I then monitored the impact of STAT3 depletion on NLRP3 and pro-IL-1 β expression and on the LPS + butyrate-induced IL-1 β secretion. STAT3 protein levels in GM-MDMs treated with specific siRNAs targeting STAT3 were decreased at day 3 after siRNA delivery and completely ablated at day 5 (Figure 4.3.5 A). STAT3 deficiency had no significant effect on the expression of NLRP3 and pro-IL-1 β or on TNF- α secretion (Figure 4.3.5 B, C), excluding a potential effect on the priming step of the NLRP3 inflammasome activation. Interestingly, the secretion of IL-1 β in human GM-MDMs treated by LPS + butyrate was elevated when STAT3 was depleted, compared to the scrambled siRNA control (Figure 4.3.5 D). Taken together, I demonstrated that STAT3 has a negative regulatory impact on the LPS + butyrate-driven IL-1 β secretion in primary human macrophages, through a mechanism independent of priming.

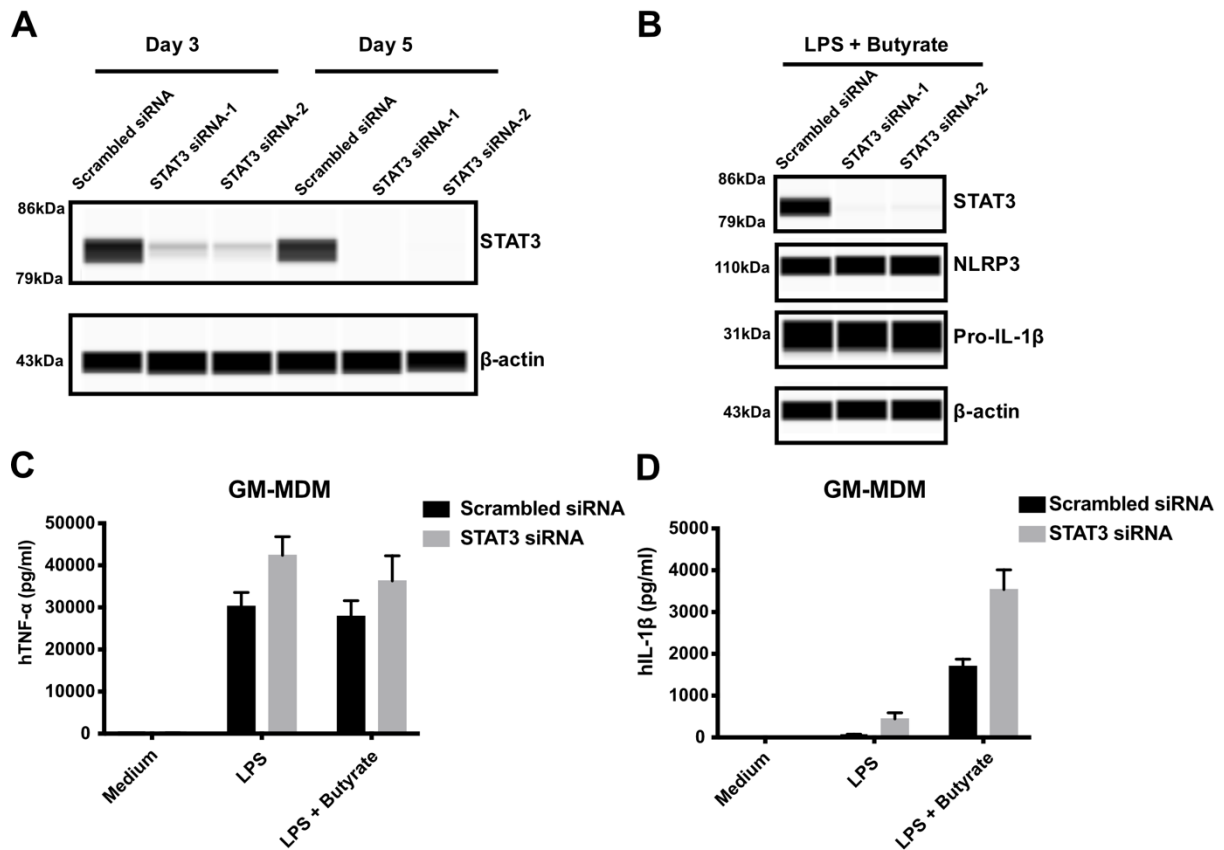


Figure 4.3.5: STAT3 exerts negative roles in the IL-1 β release driven by LPS + butyrate

(A-D): GM-MDMs were electroporated with either scrambled siRNA or STAT3 siRNA, (A) the knockdown efficiency of STAT3 was evaluated by measuring the expression of STAT3 at day 3 and day 5 after electroporation through WES, (B) the intracellular protein levels of STAT3, NLRP3, pro-IL-1 β and β -actin, serving as loading control, were evaluated by WES with the treatment of LPS (1 ng/ml) + butyrate (10 mM) for 16 hours, or the levels of (C) TNF- α and (D) IL-1 β in the cell-free supernatants were measured by HTRF with the stimulation of medium, LPS (1 ng/ml) or LPS (1 ng/ml) + butyrate (10 mM) for 16 hours. Pooled data from $n = 5$ (C, D), each in technical duplicates, mean + SEM. (A, B) Blots are representative of two independent experiments.

4.3.6 TBK1 downregulates the IL-1 β secretion driven by LPS + butyrate

Based on the RNA-Seq and proteomics data (described in section 4.1), I found that genes associated with the IFN signaling pathway were the most significantly regulated by butyrate. To fully elucidate this phenomenon, I probed the link between the IFN signaling cascade and IL-1 β secretion regulation in human GM-MDMs treated with LPS + butyrate.

Among the components of the IFN signaling pathway, TBK1-interferon regulatory factor 3 (IRF3) complex plays a crucial role in the induction of IFN- β secretion (Hu et al., 2018; Yu et al., 2012). It has also been reported that TBK1 deficiency enhanced the induction of IL-1 β in DCs (Xiao et al., 2017a) and that TBK1 could function as a suppressor of RIPK1 kinase activity (Xu et al., 2018). Given the importance of TBK1 in IFN signaling and in IL-1 β regulation, I assessed the LPS-induced TBK1 activity in the presence or absence of butyrate. I also

explored the role of TBK1 in the LPS + butyrate-driven IL-1 β secretion in human GM-MDMs using TBK1-targeting siRNA.

Interestingly, butyrate administration strongly decreased the LPS-induced TBK1 phosphorylation (Figure 4.3.6 A). Similar to the STAT3 knockdown results (Section 4.3.5), TBK1 deficiency had no effect on the NLRP3 and pro-IL-1 β expression or on TNF- α secretion (Figure 4.3.6 B, C), but it increased IL-1 β release from human GM-MDMs treated by LPS + butyrate (Figure 4.3.5 D). In summary, I found that TBK1 activity is negatively associated with IL-1 β secretion elicited by LPS + butyrate in primary human macrophages without affecting the protein levels of NLRP3 or pro-IL1 β .

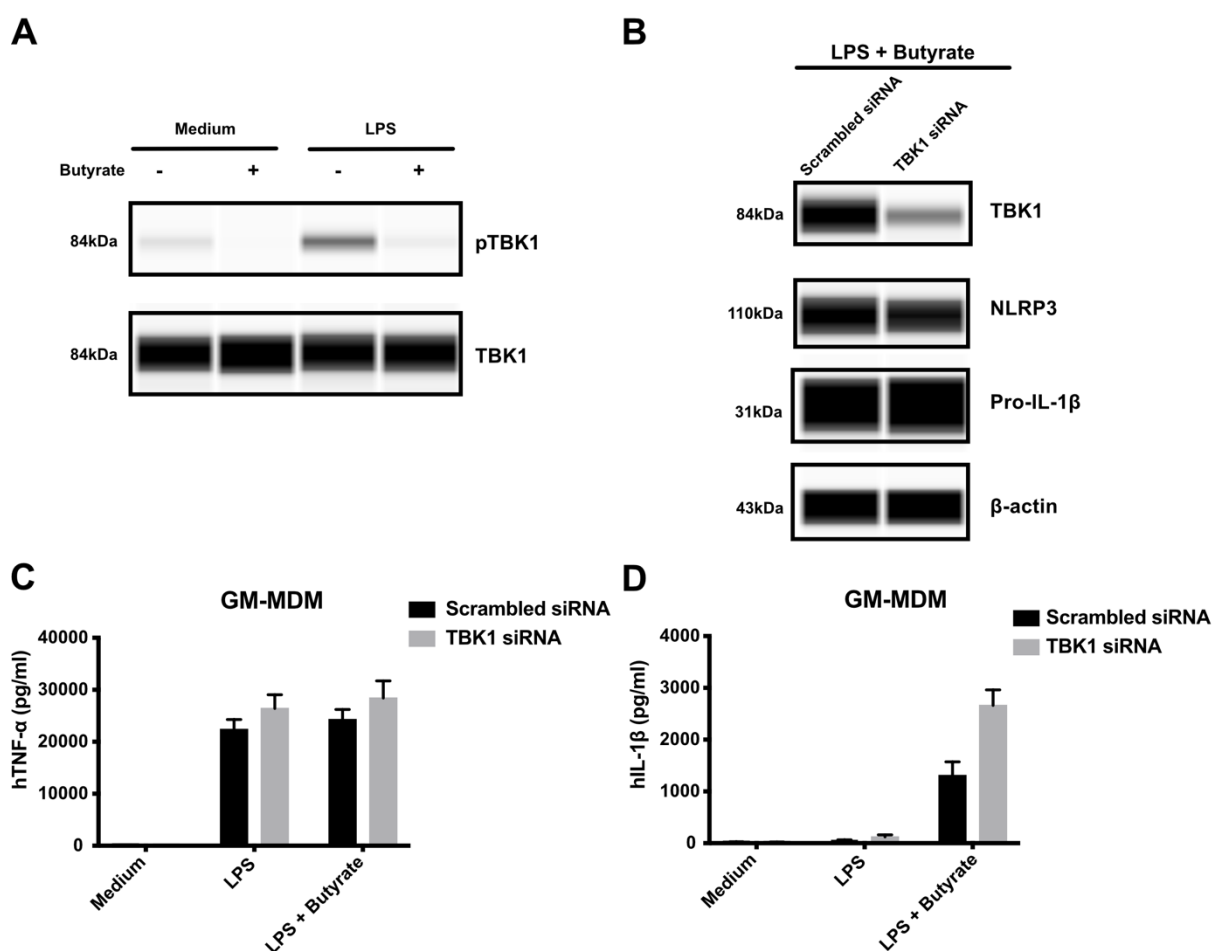


Figure 4.3.6: TBK-1 is associated with the IL-1 β secretion in response to LPS + butyrate

(A): GM-MDMs were treated with butyrate (10 mM) in the presence or absence of LPS (1 ng/ml) for 16 hours. The levels of phosphorylated TBK1 and total TBK-1 were evaluated by WES. (B): GM-MDMs were electroporated with either scrambled siRNA or TBK-1 siRNA prior to the stimulation with LPS (1 ng/ml) + butyrate (10 mM) for 16 hours. The levels of TBK-1, NLRP3, pro-IL-1 β and β -actin, serving as loading control, were evaluated by WES. (C-D): GM-MDMs were electroporated with either scrambled siRNA or TBK-1 siRNA before the stimulation with medium, LPS (1 ng/ml) or LPS (1 ng/ml) + butyrate (10 mM) for 16 hours. The levels of (C) TNF- α and (D) IL-1 β in the cell-free supernatants were measured by HTRF. Pooled data from n = 4 (C, D), each in technical duplicates, mean + SEM. (A, B) Blots are representative of three independent experiments.

4.3.7 HDAC11 modulates IL-1 β processing triggered by LPS + butyrate through the regulation of NLRP3 and pro-IL-1 β expression

SCFAs have long been known as inhibitors of histone deacetylases (HDACs). In this respect, butyrate is the most well-characterized and studied SCFA. It modifies the histone acetylation pattern and thereby regulates the expression of certain genes (Li et al., 2018; Macia et al., 2015b). Notably, emerging evidence suggests that HDAC11 is implicated in the caspase-1 independent but caspase-8 dependent maturation of IL-1 β triggered by LPS in human and murine DCs and murine macrophages (Stammler et al., 2015) .

To gain further insight into the involvement of HDAC11 in the LPS + butyrate-driven IL-1 β secretion, I knocked down HDAC11 expression in human GM-MDMs using siRNAs. Protein expression of NLRP3 and pro-IL-1 β as well as secretion of IL-1 β and TNF- α were then evaluated to assess the impact of HDAC11 silencing on the NLRP3 inflammasome-dependent IL-1 β secretion.

Both of the tested HDAC11-targeting siRNAs efficiently decreased the expression of HDAC11 in GM-MDMs (Figure 4.3.7 A). Interestingly, the siRNA-mediated HDAC11 knockdown affected the priming step of the NLRP3 inflammasome activation, as I observed the reduction in the NLRP3 and pro-IL-1 β protein expression compared to scrambled siRNA (Figure 4.3.7 B). Correspondingly, the release of IL-1 β and TNF- α induced by LPS + butyrate was also reduced, likely due to the decreased expression of NLRP3 and pro-IL-1 β associated with HDAC11 deficiency (Figure 4.3.7 C, D). Taken together, these results demonstrate that HDAC11 was able to regulate the priming step of the NLRP3 inflammasome activation, and modulate the subsequent IL-1 β maturation and processing in GM-MDMs.

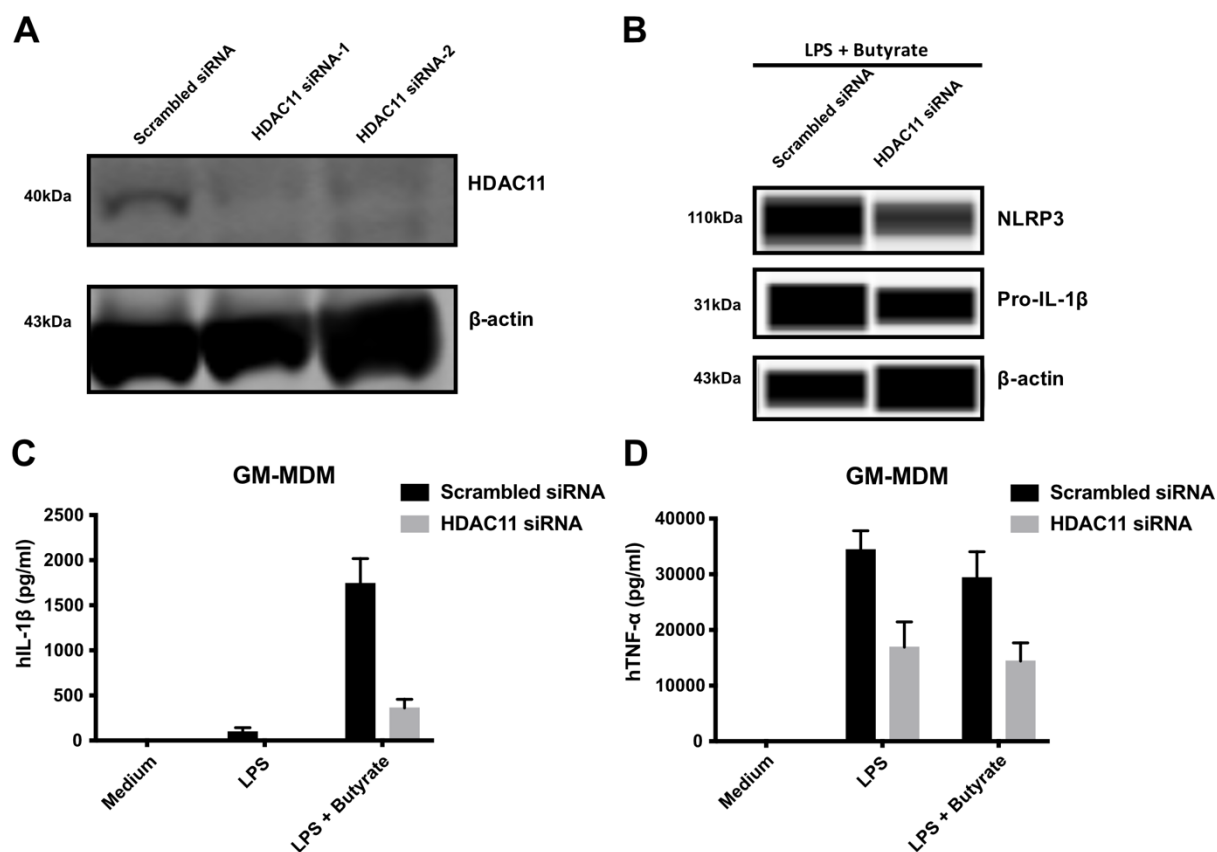


Figure 4.3.7: HDAC 11 regulates the priming signal of NLRP3 inflammasome

(A-B): GM-MDMs were electroporated with either scrambled siRNA or HDAC11 siRNA in the (A) absence or (B) presence of LPS (1 ng/ml) + butyrate (10 mM). The levels of HDAC11 and NLRP3, pro-IL-1 β and β -actin were evaluated by Western blot and WES, respectively. (C-D): GM-MDMs were electroporated with either scrambled siRNA or HDAC11 siRNA before the stimulations with medium, LPS (1 ng/ml) and LPS (1 ng/ml) + butyrate (10 mM) for 16 hours. The levels of (C) IL-1 β and (D) TNF- α in the cell-free supernatants were measured by HTRF. Pooled data from $n = 3$ (C, D), each in technical duplicates, mean + SEM. (A, B) Blots are representative of two independent experiments.

4.4 SCFAs exacerbate the inflammatory response through inhibition of the IL-10 signaling pathway

Numerous regulatory mechanisms exist to maintain immune homeostasis in response to inflammation driven by pathogen invasion and tissue damage (Dempsey et al., 2003; Drummond and Lionakis, 2019). For instance, the production of IL-10 is a well-characterized mechanism that immune cells use to counteract excessive inflammation (Kessler et al., 2017; Steen et al., 2020). The challenge with bacterial components, such as LPS, triggers the release of pro-inflammatory cytokines including TNF- α and IL-1 β . To limit the overwhelming inflammatory response driven by TNF- α and IL-1 β , the anti-inflammatory cytokine IL-10 is produced in response to LPS stimulation. IL-10 suppresses NF- κ B activity, thereby resulting in a feedback inhibition of TNF- α and pro-IL-1 β transcription (Couper et al., 2008; Yilma et al.,

2012). People deficient in IL-10 signaling suffer from early onset IBD (Shim and Seo, 2014; Yilma et al., 2012), and, correspondingly, the IL-10 receptor subunit beta-deficient (*Il10rb^{-/-}*) mouse model spontaneously develops into infant-onset IBD. These observations indicate that IL-10 signaling is vital for the intestinal homeostasis and gut health (Hurtubise et al., 2019; Jofra et al., 2019).

IL-10 is secreted and sensed by various cell types, including macrophages, DCs, and T helper cells, thus exerting a broad immunoregulatory effect. It has been demonstrated that IL-10 mainly has immune-inhibitory influence on macrophages (Ip et al., 2017). Therefore, I examined the effect of SCFAs on IL-10 signaling in primary human macrophages.

4.4.1 Butyrate inhibits TLR-induced IL-10 production in primary human macrophages

To test the impact of SCFAs on the regulation of the inflammatory response and IL-10 signaling, I first evaluated how co-stimulation with butyrate influences IL-10 secretion induced by TLR ligands in GM-MDMs, M-MDMs, or PBMCs.

I found that butyrate completely blocked the LPS-induced IL-10 production at all tested time points in both GM-MDMs and M-MDMs (Figure 4.4.1 A, B). Butyrate had a dose-dependent inhibitory effect on the LPS-induced IL-10 secretion in GM-MDMs, in which 2 mM butyrate was sufficient to fully abolish the LPS-induced release of IL-10 (Figure 4.4.1C). The LPS-driven IL-10 release in human PBMCs could also be entirely blocked by butyrate (Figure 4.4.1 D). Consistent with the impact of butyrate on the LPS-induced IL-10 secretion, butyrate also dramatically inhibited IL-10 release in response to the TLR1/2 agonist Pam3CSK4, the TLR5 ligand flagellin, and the TLR7/8 agonist R848 in both GM-MDMs and M-MDMs (Figure 4.4.1 E, F).

Taken together, these results suggest an extensive inhibitory effect of butyrate on IL-10 secretion in primary human macrophages and PBMCs.

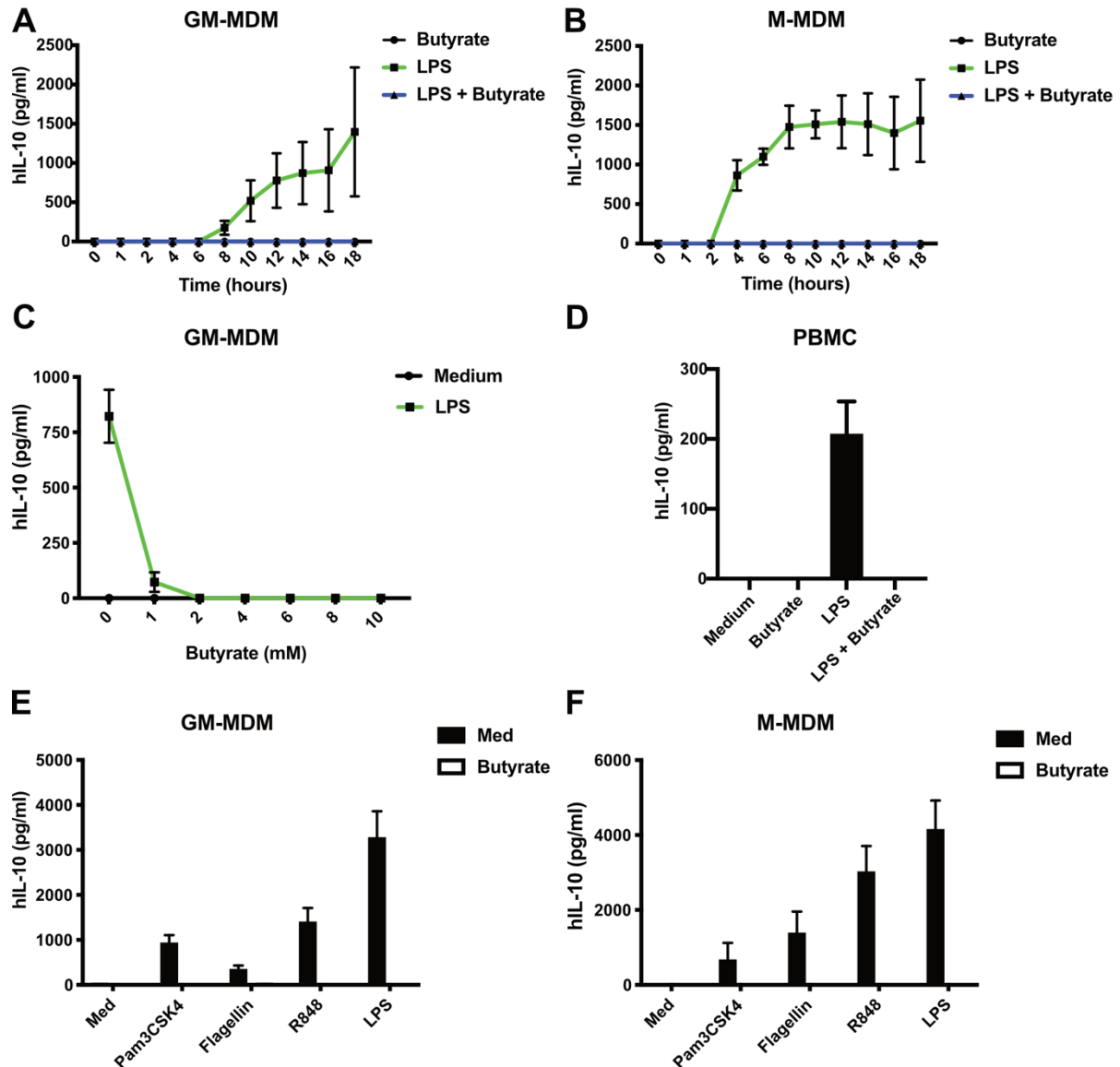


Figure 4.4.1: Butyrate inhibits TLR-induced IL-10 production

(A-B): GM-MDMs and M-MDMs were treated with butyrate (10 mM) or LPS (1 ng/ml), alone or in combination, for the indicated period of time. The levels of IL-10 in the cell-free supernatants were measured by HTRF. (C): GM-MDMs were treated with medium or LPS (1 ng/ml) in the presence of increasing concentration of butyrate for 16 hours. The levels of IL-10 in the cell-free supernatants were measured by HTRF. (D): PBMCs were treated with medium or butyrate (10 mM) in the presence or absence of LPS (1 ng/ml) for 16 hours. The levels of IL-10 in the cell-free supernatants were measured by HTRF. (E-F): (E) GM-MDMs and (F) M-MDMs were treated with medium or butyrate (10 mM) in the presence of agonists of TLR1/2/6 (Pam3CSK4, 10 ng/ml), TLR4 (LPS, 1 ng/ml), TLR5 (Flagellin, 500 ng/ml), or TLR7/8 (R848, 250 ng/ml) for 16 hours. The levels of IL-10 in the cell-free supernatants were measured by HTRF. Pooled data from $n = 3$ (A, B, C, F) or 4 (D) or 6 (E), each in technical duplicates, mean + SEM.

4.4.2 Butyrate regulates STAT3 activity through IL-10 suppression

As one of the most important targets downstream of IL-10 receptor activation, STAT3 is crucial for the IL-10-mediated anti-inflammatory response. This effect relies on a direct or indirect

transcriptional gene regulation in immune cells, especially in macrophages and DCs. (Melillo et al., 2010; Öztürk Akcora et al., 2020).

In response to IL-10 recognition, STAT3 is phosphorylated at residue Tyr705 (Y705) and translocates from the cytosol to the nucleus to function as transcription factor (Darnell et al., 1994; Ihle, 1995). In addition, emerging evidence demonstrates that STAT3 could also translocate into the mitochondria after being phosphorylated at the Ser727 residue (the so-called mito-STAT3; phospho-S727), leading to the regulation of the mitochondrial electron transport chain (ETC), ATP and ROS production (Balic et al., 2020a; Yang and Rincon, 2016). To briefly explore the impact of SCFAs on STAT3 activity, I assessed the phosphorylation of STAT3 at the Y705 and S727 residues in response to TLR agonists with or without butyrate in human GM-MDMs. Interestingly, I found that engagement of TLRs potently induced the phosphorylation of STAT3 at the Y705 and S727 residues (Figure 4.4.2 A-C), which was completely abolished by butyrate (Figure 4.4.2 B, C).

To gain further insight into the involvement of IL-10 in the LPS-induced STAT3 phosphorylation at the Y705 and S727 residues, recombinant human IL-10 (rhIL-10) was employed to compensate for the loss of LPS-induced IL-10 associated with butyrate co-stimulation. In the presence of LPS + butyrate, rhIL-10 robustly restored the phosphorylation of STAT3 at the Y705 and S727 residues (Figure 4.4.2 B, C), suggesting that butyrate suppressed the LPS-induced phosphorylation at the Y705 and S727 residues through inhibition of IL-10 signaling. rhIL-10 and rhIL-6 served as positive control for the phosphorylation of STAT3 at the Y705 and S727 residues respectively (Figure 4.4.2 B, C).

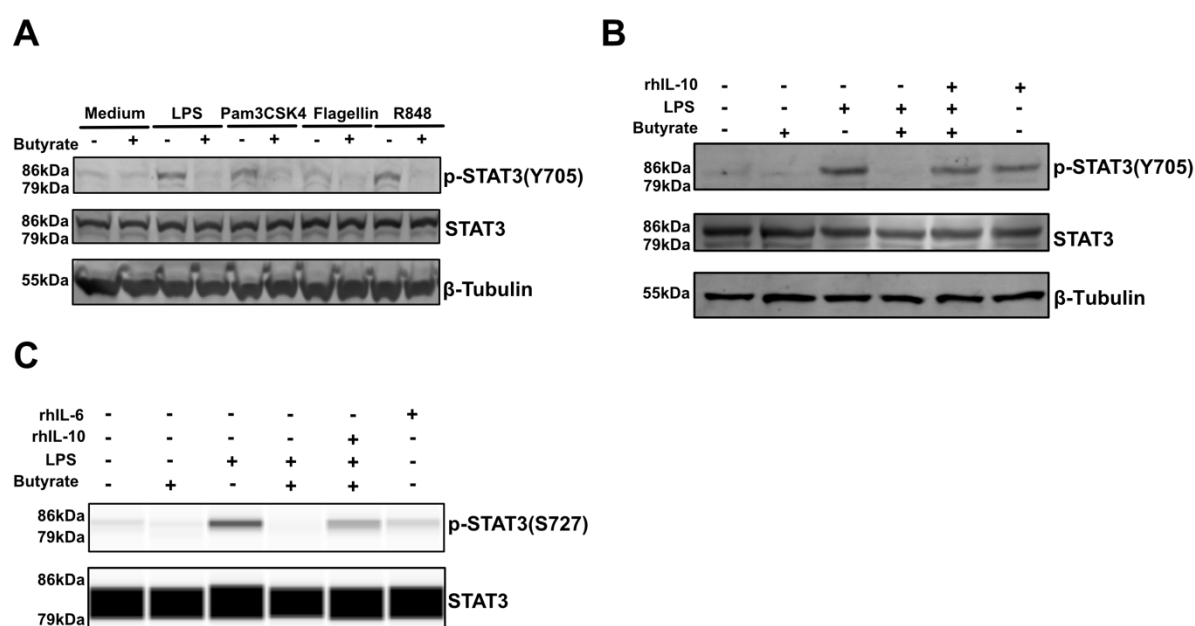


Figure 4.4.2: Butyrate inhibits STAT3 activity with the engagement of IL-10

(A): GM-MDMs were treated with medium or butyrate (10 mM) in the presence of agonists of TLR1/2/6 (Pam3CSK4, 10 ng/ml), TLR4 (LPS, 1 ng/ml), TLR5 (Flagellin, 500 ng/ml), or TLR7/8 (R848, 250 ng/ml) for 16 hours. The levels

of phosphorylated STAT3, total STAT3 and β -Tubulin, serving as loading control, were evaluated by Western blot. **(B-C)**: GM-MDMs were pre-treated with rhIL-6 (100 ng/ml, 0.5 hour) or rhIL-10 (100 ng/ml, 0.5 hour) before subsequent treatments with medium, LPS (1 ng/ml) or butyrate (10 mM), alone or in combination, for 16 hours. The levels of **(B)** phosphorylated STAT3(Y705), total STAT3 and β -Tubulin, and **(C)** phosphorylated STAT3(S727) and total STAT3 were evaluated by Western blot and WES, respectively. Blots are representative of (A) two or (B, C) three independent experiments.

4.4.3 Butyrate inhibits phosphorylation of STAT1 and p38 independently of IL-10

In conjunction with the IL-10 induced activation of STAT3, STAT1 is activated as well. These proteins can form either homodimers (STAT1/STAT1 and STAT3/STAT3) or a STAT1/STAT3 heterodimer, resulting in specific gene regulatory outcomes (Kontoyiannis et al., 2001; Mukhopadhyay et al., 2020). Whether STAT1 plays a role downstream or upstream of IL-10 signaling is still unclear (Karaghiosoff et al., 2000; Shaw et al., 2006a; Wilbers et al., 2017a). The p38 mitogen-activated protein kinases are another prominent component of the IL-10 signaling pathway and they are important for IL-10 to execute its anti-inflammatory functions. Kontoyiannis et al. demonstrated in 2001 that IL-10 could inhibit TNF- α expression in a mechanism dependent on p38 (Kontoyiannis et al., 2001). Moreover, p38 has been shown to be involved in the IL-10-induced heme oxygenase-1 (HO-1) expression, contributing to the protection against oxidative stress, apoptosis and inflammation (Lee and Chau, 2002; Tai et al., 2009; Wilbers et al., 2017a). On the other hand, p38 is also involved in the induction of IL-10 in response to viral and bacterial infections in monocytes and macrophages (Hou et al., 2012; Ma et al., 2001a). To investigate how butyrate impacts on the p38 and STAT1 modules of IL-10 signaling, I evaluated the activation of p38 and STAT1 by measuring their respective phosphorylation in human GM-MDMs in response to LPS + butyrate with or without addition of rhIL-10. Butyrate dramatically suppressed the LPS-induced p38 and STAT1 phosphorylation (Figure 4.4.3 A), but the addition of rhIL-10 did not reverse the reduction of the p38 and STAT1 phosphorylation. These observations indicate that butyrate can dramatically suppress the LPS-induced p38 and STAT1 phosphorylation, through a mechanism independent of the butyrate-mediated IL-10 suppression. Thus, SCFAs may exert and amplify pro-inflammatory responses in primary human macrophages by the regulation of p38 and STAT1 (Figure 4.4.3 B).

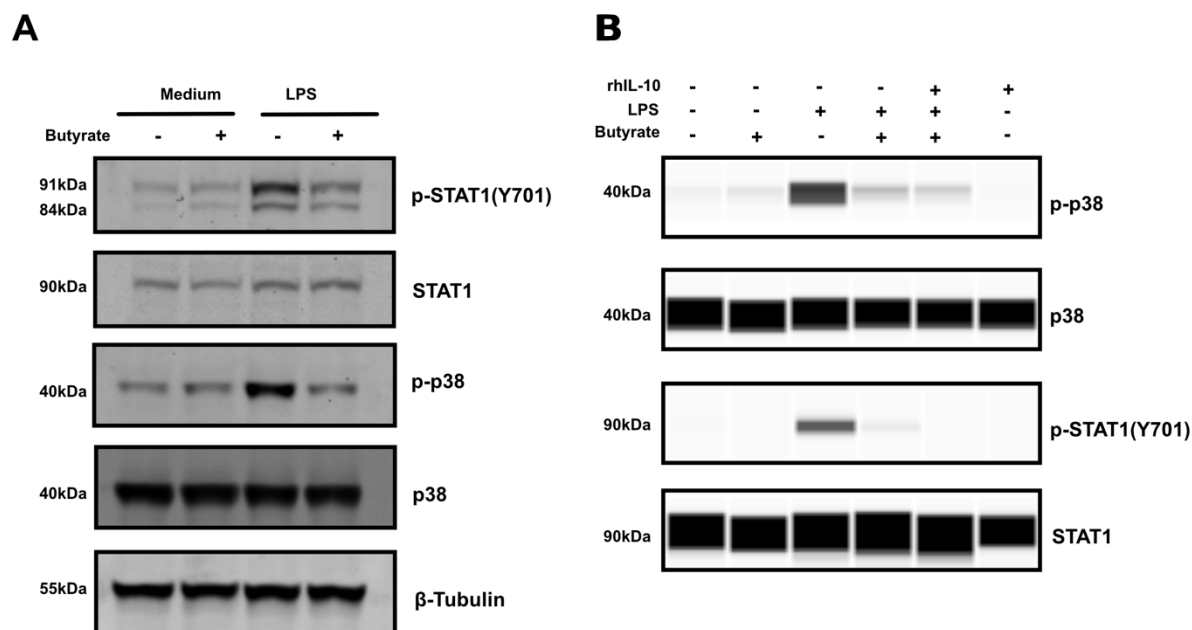


Figure 4.4.3: Butyrate suppresses the activity of STAT1 and p38

(A): GM-MDMs were treated with medium or LPS (1 ng/ml) in the presence or absence of butyrate (10 mM) for 16 hours. The phosphorylated STAT1(Y701) and p38, total STAT1 and p38 and β -Tubulin, serving as loading control, were evaluated by Western blot. (B): GM-MDMs were treated with rhIL-10 (100 ng/ml, 0.5 hour) before subsequent treatments with medium, LPS (1 ng/ml) or butyrate (10 mM), alone or in combination, for 16 hours. The levels of phosphorylated STAT1(Y701) and p38 and total STAT3 and p38 were evaluated by WES. Blots are representative of two independent experiments.

4.4.4 Butyrate modulates the Akt-mTOR signaling network

In addition to the well-characterized immunosuppressive functions of IL-10, several groups reported that IL-10 could also regulate diverse cellular processes, including cell survival, proliferation and metabolism, through the Akt-mTOR signaling network. Medzhitov and co-workers found that IL-10 could suppress mTOR activity by the up-regulation of DNA damage inducible transcript 4 (DDIT4), an mTOR inhibitor, which maintains the cellular homeostasis through eliminating the damaged mitochondria (Ip et al., 2017).

To determine the impact of butyrate on the IL-10-regulated Akt-mTOR signaling network, I used a magnetic bead-based multiplex phosphoprotein assay to screen the activity of the Akt-mTOR signaling cascades components in human GM-MDMs. Insulin-like growth factor-1 (IGF-1) and insulin served as positive controls as they were reported to activate the Akt-mTOR signaling (Haar et al., 2007; Latres et al., 2005; Nepstad et al., 2019). I observed that LPS + butyrate did not have any effect on the phosphorylation of Akt, mTOR, the insulin receptor (IR), insulin receptor substrate 1 (IRS-1), phosphatase or tensin homolog (PTEN), and tuberous sclerosis complex 2 (TSC2) (Figure 4.4.4 A-F). However, butyrate reduced the

baseline phosphorylation levels of two isoforms of glycogen synthase kinase 3 (GSK-3), GSK-3 α and GSK-3 β , and of ribosomal protein S6 (RPS6) (Figure 4.4.4 G-I). Collectively, I found that butyrate controls the activity of some of the downstream effectors of the Akt-mTOR signaling network.

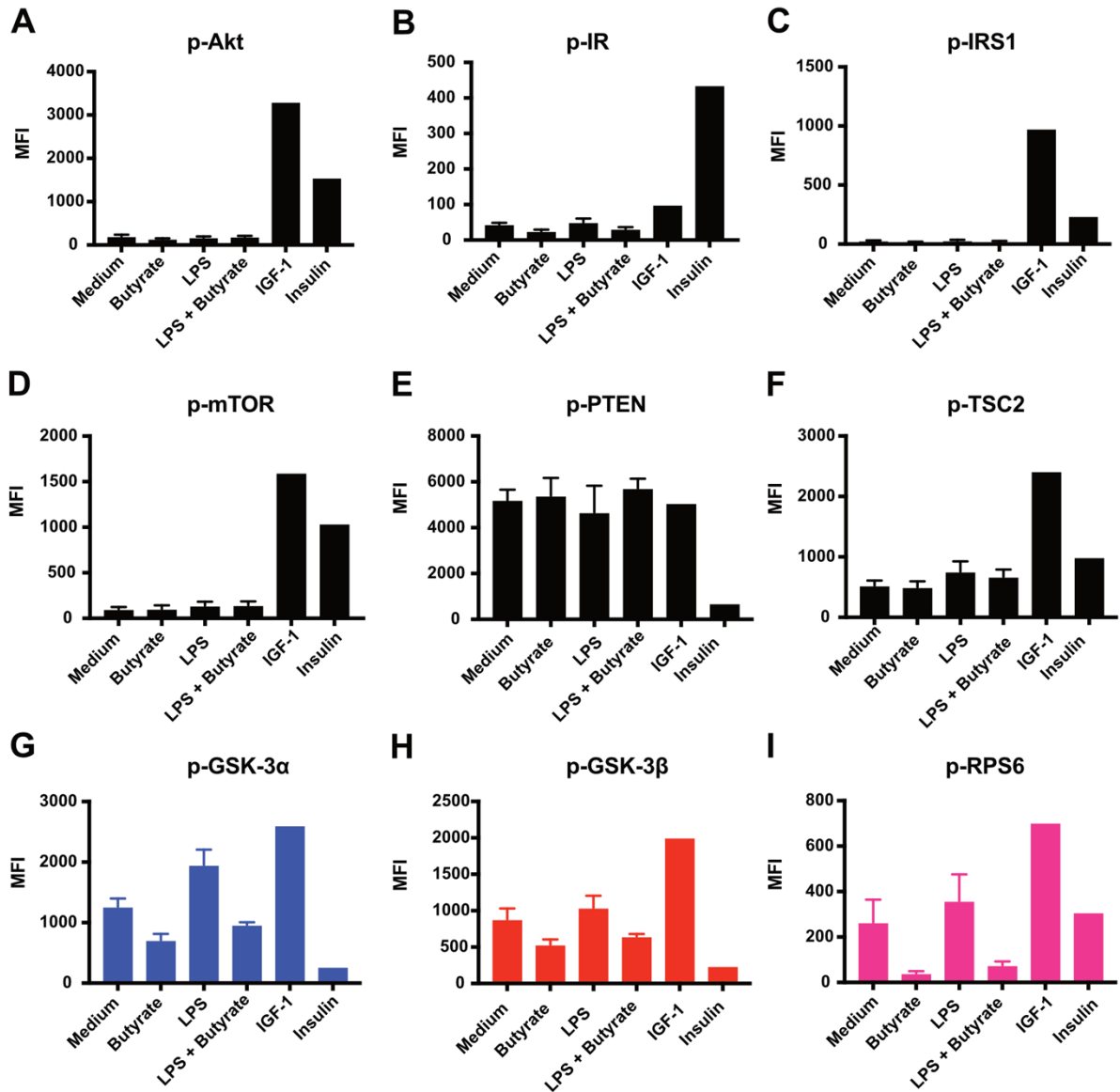


Figure 4.4.4: Butyrate regulates the phosphorylation of GSK-3 α/β and RPS6

A-I: GM-MDMs were treated with medium or LPS (1 ng/ml) in the presence or absence of butyrate (10 mM) for 16 hours. The levels of respective phosphoproteins in the cell lysates were assessed by Akt/mTOR Phosphoprotein 11-plex Magnetic Bead Kit (# 48-611MAG) including positive controls HepG2 cell lysate stimulated by Insulin or IGF1. The Median Fluorescence Intensity (MFI) is proportional to the level of phosphorylated protein. Pooled data from $n = 3$, each in technical duplicates, mean + SEM. This experiment was performed with the help of Carl Christian Kolbe (Institute of Innate Immunity, University of Bonn).

5. Discussion

For decades, it has been generally considered that SCFAs derived from commensal bacterial fermentation of dietary fibres are beneficial to gut health through regulation of a series of cellular processes, including stimulation of mucus production by epithelial cells (Thomas et al., 2013; Willemsen et al., 2003), induction of IgA production by B cells (Ishikawa and Nanjo, 2009), promoting tissue repair and wound healing, and supporting functions of inducible Treg cells (Atarashi et al., 2013; Geuking et al., 2011; Krebs et al., 2011). However, these beneficial effects of SCFAs are primarily observed in intact, healthy gut states. Conversely, in chronic inflammatory gut diseases, such as IBD, the gut mucosal barrier is damaged and leaky, leading to accumulation of bacterial components (LPS, flagellin and bacterial metabolites such as SCFAs or ATP) in a new niche infiltrated by phagocytes – macrophages, DCs, and neutrophils (Blaak et al., 2020; Silva et al., 2020; Venegas et al., 2019).

Recent studies unexpectedly indicated that some patients with IBD showed poor tolerance to certain dietary fibres. Consistent with these reports, in a (Dextran sulfate sodium) DSS-induced mouse IBD model, a high content of dietary fibres led to exacerbated inflammation (Singh et al., 2019; Zhang et al., 2016). Altogether, these results put forward the question whether dietary fibres are still as beneficial to people under inflammatory conditions as they are to the healthy population.

In this study, I co-stimulated primary human macrophages with LPS and SCFAs to partially mimic the new niche formed in damaged, leaky guts *in vitro*. The aim of this model was to explore the previously unexplored physiological characteristics and regulatory potential of SCFAs under inflammatory conditions.

5.1 Multifaceted consequences of SCFAs co-stimulation on the TLR-mediated immune response

At the beginning of this study, I systemically explored the impact of SCFAs on the TLR-mediated immune response using both transcriptomic and proteomic approaches. Thereby, I could show that the potency of SCFAs as regulators of gene transcription in primary human macrophages increased in the following order: acetate – propionate – butyrate. This might be attributed to the HDAC-inhibitory properties of propionate and butyrate but not acetate (Li et al., 2018). This hypothesis was strengthened by the detected similarities between the impact of TSA and butyrate on the LPS-induced change in gene expression. Furthermore, it has been previously demonstrated that butyrate has a broader HDAC-inhibitory effect than propionate (Silva et al., 2018), which could partially explained why butyrate targeted the expression of

twice as many genes as propionate did. For these reasons, butyrate was selected as the representative commensally-derived SCFA for the subsequent experiments.

Of note, even though TSA and butyrate had similar effects on the LPS-induced changes in gene expression, on the proteomic level butyrate targeted three times as many proteins as TSA did. This analysis showed a relatively poor correlation between gene transcription and protein translation, which could be due to post-transcriptional modifications, post-translational modifications, protein stability (Koussounadis et al., 2015; Maier et al., 2009; Vogel and Marcotte, 2012).

Interestingly, the GSEA in both the transcriptomic and proteomic profiles indicated that butyrate and TSA stimulation led to an enrichment of similar gene sets. The commonly shared gene sets were responses to IFN- α and - γ , consistent with previous reports suggesting that SCFAs are involved in virus-induced inflammatory responses. Trompette et al. found that dietary fibres could exert a protective effect against influenza-induced pathology by dampening neutrophil-mediated tissue damage and amplifying the anti-viral effects of CD8⁺ T cells (Trompette et al., 2018). On the other hand, Prow et al. demonstrated that mice fed with high a fibre diet, or with butyrate supplementation in the drinking water, had an exacerbated arthropathy after infection with chikungunya virus (Prow et al., 2019). Thus, in specific pathological settings, my results provide new evidences on the roles of SCFAs in the virus-mediated inflammatory responses.

Compared to the treatment with TSA, the only gene set selectively enriched upon butyrate stimulation was the inflammatory response gene set, supporting the notion that dietary fibres are extensively associated with inflammation-related diseases (Swann et al., 2020; Telle-Hansen et al., 2018). In summary, my experiments provide novel insights into the roles of SCFAs as modulators of the TLR-induced changes in gene transcription and protein translation in macrophages and possibly other cell types. These findings will be beneficial for future studies investigating the impact of SCFAs on further cell types and to understand their role in inflammation.

5.2 SCFAs trigger NLRP3 inflammasome-mediated IL-1 β release

On the whole, the impact that SCFAs had on the LPS-induced cytokines secretion was consistent with the influence exerted on the gene expression profile (Section 4.1). Propionate and butyrate, but not acetate, exhibited a similar potency in modulating the LPS-induced cytokines release from primary human macrophages. Strikingly, among all the LPS-induced cytokines regulated by butyrate, IL-1 β , IP-10, TNF- α , IL-12p70, and IL-10 have all been reported to be associated with the pathogenesis and development of IBD. All the four pro-

inflammatory cytokines: IL-1 β , IP-10, TNF- α , and IL-12p70 have been shown to be increased in the serum, stool, and biopsy specimens of colonic mucosa from patients with IBD (Fuss et al., 2006; Koelink et al., 2020; Singh et al., 2016; Ugucioni et al., 1999; Vulliamoz et al., 2020). In the past 20 years, anti-TNF- α antagonists have become a treatment option for patients suffering from IBD, however, approximately 30 – 50% of IBD patients do not respond to anti-TNF- α therapy (Rundquist et al., 2021; Siegel and Melmed, 2009). In addition, the IL-1 receptor antagonist Anakinra has been tested in clinical trials for the treatment of acute severe ulcerative colitis (Kashani and Schwartz, 2019). To further target cytokines in IBD, monoclonal antibodies against IP-10 and IL-12/-23p40 are currently in clinical trials for the treatment of ulcerative colitis and Crohn's disease (Kashani and Schwartz, 2019; Sandborn et al., 2016). IL-10, an important anti-inflammatory cytokine, is critical for the protection against the initiation of IBD, which will be discussed in detail in Section 5.4.

In this study, I found that the SCFA butyrate dramatically increased secretion of IL-1 β and IP-10 by macrophages, which might point to the potential causes of the dietary fibre-mediated exacerbation of IBD development. Mechanistically, SCFAs were shown to regulate the release of IP-10 via mediating histone hyperacetylation, at least partially (Inatomi et al., 2005; Vinolo et al., 2011). However, the mechanisms by which SCFAs regulate IL-1 β responses in primary human macrophages were still underexplored (Li et al., 2018; Macia et al., 2015b; Schulthess et al., 2019; Yuan et al., 2018). During my work, I found that the bacterial outer membrane component LPS combined with the bacterial metabolite butyrate triggers secretion of IL-1 β by primary human macrophages, but not by primary human monocytes. Furthermore, I could show that this butyrate elicited IL-1 β secretion is dependent on the activation of the NLRP3 inflammasome. My observations were, to some extent, in line with the previous report that elevated butyrate levels promote IL-1 β activity, resulting in exacerbated colitis that could be alleviated by inhibition of NLRP3 (Singh et al., 2019). Conversely, Wang et al. demonstrated that butyrate has an anti-inflammatory effect on obesity-induced inflammation through suppressing the NLRP3 pathway (Wang et al., 2015). Furthermore, Yuan et al. observed that butyrate could completely block the NLRP3 inflammasome complex formation in a model of endothelial dysfunction and atherosclerosis (Yuan et al., 2018). The discrepancies between the observed roles of butyrate in the NLRP3 inflammasome activation could be attributed to the differences in the investigated cell types and the comparability between in vivo and in vitro results. For example, I found that butyrate does not induce IL-1 β release in human PBMC and human monocyte-like cell line THP-1.

Upon engagement of TLRs, NF- κ B is essential for the priming signal for the NLRP3 inflammasome. Interestingly, butyrate suppressed the LPS-induced NF- κ B phosphorylation and the subsequent expression of NLRP3 and pro-IL-1 β mRNA, but did not affect the LPS-induced expression of NLRP3 and pro-IL-1 β at the protein level. The explanations of this

discrepancy could be attributed to the post-transcriptional modifications (PTMs) and protein stability. For example, it is possible that the rate of translation is still sufficient to compensate the decrease of mRNA expression, resulting in the same amount of translated proteins. In addition, butyrate could influence the protein stability or degradation, for example by modulating PTMs involved in protein degradation.

In accordance with the canonical mechanism whereby the NLRP3 inflammasome is activated by a series of priming and activating triggers, the activating stimuli include nigericin (Mariathasan et al., 2006b), cholesterol crystals (Dewell et al., 2010c), or monosodium urate crystals (Martinon et al., 2006). For these activators, K^+ efflux is a common event upstream of the NLRP3 inflammasome assembly. The dependence of the IL-1 β release in response to LPS + butyrate in primary human macrophages on K^+ efflux implies that butyrate triggers the canonical NLRP3 activation pathway.

In addition to K^+ efflux, another event occurring during NLRP3 activation is ROS production (Cruz et al., 2007; Dostert et al., 2008; Menu et al., 2012). Furthermore, most studies hold the notion that ROS produced by mitochondria or through NADPH oxidases is able to lead to NLRP3 inflammasome activation (Dostert et al., 2008; Di Meo et al., 2016; Morgan and Liu, 2011; Wang et al., 2017). However, the importance of ROS for the NLRP3 inflammasome assembly has been questioned by Núñez and co-workers, who demonstrated that ROS production is not essential for NLRP3 priming and activation (Muñoz-Planillo et al., 2013). In this study, I observed that butyrate potently induced cytosolic ROS production in primary human macrophages. Thus, I hypothesized that the butyrate-induced ROS could contribute to the inflammasome activation under the tested conditions. Contrary to these expectations, the antioxidants PDTC and Ebselen failed to inhibit the LPS + butyrate-driven IL-1 β secretion, indicating that the butyrate-induced ROS production is likely not involved in inflammasome activation.

Numerous reports investigating the NLRP3 inflammasome commonly use LPS + nigericin or LPS + ATP as the priming and activation triggers to induce NLRP3 inflammasome assembly. In addition to this two-step model, the lab of Veit Hornung found that LPS alone could induce NLRP3-dependent IL-1 β maturation and secretion in human monocytes in the absence of pyroptosis (alternative NLRP3 activation). Moreover, this mechanism was demonstrated to be independent of K^+ efflux or the assembly of pyroptosome complex (Gaidt et al., 2016).

Here, I found that the NLRP3 inflammasome activation by LPS + butyrate in primary human macrophages does not involve pyroptosome formation and pyroptosis, as indicated by the lack of ASC aggregation and LDH release. These observations pointed to the characteristics of the alternative NLRP3 inflammasome activation pathway. Conversely, IL-1 β release induced by LPS + butyrate is K^+ efflux-dependent, which is contradictory to the K^+ efflux-independent mechanism of the alternative NLRP3 inflammasome activation but instead one

of the hallmarks of the canonical NLRP3 inflammasome pathway. Based on the current knowledge, it is difficult to explain why the LPS + butyrate-induced NLRP3 inflammasome activation shares characteristics of both the canonical and the alternative inflammasome pathways in primary human macrophages. Due to the lack of a proper definition for this phenomenon, hereafter I termed it as the “novel NLRP3 inflammasome activation” pathway. In this scenario, the mechanisms for IL-1 β secretion in the absence of cell death still need to be determined. However, similar observations have been reported by the lab of Jonathan Kagan, in which they demonstrated that two components of oxidized phospholipids, PGPC (1-palmitoyl-2-glutaryl-sn-glycero-3-phosphocholine) and POVPC (1-palmitoyl-2-(5-oxovaleroyl)-sn-glycero-3-phosphocholine), could induce inflammasome-dependent macrophages hyperactivation and IL-1 β release without pyroptosis (Zanoni et al., 2016, 2017). Taken together, I demonstrated that SCFAs exhibit a pro-inflammatory effect in combination with the bacterial component LPS in primary human macrophages. This effect is mediated through a novel NLRP3 inflammasome-mediated IL-1 β secretion, suggesting a potential therapeutic strategy for the treatment of IBD. To gain more insight into and further characterize the novel mechanism for NLRP3 inflammasome activation identified in my presented work here, the following questions are of great interest:

1. is it possible for the canonical and alternative NLRP3 inflammasome pathways to be active simultaneously and under which conditions does it happen?
2. are there any other triggers of the novel NLRP3 inflammasome activation in addition to the LPS + butyrate combination?
3. do LPS + butyrate regulate IL-1 β secretion in cell types other than macrophages, such as DCs or neutrophils and, if yes, is this process similar to the novel NLRP3 inflammasome activation?
4. do LPS + butyrate promote IL-1 β release through inflammasome-dependent macrophages hyperactivation?
5. what is the physiological relevance of the newly identified NLRP3 inflammasome activation machinery?

5.3 LPS + butyrate promote IL-1 β release orchestrated by multiple targets

To date, the NLRP3 inflammasome has been associated with the pathogenesis of more than 30 chronic inflammatory and neuro-degenerative diseases (Mangan et al., 2018; Wang et al., 2020). Accordingly, a great number of low molecular weight compounds (He et al., 2014; Juliana et al., 2010; Toldo and Abbate, 2018; Wannamaker et al., 2007b) and antibodies (Abbate et al., 2020; Desu et al., 2020b) targeting the NLRP3 inflammasome components

have been developed and are currently in clinical trials. The potential success of these efforts will likely depend on a comprehensive understanding of the NLRP3 inflammasome activation mechanism as well as the respective disease context. In this study, I found several mediators of this process, including cFLIP/caspase-8, RIPK1/RIPK3, STAT3/TBK1, and HDAC11, which are all potentially involved in the IL-1 β release induced by LPS + butyrate in primary human macrophages.

5.3.1 LPS + butyrate induce IL-1 β through a novel NLRP3 inflammasome activation pathway

Having identified a novel inflammasome activation mechanism mediating the butyrate-driven IL-1 β secretion in primary human macrophages, I went on to explore which proteins are involved in this process. Based on the RNA-Seq data and previous reports on the alternative NLRP3 activation pathway, I focused on the prospective roles of cFLIP, caspase-8, and RIPK1. Butyrate completely abolished cFLIP expression and robustly activated caspase-8. Moreover, pharmacological inhibition or siRNA-mediated silencing of caspase-8 demonstrated the involvement of caspase-8 in the novel NLRP3 inflammasome activation mechanism. Given the importance of cFLIP and caspase-8 on the TNFR1 complex II-driven IL-1 β regulation (Muendlein et al., 2020), I put forward two potential models of the novel NLRP3 inflammasome activation.

Model 1: Butyrate enables LPS to elicit IL-1 β secretion by cFLIP deficiency-induced TNFR1 complex II formation

In model 1, upon LPS binding to TLR4 on the plasma membrane, TNF- α is expressed as a result of the activation of the NF- κ B signaling pathway (Hoareau et al., 2010). Secreted TNF- α then binds to TNFR1, leading to the recruitment of TRADD, TRAF and RIPK1 to form complex I and the transcriptional induction of cFLIP through activation of NF- κ B. Complex I can dissociate from the plasma membrane upon the ubiquitination of RIPK1 (Barnhart and Peter, 2003; Dondelinger et al., 2016; Kimberley et al., 2007; Legler et al., 2003)

After dissociation from TNFR1, FADD, pro-caspase-8, pro-caspase-10 and cFLIP are recruited to form complex II, which functions as an intracellular death-inducing signaling complex. As the vital executor of apoptosis in complex II, caspase-8 activity is blocked by its endogenous inhibitor cFLIP, whose expression is an outcome of the complex I-induced NF- κ B signaling. This explains why LPS alone does not lead to apoptosis in most cell types (Barnhart and Peter, 2003; Micheau and Tschopp, 2003). Recently, Muendlein et al. demonstrated that LPS alone induced K⁺ efflux- and NLRP3-dependent IL-1 β secretion and

pyroptosis in BMDMs through regulation of the complex II formation under conditions of cFLIP knockdown (Muendlein et al., 2020). In analogy to the processes described above, I hypothesize that butyrate intrinsically blocks cFLIP expression, enabling LPS-induced complex II formation and caspase-8 activation, thereby inducing NLRP3- and caspase-1-dependent IL-1 β secretion in primary human macrophages (Figure 5.1). To further validate this model, it will be helpful to test whether reconstitution/overexpression of cFLIP is able to repress the induction of IL-1 β in response to LPS + butyrate. Blocking the formation of the TNFR1 complex II by a TNF- α neutralizing antibody could be another tool to validate the dependence of the NLRP3 inflammasome-mediated IL-1 β driven by LPS + butyrate on complex II.

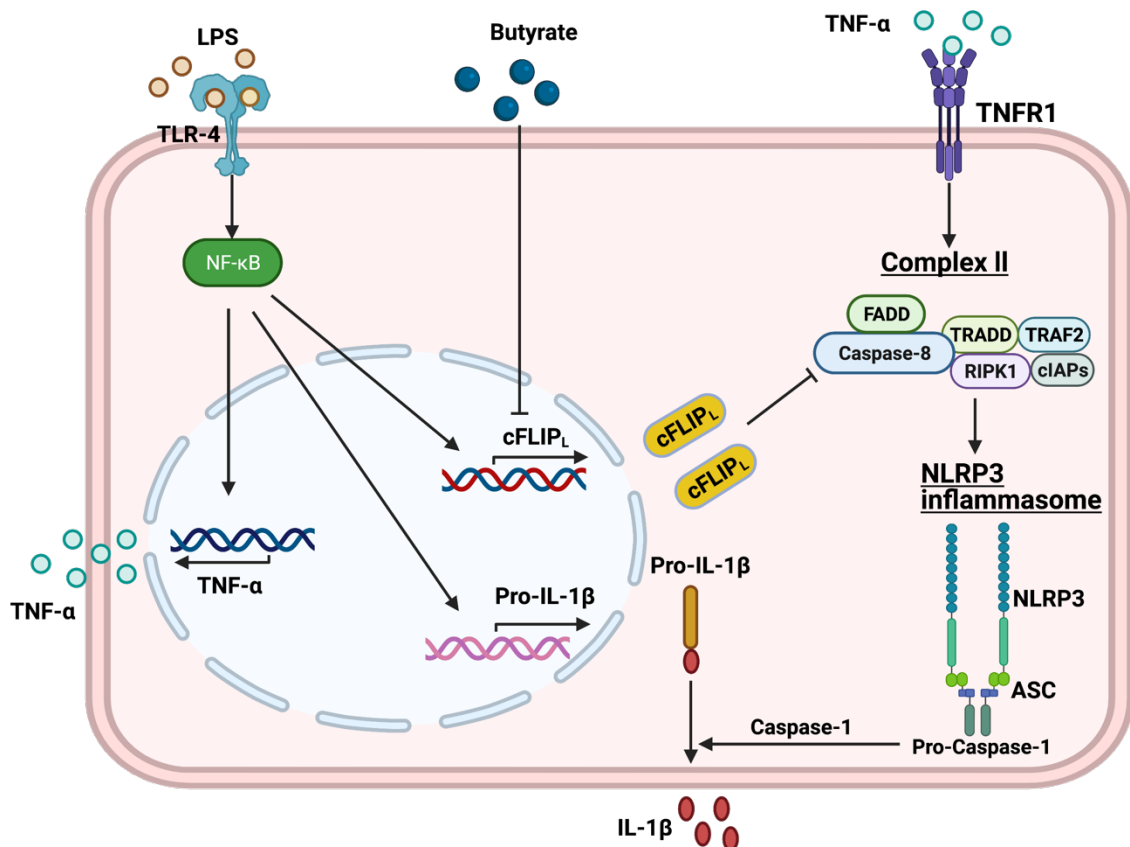


Figure 5.1: Butyrate enables LPS to elicit IL-1 β secretion by cFLIP deficiency-induced TNFR1 complex II formation.

Schematic representation of model 1. LPS binding to TLR-4 induces NF- κ B-mediated transcription of TNF- α , cFLIP and pro-IL-1 β . The engagement of TNF- α with TNFR1 promotes complex II formation, which under steady-state conditions is blocked by cFLIP. Whereas butyrate could inhibit the expression of cFLIP, whereby the inhibitory effect of cFLIP on caspase-8 is abrogated, allowing for caspase-8-driven NLRP3 inflammasome activation and subsequent IL-1 β maturation.

LPS, Lipopolysaccharide; TLR4, toll-like receptor 4; NF- κ B, nuclear factor- κ B; TNF- α , tumour necrosis factor- α ; cFLIP, cellular FLICE-inhibitory protein; IL-1 β , interleukine-1 β ; TNFR1, tumour necrosis factor receptor 1; NLRP3, NLR family pyrin domain containing 3.

Model 2: Both the canonical and the alternative inflammasome pathways are at play in the induction of IL-1 β driven by LPS + butyrate

Model 1 offers a plausible mechanism for the novel NLRP3 inflammasome activation pathway, however, it does not explain the lack of pyroptosome formation and the absence of pyroptosis in response to LPS + butyrate. Veit Hornung and colleagues reported that LPS, as a single signal, could induce IL-1 β release in primary human monocytes without pyroptosome formation and pyroptosis, in a manner dependent on the TRIF-FADD-RIPK1-caspase-8 pathway (Gaidt et al., 2016). Given the involvement of similar factors between the alternative and the novel NLRP3 inflammasome activation pathways and the dependence of the novel NLRP3 activation on K⁺ efflux, I propose that LPS + butyrate could induce IL-1 β production through a combination of the canonical and the alternative NLRP3 inflammasome pathways (Figure 5.2). To validate the credibility of this hypothesis, the following questions need to be addressed:

1. Why is there no pyroptosome formation detectable following K⁺ efflux in response to LPS + butyrate? Firstly, ASC speck measurements using microscopy are not as sensitive as flow cytometry, so it is possible that a small population of specking cells could be detected by flow cytometry methods. Secondly, it is possible that living cells are degrading ASC specks, for example through autophagy or the proteasome (Biasizzo and Kopitar-Jerala, 2020; Lopez-Castejon, 2020; Shi et al., 2012).
2. Can cells lacking the pyroptosome secrete IL-1 β in the presence of LPS + butyrate? This question could be answered by performing an Elispot assay, localizing active IL-1 β -secreting cells, which could be correlated with ASC speck formation.
3. Is pyroptosome formation reversible, possibly connecting the classical and alternative inflammasome activation pathways during the treatment with LPS + butyrate? Though previous reports have suggested that pyroptosome formation is irreversible (Cai et al., 2014; Lu et al., 2014), more work could be focused on primary human cells to explore this notion.

Of note, RIPK1, as the node orchestrating both the NF- κ B/cFLIP-mediated cell survival and the caspase-8-dependent apoptosis, is believed to be crucial for the signaling downstream of death receptors and PRRs (Declercq et al., 2009; Ofengeim and Yuan, 2013). However, the role of RIPK1 varies between different cell types. For example, RIPK1 mediates a protective and antiapoptotic effect in epithelial cells in a manner independent of the NF- κ B pathway (Takahashi et al., 2014b). Intriguingly, I found that RIPK1 is a negative regulator of IL-1 β

secretion in response to LPS + butyrate through its kinase-independent platform function, as pharmacological inhibition of RIPK1 kinase activity did not have any effect on IL-1 β release, while the siRNA-mediated RIPK1 knockdown enhanced IL-1 β release in primary human macrophages.

Contrary to the requirement for RIPK1 in the TNFR1 complex II-driven and the alternative NLRP3 inflammasome-mediated IL-1 β activation, RIPK1 had a negative impact on the IL-1 β response to LPS + butyrate. Additionally, the siRNA-mediated RIPK1 deficiency had no effect on the viability of primary human macrophages (Supplementary Figure 2), which excluded the impact of cell death in the absence of RIPK1 on the IL-1 β secretion induced by LPS + butyrate. However, it remains unclear how and why RIPK1 displayed negative roles under this circumstance and more work needs to be done in the future to explain this effect.

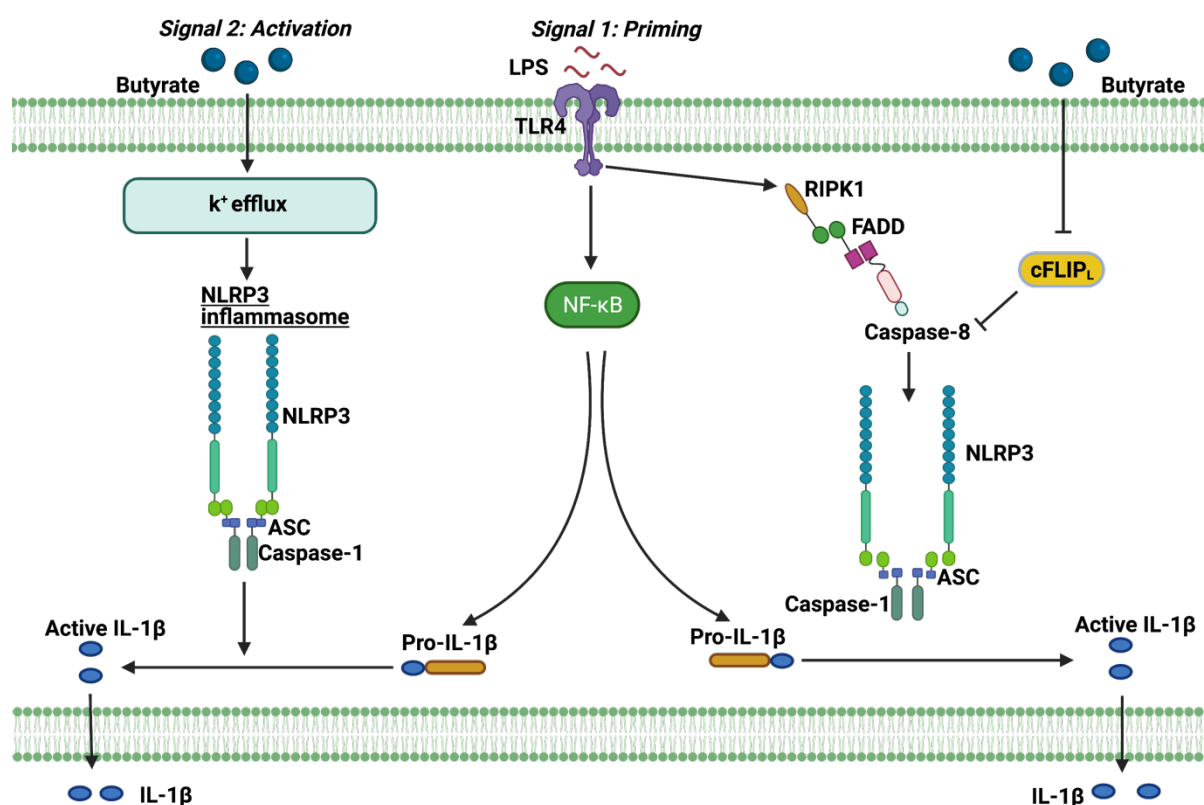


Figure 5.2: Both the canonical and the alternative inflammasome pathways are at play in the induction of IL-1 β driven by LPS + butyrate.

Schematic representation of model 2. LPS binding to TLR-4 provides the priming signal and, in parallel, butyrate elicits K⁺ efflux enabling the assembly of the NLRP3 inflammasome complex. The canonical NLRP3 inflammasome activation leads to the maturation and secretion of IL-1 β . Simultaneously, the combination of LPS and butyrate could activate the alternative inflammasome pathway with the removal of the inhibitory effect of cFLIP on caspase-8 by butyrate. Together, the IL-1 β secretion in response to LPS + butyrate could be mediated by the canonical NLRP3 inflammasome activation in concert with the alternative inflammasome pathway.

LPS, Lipopolysaccharide; TLR4, toll-like receptor 4; cFLIP, cellular FLICE-inhibitory protein; IL-1 β , interleukine-1 β ; NLRP3, NLR family pyrin domain containing 3.

5.3.2 TBK1 and STAT3 act as negative regulators of IL-1 β secretion induced by LPS + Butyrate

The IL-10-STAT3-DDIT4 axis has been identified as a novel signaling pathway for the maintenance of mitochondrial integrity in response to LPS. Deficiencies in the components of this pathway enable LPS alone to induce inflammasome-dependent IL-1 β secretion through aberrant activation of mTORC1 signaling, resulting in increased ROS production and accumulation of damaged mitochondria (Ip et al., 2017). In agreement with these findings, I also detected increased IL-1 β production in response to LPS with or without butyrate stimulation when STAT3 was knocked down using siRNA in primary human macrophages. Based on these observations, I hypothesized that the butyrate-mediated ablation of IL-10 allows LPS to trigger the inflammasome-mediated IL-1 β secretion through the IL-10-STAT3-DDIT4-mTORC1 signaling pathway. However, I did not observe any regulatory effect of butyrate on the expression of DDIT4 (Supplementary figure 3) and on the activation of Akt and mTOR (Section 4.4.4), and the ROS scavengers PDTC and Ebselen did not inhibit IL-1 β induction in response to LPS + butyrate. These results indicate that it is unlikely that DDIT4 and mTOR are involved in the IL-1 β regulation driven by LPS + butyrate. At the same time, STAT3 appears to limit the NLRP3 inflammasome activation through a mechanism independent of the NLRP3 priming signal.

It has been previously reported that the combination of an HDACi and a TLR4 agonist could induce IL-1 β secretion in bone marrow-derived dendritic cells (BMDCs) through a caspase-8-dependent but TBK1- and RIPK1-independent mechanism (Stammli et al., 2015). Conversely, I observed enhanced induction of IL-1 β in response to LPS + butyrate when RIPK1 and TBK1 were knocked down using siRNA in primary human macrophages. One explanation for the discrepancy might be the cell type difference, as, in contrast to primary human macrophages, the HDACi-driven IL-1 β secretion is independent of the NLRP3 inflammasome in BMDCs.

In line with the observation that STAT3 and TBK1 physically interact in splenic DCs (Xiao et al., 2017b), a recent report from the Ashley Mansell lab demonstrated that upon LPS stimulation, TBK1 could interact with STAT3, modulating the metabolic reprogramming and subsequent production of inflammatory cytokines, including IL-1 β (Balic et al., 2020b). Given the similar effects of TBK1 and STAT3 knockdowns on the IL-1 β response to LPS + butyrate (Sections 4.3.6-7), I speculate that the interplay between TBK1 and STAT3 could be another regulator involved in the butyrate-driven IL-1 β secretion in primary human macrophages. To further validate this hypothesis, it would be helpful to perform a co-immunoprecipitation assay

to test the interaction between STAT3 and TBK1 during a challenge with LPS + butyrate in primary human macrophages.

5.3.3 HDAC11 modulates the NLRP3 priming signal

Stammler et al. speculated that the HDACi-driven IL-1 β secretion of DCs and macrophages likely depends on the inhibition of HDAC11 after excluding the involvement of other HDACs, due to the lack of commercially available inhibitors of HDAC11. I find this notion debatable, as there was no direct evidence provided to prove the involvement of HDAC11. In this study, I employed HDAC11-targeting siRNA and found that HDAC11 knockdown dramatically decreased the IL-1 β release in response to LPS + butyrate in primary human macrophages. This observation may appear to support the findings that the HDACi-induced IL-1 β secretion depends on the inhibition of HDAC11 (Stammler et al., 2015). However, LPS alone failed to induce IL-1 β secretion when HDAC11 was knocked down (Section 4.3.7), indicating that HDAC11 deficiency is not sufficient for IL-1 β secretion in response to LPS and thus providing evidence against the speculation from the study by Stammler et al. (2015). On the other hand, the deficiency in HDAC11 significantly reduced the expression of NLRP3 and pro-IL-1 β in the presence of LPS + butyrate (Section 4.3.7), suggesting that the NLRP3 priming signal was suppressed. This could be the cause of the observed reduction in IL-1 β secretion.

Among all the factors involved in the IL-1 β regulation in response to LPS + butyrate described above, none had a regulatory effect on the priming signal with the exception of HDAC11, as indicated by the reduced expression of NLRP3 and pro-IL-1 β with the knockdown of HDAC11. However, it still needs to be investigated how HDAC11 is involved in the regulation of NLRP3 and pro-IL-1 β expression. As no commercially available inhibitors of HDAC11 exist, the NF- κ B and MAPK signaling pathways activity could be tested under the conditions of siRNA-mediated HDAC11 knockdown. In addition, the identification of the exact HDAC isoform(s) downstream of butyrate could be facilitated by targeting class I (1, 2, 3, and 8) and class IIa (4, 5, 7, and 9) HDACs with specific siRNAs or inhibitors.

5.4 Butyrate inhibits the IL-10 downstream signaling pathway

As the most pleiotropic anti-inflammatory cytokine signaling network, the IL-10 signaling has been shown to play essential roles in the regulation of inflammatory responses and autoimmune pathologies in T cells (Trinchieri, 2007), B cells (Hilgenberg et al., 2014), DCs (De Smedt et al., 1997), macrophages (Chung et al., 2007), and neutrophils (Kasten et al., 2010).

In my thesis, I observed that butyrate completely blocked the TLR-mediated IL-10 production in both primary human macrophages and PBMCs. This potent inhibition of the TLR-mediated IL-10 induction is reminiscent of the spontaneous development of IBD in IL-10 signaling-deficient mouse models (Keubler et al., 2015; Zhu et al., 2017). Without the homeostatic activity of IL-10, the excessive pro-inflammatory cytokine secretion and alterations of mitochondria integrity (Ip et al., 2017) could enable bacterial components such as the TLR4 ligand LPS to exacerbate gut inflammation through inflammasome-dependent IL-1 β release. To validate this hypothesis, I employed an IL-10 neutralizing antibody and an IL-10Ra antagonist to mimic the effect of butyrate on IL-10 signaling. Unexpectedly, both of these treatments failed to induce IL-1 β secretion in LPS-stimulated primary human macrophages (Supplementary Figure 4). These results implied that the butyrate-induced deficiency in IL-10 is unlikely to contribute to the inflammasome-mediated IL-1 β secretion under these conditions. To some extent, this is in line with the failed clinical trial attempting to administer IL-10 to patients with IBD (Marlow et al., 2013). Given the importance of IL-10 signaling in the pathogenesis of IBD, it will be highly meaningful to determine the mechanisms by which butyrate suppresses the TLR-induced IL-10 production, providing potential therapeutic targets for the treatment of IBD in the future.

Villagra et al. (2009) found that HDAC11 could inhibit the transcription of IL-10 by interacting with the IL-10 promoter. Intact enzymatic activity of HDAC11 was indispensable for this regulation (Villagra et al., 2009). Contradictory to this finding, siRNA-mediated knockdown of HDAC11 decreased IL-10 production in response to LPS stimulation in GM-MDMs (Supplementary figure 5), indicating that HDAC11 is required for the LPS-induced IL-10 secretion in primary human macrophages. On the other hand, the requirement of HDAC11 on the LPS-induced IL-10 regulation might be the mechanism by which butyrate exerts its inhibitory effect on the TLR-mediated IL-10 production.

Following the observation that butyrate inhibits IL-10 production in primary human macrophages, I found that butyrate strongly suppressed the LPS-induced STAT1 phosphorylation. Initially, I reasoned that the decreased STAT1 phosphorylation could be attributed to the loss of IL-10, based on early reports suggesting that IL-10 is upstream of STAT1 (Larner et al., 1993; Shaw et al., 2006b; Wehinger et al., 1996). This notion is now considered controversial (Williams et al., 2004). The addition of IL-10 prior to the stimulation of LPS + butyrate failed to rescue STAT1 phosphorylation, consistent with the latter notion that the IL-10 signaling is not linked to STAT1 phosphorylation in macrophages (Wilbers et al., 2017b). Even though the association between IL-10 and STAT1 in different cell types remains a matter of debate, a possible explanation of the observed effect is that butyrate inhibits the LPS-induced IL-10 production through downregulation of STAT1 phosphorylation.

(VanDeusen et al., 2006). STAT1 inhibitors and STAT1-targeting siRNAs could be helpful to validate this hypothesis.

In addition to STAT1, p38 is also believed to be required for the LPS-induced IL-10 production in macrophages and B cells (Ma et al., 2001b; Mion et al., 2014). Here, I found that LPS dramatically elicited p38 phosphorylation, which was significantly suppressed by butyrate. Therefore, the downregulation of IL-10 by butyrate could also be an effect of decreased p38 signaling. Further experiments would still need to be performed with p38 inhibitors (SB203580 and BIRB796) to confirm the role of p38 in the butyrate-mediated IL-10 regulation.

As discussed in section 5.3.2, STAT3, as a negative regulator of the inflammasome-dependent IL-1 β secretion, might be a new therapeutic target for the treatment of IBD (Li et al., 2012; Mitsuyama et al., 2007; Sugimoto, 2008). I found that butyrate completely abolishes the TLR-induced STAT3 phosphorylation at both Y705 and S727 residues through its inhibition on IL-10 production. Given the involvement of STAT3 phosphorylation at S727 residue, but not at Y705 residue, in IL-1 β regulation (Balic et al., 2020a), I propose that it is likely that butyrate could induce IL-1 β production through the regulation of STAT3 phosphorylation at S727. However, additional experiments with STAT3 S727 point mutants could be performed to investigate the role of STAT3 S727 in butyrate-driven IL-1 β release. This could provide new insights into the role of STAT3 S727 phosphorylation in inflammatory responses.

Another important downstream effector of IL-10 is the PI3K-Akt-mTOR pathway, which has been suggested as a new target for Crohn's disease therapy (Tokuhira et al., 2015). However, in primary human macrophages, neither LPS nor butyrate appeared to have an impact on the Akt-mTOR phosphorylation status. Interestingly, butyrate potently decreased the basal and the LPS-induced GSK-3 α and GSK-3 β phosphorylation. As moonlighting proteins targeting a great number of substrates (Nagini et al., 2019; Schrecengost et al., 2018a), GSK-3 isoforms have been associated with multiple diseases with inflammatory components, including multiple sclerosis, Alzheimer's disease, colitis, arthritis, and diabetes (Duda et al., 2018; Lal et al., 2015; Llorens-Martín et al., 2014). Hence, further *in vivo* experiments need to be performed to identify the systemic effect of butyrate on various pathologies with the possible involvement of GSK-3 regulation. Apart from GSK-3 α and β , the phosphorylation status of ribosomal protein S6 (RPS6) is also modulated by butyrate. The most well-defined characteristic of RPS6 is inhibition of autophagy, serving as a buffering machinery to remove abundant ROS in the cytosol (Fang et al., 2017). Thus, it is likely that butyrate could induce autophagy, as indicated by the processing of LC3B-II (Supplementary figure 6), through suppression of RPS6. This would allow to balance the intracellular levels of butyrate-elicited ROS, suggesting a potential explanation for why primary human macrophages (GM-MDMs) do not undergo cell death in response to LPS + butyrate.

5.5 Conclusion

At the beginning of this project, to obtain a comprehensive understanding of the roles of SCFAs in the TLR-mediated immune responses, transcriptomic and proteomic analyses were performed. These demonstrated that SCFAs dramatically shaped the TLR-induced IFN- α/γ responses and the inflammatory response. Thus, the findings described in the first part of my thesis provided some hints that SCFAs might be involved in the development of IBD by impacting on TLR-mediated inflammatory responses.

Therefore, the next part of my project aimed to explore the effect of SCFAs on the inflammatory response through regulation of cytokine production in primary human macrophages. Strikingly, I found that the SCFA butyrate combined with LPS induced IL-1 β secretion, while simultaneously inhibiting the LPS-mediated IL-10 production. Moreover, I demonstrated that the IL-1 β release driven by LPS + butyrate is NLRP3 inflammasome-dependent, and the mechanisms underlying this response involve multiple molecules including cFLIP, caspase-8, RIPK1, TBK1, STAT3 and HDAC11. Notably, I discovered that the NLRP3 inflammasome could be activated by LPS + butyrate, possibly in a novel pathway, distinct from all the known and previously characterized NLRP3 inflammasome activation models.

Furthermore, due to the crucial roles of IL-1 β and IL-10 in the development of IBD, this study provided a novel insight that the combination of SCFAs and LPS could aggravate the inflammatory response through IL-1 β and IL-10 regulation. While IL-1 β upregulation may drive the inflammatory response, the inhibitory effect of butyrate on the TLR-induced IL-10 signaling pathway could dampen the protective mechanisms in the gut.

In summary, the findings presented in my thesis suggested novel effects of SCFAs on gut health under an impaired, inflammatory state. All of the molecules identified to be involved in the butyrate-mediated regulation of IL-1 β and IL-10 could be promising therapeutic targets for the treatment of IBD. Thus, future work should focus on the roles of SCFAs in the inflammatory response in IBD *in vivo*.

6. List of Abbreviations

AD	Alzheimer's Disease
AIM2	Absent melanoma 2
ALR	AIM2-like receptor
APAF-1	Apoptotic peptidase activating factor 1
APC	Antigen-presenting cells
ASC	Apoptosis-associated speck-like protein containing a CARD
ATP	Adenosine triphosphate
BAK	BCL-2 antagonist or killer
BAX	BCL-2-associated X protein
BCA	Bicinchoninic acid
BCL-2	B-cell lymphoma 2
BH3	Bcl-2 homology domain 3
BID	BHD-interacting domain death agonist
BMDMs	Bone marrow derived macrophages
CAPS	Cryopyrin-associated periodic syndrome
CARD	Caspase activation and recruitment domain
CD	Crohn's disease
CD14	Cluster of differentiation 14
cDNA	Complementary DNA
cFLIP	Cellular FLICE-inhibitory protein
CLR	C-type lectin-like receptor
DAMPs	Danger-associated molecular patterns
DC	Dendritic cell
DCFDA	Dichlorofluorescein diacetate
DE	Differentially expressed
DEGs	Differentially expressed genes
DISC	Death inducing signaling complex
DMEM	Dulbecco's Modified Eagle Medium
DSS	Dextran sulfate sodium
ELISA	Enzyme-linked immunosorbent assay
EMCV	Encephalomyocarditis virus
ENS	Enteric nerve system
ETC	Electron transport chain
FADD	Fas-associated death domain

FC	Fold change
FCAS	Familial cold autoinflammatory syndrome
FDR	False discovery rate
GM-MDM	GM-CSF-differentiated primary human monocytes-derived macrophage
GPR	G-protein coupled receptor
GSDMD	Gasdermin D
GSEA	Gene set enrichment analysis
GSK3	Glycogen synthase kinase 3
HATs	Histone acetyltransferases
HDACi	Inhibitor of histone deacetylase
HDACs	Histone deacetylases
HMDMs	Primary human monocytes-derived macrophages
HO-1	Heme oxygenase-1
HSP	Heat-shock proteins
HTRF	Homogeneous time resolved fluorescence
IAV	Infuenza A virus
IBD	Inflammatory bowel disease
IEC	Intestinal epithelial cells
IFN	Interferon
IGF-1	Insulin-like growth factor-1
IL	Interleukin
IP10	Interferon gamma-induced protein 10
IR	Insulin receptor
IRF3	Interferon regulatory factor 3
IRS-1	Insulin receptor substrate 1
LPS	Lipopolysaccharide
LDH	Lactate dehydrogenase
M-MDM	M-CSF-differentiated primary human monocytes-derived macrophage
MCP	Monocyte chemoattractant protein
MCT-1	Monocarboxylate-transporter 1
MD2	Myeloid differentiation factor 2
MDS	Multidimensional scaling
MHC	major histocompatibility complex
MLKL	Mixed lineage kinase domain like

MOMP	Mitochondrial outer membrane permeabilization
MSigDB	Molecular Signatures Database
MSU	Monosodium urate
mtDNA	Mitochondria DNA
mtROS	Mitochondria reactive oxygen species
MWS	Muckle-Wells syndrome
NCDs	Non-communicable diseases
NF- κ B	Nuclear factor kappa B
NK	Natural killer
NLR	Nucleotide-binding oligomerization domain-like receptor
NLRP3	NLR family pyrin domain containing 3
NOD2	Nucleotide-binding oligomerization domain 2
NOMID	Neonatal onset multisystem inflammatory disease
OlfR 78	Olfactory receptor 78
OMV	Outer membrane vesicle
OSM	Oncostatin M
PAMPs	Pathogen-associated molecular patterns
PBMCs	Peripheral blood mononuclear cells
PCD	Programmed cell death
PCR	Polymerase chain reaction
PGPC	1-palmitoyl-2- glutaryl-sn-glycero-3-phosphocholine
POVPC	1-palmi- toyl-2-(50-oxo-valeroyl)-sn-glycero-3-phosphocholine
PRR	Pattern recognition receptor
PTEN	Phosphatase and tensin homolog
PYD	Pyrin domain
qPCR	Reverse transcription quantitative real-time PCR
RIPK1	Receptor-interacting serine-threonine kinase 1
RIPK3	Receptor-interacting serine-threonine kinase 3
RLR	Retinoci acid-inducible gene-I
ROS	Reactive oxygen species
RPS6	Ribosomal protein S6
RT-PCR	Reverse transcription PCR
SCFAs	Short chain fatty acids
SMAC	Second mitochondria-derived activator of caspases
SMCT-1	Sodium-dependent monocarboxylate-transporter 1
STAT	Signal transducer and activator of transcription

TBK1	TANK-binding kinase 1
TGF- β	Transforming growth factor- β
TLRs	Toll-like receptors
TRADD	TNFR type-1 associated death domain protein
TRIF	TIR domain-containing adaptor-inducing interferon- β
TSA	Trichostatin
UC	Ulcerative colitis
VEGF	Vascular endothelial growth factor
VEO-IBD	Very early onset inflammatory bowel disease
VSV	Vesicular stomatitis virus
WCL	Whole cell lysates
WT	Wild type
XIAP	X-linked inhibitor of apoptosis protein
ZBP1	Z-DNA Binding Protein 1

7. List of Figures and Tables

List of Figures

Figure 2.1: Pattern recognition receptors (PRRs) and their ligands.	9
Figure 2.2: NLRP3 inflammasome activation pathways.....	11
Figure 4.1.1: SCFAs regulate TLR-induced gene transcriptional profile.....	47
Figure 4.1.2: LPS + butyrate and LPS + TSA have a similar effect on the cellular processes based on hallmark gene sets enrichment.....	49
Figure 4.1.3: SCFAs regulate TLR-induced proteomics profile.....	52
Figure 4.2.1: SCFAs regulate LPS-induced cytokines production in primary human macrophages.	55
Figure 4.2.2: LPS plus butyrate elicit human macrophages, but not monocytes, to secrete IL-1 β	57
Figure 4.2.3: Butyrate in combination with TLR agonists induce IL-1 β secretion.....	58
Figure 4.2.4: The IL-1 β secretion driven by LPS + butyrate is NLRP3 inflammasome-dependent.	60
Figure 4.2.5: Butyrate has no effect on the priming signal of NLRP3 inflammasome	62
Figure 4.2.6: Butyrate drives NLRP3 inflammasome activation through potassium efflux	64
Figure 4.2.7: LPS + butyrate induce no cell death and ASC specks formation.....	67
Figure 4.3.1: Butyrate inhibits the expression of cFLIP at gene and protein level.....	69
Figure 4.3.2: Caspase-8 is involved in the IL-1 β production driven by LPS + butyrate	71
Figure 4.3.3: The IL-1 β secretion elicited by LPS + butyrate is RIPK3-dependent	73
Figure 4.3.4: RIPK1 is involved in the IL-1 β induction in response to LPS + butyrate	74
Figure 4.3.5: STAT3 exerts negative roles in the IL-1 β release driven by LPS + butyrate	76
Figure 4.3.6: TBK-1 is associated with the IL-1 β secretion in response to LPS + butyrate	77
Figure 4.3.7: HDAC 11 regulates the priming signal of NLRP3 inflammasome	79
Figure 4.4.1: Butyrate inhibits TLR-induced IL-10 production	81
Figure 4.4.2: Butyrate inhibits STAT3 activity with the engagement of IL-10.....	82
Figure 4.4.3: Butyrate suppresses the activity of STAT1 and p38	84
Figure 4.4.4: Butyrate regulates the phosphorylation of GSK-3 α/β and RPS6	85
Figure 5.1: Butyrate enables LPS to elicit IL-1 β secretion by cFLIP deficiency-induced TNFR1 complex II formation.	92
Figure 5.2: Both the canonical and the alternative inflammasome pathways are at play in the induction of IL-1 β driven by LPS + butyrate.	94
Figure S1: RIPK3 siRNAs fail to knock down the expression of RIPK3.....	106
Figure S2: RIPK1 siRNA has no toxic effect on the GM-MDMs	106
Figure S3: Butyrate has no regulatory effect on the expression of DDIT4.....	107
Figure S4: IL-1 β is not induced by LPS with the blockade of IL-10 signaling	107
Figure S5: HDAC11 is required for the LPS-induced IL-10 production.....	108
Figure S6: Butyrate upregulates the processing of LC3B-II.....	108

List of Tables

Table 1: List of antibodies used for Western blot and WES	28
Table 2: List of siRNAs used for electroporation	29
Table 3: List of qPCR primers used for amplification of human genes	30
Table 4: List of cell culture medium	30
Table 5: List of buffers and solutions	31
Table 6: List of primary cells and cell lines	32

8. Appendix

Supplementary figure:

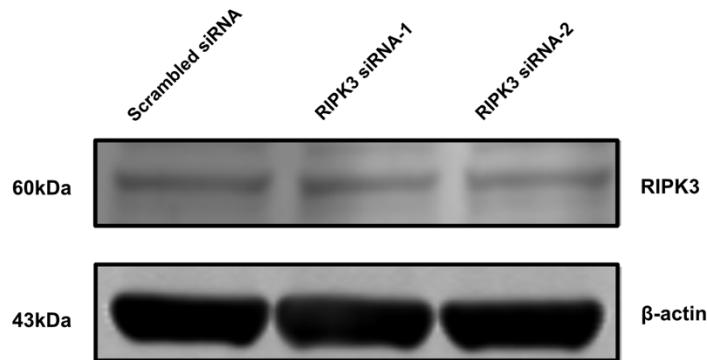


Figure S1: RIPK3 siRNAs fail to knock down the expression of RIPK3

GM-MDMs were electroporated with either scrambled siRNA or RIPK3 siRNA-1 and -2, the levels of RIPK3 and β -actin, serving as loading control, were evaluated by Western blot. Blots are representative of two independent experiments.

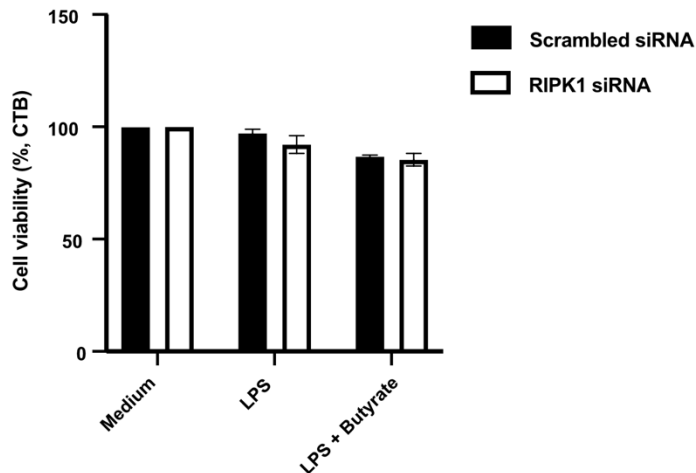


Figure S2: RIPK1 siRNA has no toxic effect on the GM-MDMs

GM-MDMs were treated with medium, LPS (1 ng/ml) or LPS (1 ng/ml) + butyrate (10 mM) for 16 hours. The CTB assay was performed to determine the cell viability. Pooled data from $n = 3$, each in technical duplicates, mean + SEM.

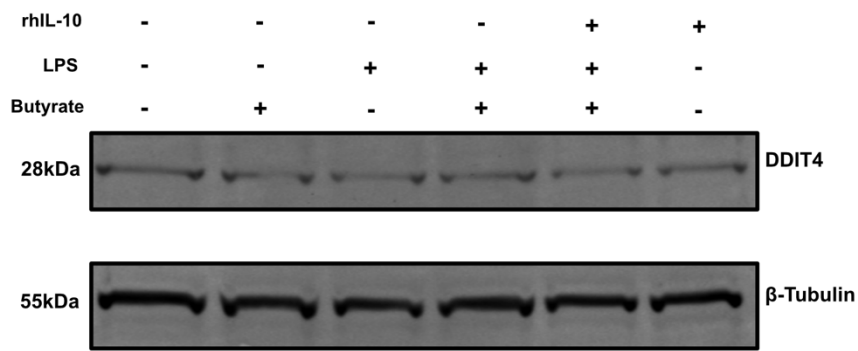


Figure S3: Butyrate has no regulatory effect on the expression of DDIT4

GM-MDMs were treated rhIL-10 (100 ng/ml, 0.5 hour) before subsequent treatments with medium, LPS (1 ng/ml) or butyrate (10 mM), alone or in combination, for 16 hours. The levels of DDIT4 and β -Tubulin, serving as loading control, were evaluated by Western blot. Blots are representative of two independent experiments.

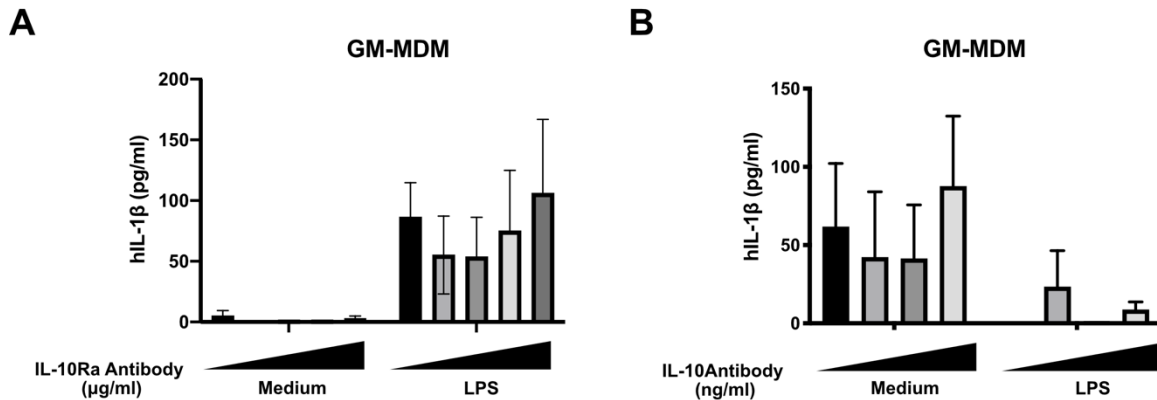


Figure S4: IL-1 β is not induced by LPS with the blockade of IL-10 signaling

(A-B): GM-MDMs were treated with increasing concentrations of (A) IL-10Ra antibody (0.1, 10, 20, or 40 μ g/ml) or (B) IL-10 antibody (5, 50, or 500 ng/ml) for 0.5 hour prior to subsequent treatments with medium (control) or LPS (1 ng/ml) for 16 hours. The levels of IL-1 β in the cell-free supernatants were measured by HTRF. Pooled data from $n = 3$ (A) or 4 (B), each in technical duplicates, mean + SEM.

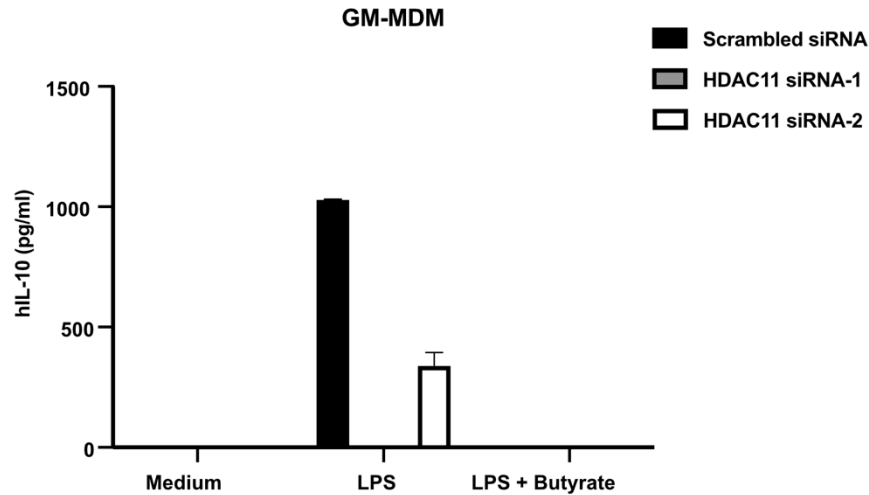


Figure S5: HDAC11 is required for the LPS-induced IL-10 production

GM-MDMs were electroporated with either scrambled siRNA or HDAC11 siRNA before the stimulations with medium, LPS (1 ng/ml) or LPS (1 ng/ml) + butyrate (10 mM) for 16 hours. The levels of IL-10 in the cell-free supernatants were measured by HTRF. Pooled data from $n = 2$, each in technical duplicates, mean + SD.

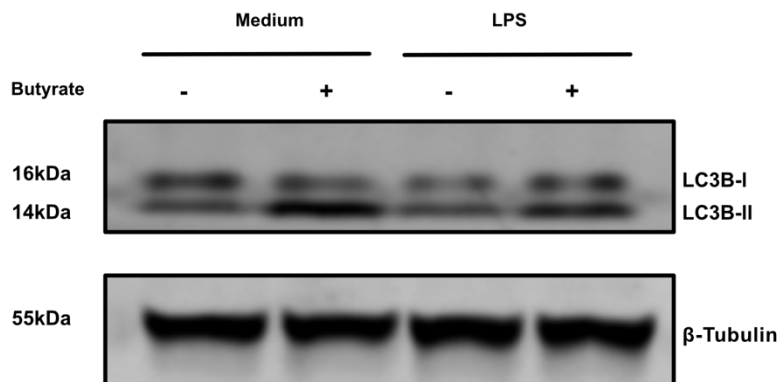


Figure S6: Butyrate upregulates the processing of LC3B-II

GM-MDMs were treated with medium or LPS (1 ng/ml) in the presence or absence of butyrate (10 mM) for 16 hours. The level of LC3B-I/II and β -Tubulin, serving as loading control, were evaluated by Western blot. Blots are representative of two independent experiments.

9. References

- Abais, J.M., Xia, M., Zhang, Y., Boini, K.M., and Li, P.L. (2015). Redox Regulation of NLRP3 Inflammasomes: ROS as Trigger or Effector? *Antioxidants Redox Signal.* 22, 1111–1129.
- Abbate, A., Toldo, S., Marchetti, C., Kron, J., Van Tassell, B.W., and Dinarello, C.A. (2020). Interleukin-1 and the Inflammasome as Therapeutic Targets in Cardiovascular Disease. *Circ. Res.* 1260–1280.
- Abderrazak, A., Syrovets, T., Couchie, D., El Hadri, K., Friguet, B., Simmet, T., and Rouis, M. (2015). NLRP3 inflammasome: From a danger signal sensor to a regulatory node of oxidative stress and inflammatory diseases. *Redox Biol.* 4, 296–307.
- Abegunde, A.T., Muhammad, B.H., Bhatti, O., and Ali, T. (2016). Environmental risk factors for inflammatory bowel diseases: Evidence based literature review. *World J. Gastroenterol.* 22, 6296–6317.
- Aberle, J.H., Stiasny, K., Kundi, M., and Heinz, F.X. (2013). Mechanistic insights into the impairment of memory B cells and antibody production in the elderly. *Age (Omaha).* 35, 371–381.
- Aglietti, R.A., Estevez, A., Gupta, A., Ramirez, M.G., Liu, P.S., Kayagaki, N., Ciferri, C., Dixit, V.M., and Dueber, E.C. (2016). GsdmD p30 elicited by caspase-11 during pyroptosis forms pores in membranes. *Proc. Natl. Acad. Sci. U. S. A.* 113, 7858–7863.
- Agostini, L., Martinon, F., Burns, K., McDermott, M.F., Hawkins, P.N., and Rg Tschopp, J. (2004). NALP3 Forms an IL-1-Processing Inflammasome with Increased Activity in Muckle-Wells Autoinflammatory Disorder containing protein called ASC binds and activates pro-caspase-1 (Martinon et al ASC contains a C-terminal CARD motif as well as an N-terminal CAR. *Immunity* 20, 319–325.
- Alatab, S., Sepanlou, S.G., Ikuta, K., Vahedi, H., Bisignano, C., Safiri, S., Sadeghi, A., Nixon, M.R., Abdoli, A., Abolhassani, H., et al. (2020). The global, regional, and national burden of inflammatory bowel disease in 195 countries and territories, 1990–2017: a systematic analysis for the Global Burden of Disease Study 2017. *Lancet Gastroenterol. Hepatol.* 5, 17–30.
- Alfano, M., and Poli, G. (2005). Role of cytokines and chemokines in the regulation of innate immunity and HIV infection. *Mol. Immunol.* 42, 161–182.
- Andersen, M.H., Schrama, D., Thor Stratén, P., and Becker, J.C. (2006). Cytotoxic T cells. *J. Invest. Dermatol.* 126, 32–41.
- Ang, Z., Er, J.Z., Tan, N.S., Lu, J., Liou, Y.C., Grosse, J., and Ding, J.L. (2016). Human and mouse monocytes display distinct signalling and cytokine profiles upon stimulation with FFAR2/FFAR3 short-chain fatty acid receptor agonists. *Sci. Rep.* 6, 1–15.
- Anunziato, L., Amoroso, S., Pannaccione, A., Cataldi, M., Pignataro, G., D'Alessio, A., Sirabella, R., Secondo, A., Sibaud, L., and Di Renzo, G.F. (2003). Apoptosis induced in neuronal cells by oxidative stress: Role played by caspases and intracellular calcium ions. In *Toxicology Letters, (Toxicol Lett)*, pp. 125–133.
- Antonopoulos, C., Russo, H.M., El Sanadi, C., Martin, B.N., Li, X., Kaiser, W.J., Mocarski, E.S., and

- Dubyak, G.R. (2015). Caspase-8 as an effector and regulator of NLRP3 inflammasome signaling. *J. Biol. Chem.* 290, 20167–20184.
- Asarat, M., Apostolopoulos, V., Vasiljevic, T., and Donkor, O. (2016). Short-chain fatty acids regulate cytokines and Th17/treg cells in human peripheral blood mononuclear cells in vitro. *Immunol. Invest.* 45, 205–222.
- Atarashi, K., Tanoue, T., Oshima, K., Suda, W., Nagano, Y., Nishikawa, H., Fukuda, S., Saito, T., Narushima, S., Hase, K., et al. (2013). Treg induction by a rationally selected mixture of Clostridia strains from the human microbiota. *Nature* 500, 232–236.
- Atreya, R., and Neurath, M.F. (2005). Involvement of IL-6 in the pathogenesis of inflammatory bowel disease and colon cancer. *Clin. Rev. Allergy Immunol.* 28, 187–195.
- Atreya, R., Mudter, J., Finotto, S., Müllberg, J., Jostock, T., Wirtz, S., Schütz, M., Bartsch, B., Holtmann, M., Becker, C., et al. (2000). Blockade of interleukin 6 trans signaling suppresses T-cell resistance against apoptosis in chronic intestinal inflammation: Evidence in Crohn disease and experimental colitis in vivo. *Nat. Med.* 6, 583–588.
- Balic, J.J., Albargy, H., Luu, K., Kirby, F.J., Jayasekara, W.S.N., Mansell, F., Garama, D.J., De Nardo, D., Baschuk, N., Louis, C., et al. (2020a). STAT3 serine phosphorylation is required for TLR4 metabolic reprogramming and IL-1 β expression. *Nat. Commun.* 11, 1–11.
- Balic, J.J., Albargy, H., Luu, K., Kirby, F.J., Jayasekara, W.S.N., Mansell, F., Garama, D.J., De Nardo, D., Baschuk, N., Louis, C., et al. (2020b). STAT3 serine phosphorylation is required for TLR4 metabolic reprogramming and IL-1 β expression. *Nat. Commun.* 11, 1–11.
- Barnhart, B.C., and Peter, M.E. (2003). The TNF receptor 1: A split personality complex. *Cell* 114, 148–150.
- Bauernfeind, F.G., Horvath, G., Stutz, A., Alnemri, E.S., MacDonald, K., Speert, D., Fernandes-Alnemri, T., Wu, J., Monks, B.G., Fitzgerald, K.A., et al. (2009). Cutting Edge: NF- κ B Activating Pattern Recognition and Cytokine Receptors License NLRP3 Inflammasome Activation by Regulating NLRP3 Expression. *J. Immunol.* 183, 787–791.
- Beachy, P.A., Karhadkar, S.S., and Berman, D.M. (2004). Tissue repair and stem cell renewal in carcinogenesis. *Nature* 432, 324–331.
- Bedoui, S., Herold, M.J., and Strasser, A. (2020). Emerging connectivity of programmed cell death pathways and its physiological implications. *Nat. Rev. Mol. Cell Biol.* 21, 678–695.
- Benítez-Burraco, A., Marotta, F., Torres Fuentes, C., Agustí, A., García-Pardo, M.P., López-Almela, I., Campillo, I., Maes, M., Romani-Pérez, M., and Sanz, Y. (2018). Interplay Between the Gut-Brain Axis, Obesity and Cognitive Function. *Front. Neurosci. | Wwww.Frontiersin.Org* 1, 155.
- Bergsbaken, T., Fink, S.L., and Cookson, B.T. (2009). Pyroptosis: Host cell death and inflammation. *Nat. Rev. Microbiol.* 7, 99–109.
- Bertrand, M.J.M., and Vandenabeele, P. (2010). Editorial: RIP1's function in NF-B activation: From master actor to onlooker. *Cell Death Differ.* 17, 379–380.
- Den Besten, G., Van Eunen, K., Groen, A.K., Venema, K., Reijngoud, D.J., and Bakker, B.M. (2013). The role of short-chain fatty acids in the interplay between diet, gut microbiota, and host energy metabolism. *J. Lipid Res.* 54, 2325–2340.

- Biasizzo, M., and Kopitar-Jerala, N. (2020). Interplay Between NLRP3 Inflammasome and Autophagy. *Front. Immunol.* *11*, 591803.
- Bilotta, A.J., and Cong, Y. (2019). Gut microbiota metabolite regulation of host defenses at mucosal surfaces: implication in precision medicine. *Precis. Clin. Med.* *2*, 110–119.
- Binder, H.J. (2009). Role of colonic short-chain fatty acid transport in diarrhea. *Annu. Rev. Physiol.* *72*, 297–313.
- Blaak, E.E., Canfora, E.E., Theis, S., Frost, G., Groen, A.K., Mithieux, G., Nauta, A., Scott, K., Stahl, B., van Harselaar, J., et al. (2020). Short chain fatty acids in human gut and metabolic health. *Benef. Microbes* *11*, 411–455.
- Bordon, Y. (2017). Cytokines: Oncostatin M - A new target in IBD? *Nat. Rev. Immunol.* *17*, 280.
- Braga, T.T., Forni, M.F., Correa-Costa, M., Ramos, R.N., Barbuto, J.A., Branco, P., Castoldi, A., Hiyane, M.I., Davanso, M.R., Latz, E., et al. (2017). Soluble Uric Acid Activates the NLRP3 Inflammasome. *Sci. Rep.* *7*.
- Broecker, F., and Moelling, K. (2019). Evolution of immune systems from viruses and transposable elements. *Front. Microbiol.* *10*, 51.
- Brynskov, J., Tvede, N., Andersen, C.B., and Vilien, M. (1992). Increased concentrations of interleukin 113, interleukin-2, and soluble interleukin-2 receptors in endoscopical mucosal biopsy specimens with active inflammatory bowel disease. *Gut* *33*, 55–58.
- Cai, J., Yang, J., and Jones, D.P. (1998). Mitochondrial control of apoptosis: The role of cytochrome c. *Biochim. Biophys. Acta - Bioenerg.* *1366*, 139–149.
- Cai, X., Chen, J., Xu, H., Liu, S., Jiang, Q.X., Halfmann, R., and Chen, Z.J. (2014). Prion-like polymerization underlies signal transduction in antiviral immune defense and inflammasome activation. *Cell* *156*, 1207–1222.
- Canfora, E.E., Jocken, J.W., and Blaak, E.E. (2015). Short-chain fatty acids in control of body weight and insulin sensitivity. *Nat. Rev. Endocrinol.* *11*, 577–591.
- Casén, C., Vebø, H.C., Sekelja, M., Hegge, F.T., Karlsson, M.K., Cierniejewska, E., Dzankovic, S., Frøyland, C., Nestestog, R., Engstrand, L., et al. (2015). Deviations in human gut microbiota: A novel diagnostic test for determining dysbiosis in patients with IBS or IBD. *Aliment. Pharmacol. Ther.* *42*, 71–83.
- Caspani, G., Kennedy, S., Foster, J.A., and Swann, J. (2019). Gut microbial metabolites in depression: Understanding the biochemical mechanisms. *Microb. Cell* *6*, 454–481.
- Chaplin, D.D. (2003). 1. Overview of the immune response. *J. Allergy Clin. Immunol.* *111*.
- Chauhan, D., Vande Walle, L., and Lamkanfi, M. (2020). Therapeutic modulation of inflammasome pathways. *Immunol. Rev.* *297*, 123–138.
- Chen, J., Wang, S., Fu, R., Zhou, M., Zhang, T., Pan, W., Yang, N., and Huang, Y. (2018). RIP3 dependent NLRP3 inflammasome activation is implicated in acute lung injury in mice. *J. Transl. Med.* *16*.
- Chen, Q.L., Yin, H.R., He, Q.Y., and Wang, Y. (2021). Targeting the NLRP3 inflammasome as new therapeutic avenue for inflammatory bowel disease. *Biomed. Pharmacother.* *138*, 111442.
- Chen, S., Lv, X., Hu, B., Shao, Z., Wang, B., Ma, K., Lin, H., and Cui, M. (2017). RIPK1/RIPK3/MLKL-

mediated necroptosis contributes to compression-induced rat nucleus pulposus cells death. *Apoptosis* 22, 626–638.

Chung, E.Y., Liu, J., Homma, Y., Zhang, Y., Brendolan, A., Saggese, M., Han, J., Silverstein, R., Selleri, L., and Ma, X. (2007). Interleukin-10 Expression in Macrophages during Phagocytosis of Apoptotic Cells Is Mediated by Homeodomain Proteins Pbx1 and Prep-1. *Immunity* 27, 952–964.

Cirillo, G., Soreq, H., Qing Wang, D., Li, J., Wei, P., Yang, F., Zheng, Q., and Tang, W. (2019). The Potential Role of the NLRP3 Inflammasome Activation as a Link Between Mitochondria ROS Generation and Neuroinflammation in Postoperative Cognitive Dysfunction. *HYPOTHESIS AND THEORY* 21.

Coll, R.C., Robertson, A.A.B., Chae, J.J., Higgins, S.C., Muñoz-Planillo, R., Inserra, M.C., Vetter, I., Dungan, L.S., Monks, B.G., Stutz, A., et al. (2015). A small-molecule inhibitor of the NLRP3 inflammasome for the treatment of inflammatory diseases. *Nat. Med.* 21, 248–257.

Cooper, M.D., and Alder, M.N. (2006). The evolution of adaptive immune systems. *Cell* 124, 815–822.

Corrêa-Oliveira, R., Fachi, J.L., Vieira, A., Sato, F.T., and Vinolo, M.A.R. (2016). Regulation of immune cell function by short-chain fatty acids. *Clin. Transl. Immunol.* 5, 1–8.

da Costa, L.S., Outlioua, A., Anginot, A., Akarid, K., and Arnoult, D. (2019). RNA viruses promote activation of the NLRP3 inflammasome through cytopathogenic effect-induced potassium efflux. *Cell Death Dis.* 10.

Couper, K.N., Blount, D.G., and Riley, E.M. (2008). IL-10: The Master Regulator of Immunity to Infection. *J. Immunol.* 180, 5771–5777.

Crotty, S., Felgner, P., Davies, H., Glidewell, J., Villarreal, L., and Ahmed, R. (2003). Cutting Edge: Long-Term B Cell Memory in Humans after Smallpox Vaccination. *J. Immunol.* 171, 4969–4973.

Cruz, C.M., Rinna, A., Forman, H.J., Ventura, A.L.M., Persechini, P.M., and Ojcius, D.M. (2007). ATP activates a reactive oxygen species-dependent oxidative stress response and secretion of proinflammatory cytokines in macrophages. *J. Biol. Chem.* 282, 2871–2879.

Danese, S., Vermeire, S., Hellstern, P., Panaccione, R., Rogler, G., Fraser, G., Kohn, A., Desreumaux, P., Leong, rupert W., Comer, gail M., et al. (2019). Randomised trial and open-label extension study of an anti-interleukin-6 antibody in Crohn's disease (ANDANTE I and II). *Gut* 68, 40–48.

Darnell, J.E., Kerr, I.M., and Stark, G.R. (1994). Jak-STAT pathways and transcriptional activation in response to IFNs and other extracellular signaling proteins. *Science* (80-.). 264, 1415–1421.

Declercq, W., Vanden Berghe, T., and Vandenabeele, P. (2009). RIP Kinases at the Crossroads of Cell Death and Survival. *Cell* 138, 229–232.

Dempsey, P.W., Vaidya, S.A., and Cheng, G. (2003). The Art of War: Innate and adaptive immune responses. *Cell. Mol. Life Sci.* 60, 2604–2621.

Desu, H.L., Plastini, M., Illiano, P., Bramlett, H.M., Dietrich, W.D., De Rivero Vaccari, J.P., Brambilla, R., and Keane, R.W. (2020a). IC100: A novel anti-ASC monoclonal antibody improves functional outcomes in an animal model of multiple sclerosis. *J. Neuroinflammation* 17.

Desu, H.L., Plastini, M., Illiano, P., Bramlett, H.M., Dietrich, W.D., De Rivero Vaccari, J.P., Brambilla, R., and Keane, R.W. (2020b). IC100: A novel anti-ASC monoclonal antibody improves functional

- outcomes in an animal model of multiple sclerosis. *J. Neuroinflammation* 17.
- Dhuriya, Y.K., and Sharma, D. (2018). Necroptosis: A regulated inflammatory mode of cell death. *J. Neuroinflammation* 15, 1–9.
- Dick, M.S., Sborgi, L., Rühl, S., Hiller, S., and Broz, P. (2016). ASC filament formation serves as a signal amplification mechanism for inflammasomes. *Nat. Commun.* 7, 1–13.
- Dinareello, C.A. (2011). Blocking interleukin-1 β in acute and chronic autoinflammatory diseases. In *Journal of Internal Medicine*, pp. 16–28.
- Ding, J., and Shao, F. (2017). SnapShot: The Noncanonical Inflammasome. *Cell* 168, 544-544.e1.
- Dondelinger, Y., Darding, M., Bertrand, M.J.M., and Walczak, H. (2016). Poly-ubiquitination in TNFR1-mediated necroptosis. *Cell. Mol. Life Sci.* 73, 2165–2176.
- Dostert, C., Pétrilli, V., Van Bruggen, R., Steele, C., Mossman, B.T., and Tschopp, J. (2008). Innate immune activation through Nalp3 inflammasome sensing of asbestos and silica. *Science* (80-.). 320, 674–677.
- Drummond, R.A., and Lionakis, M.S. (2019). Organ-specific mechanisms linking innate and adaptive antifungal immunity. *Semin. Cell Dev. Biol.* 89, 78–90.
- Du, C., Fang, M., Li, Y., Li, L., and Wang, X. (2000). Smac, a mitochondrial protein that promotes cytochrome c-dependent caspase activation by eliminating IAP inhibition. *Cell* 102, 33–42.
- Duda, P., Wiśniewski, J., Wójtowicz, T., Wójcicka, O., Jaśkiewicz, M., Drulis-Fajdasz, D., Rakus, D., McCubrey, J.A., and Gizak, A. (2018). Targeting GSK3 signaling as a potential therapy of neurodegenerative diseases and aging. *Expert Opin. Ther. Targets* 22, 833–848.
- Duewell, P., Kono, H., Rayner, K.J., Sirois, C.M., Vladimer, G., Bauernfeind, F.G., Abela, G.S., Franchi, L., Núñez, G., Schnurr, M., et al. (2010a). NLRP3 inflammasomes are required for atherogenesis and activated by cholesterol crystals. *Nature* 464, 1357–1361.
- Duewell, P., Kono, H., Rayner, K.J., Sirois, C.M., Vladimer, G., Bauernfeind, F.G., Abela, G.S., Franchi, L., Núñez, G., Schnurr, M., et al. (2010b). NLRP3 inflammasomes are required for atherogenesis and activated by cholesterol crystals. *Nature* 464, 1357–1361.
- Duewell, P., Kono, H., Rayner, K.J., Sirois, C.M., Vladimer, G., Bauernfeind, F.G., Abela, G.S., Franchi, L., Nuñez, G., Schnurr, M., et al. (2010c). LETTERS NLRP3 inflammasomes are required for atherogenesis and activated by cholesterol crystals.
- Fang, C., Gu, L., Smerin, D., Mao, S., and Xiong, X. (2017). The Interrelation between Reactive Oxygen Species and Autophagy in Neurological Disorders. *Oxid. Med. Cell. Longev.* 2017.
- Feagan, B.G., Sandborn, W.J., D’Haens, G., Panés, J., Kaser, A., Ferrante, M., Louis, E., Franchimont, D., Dewit, O., Seidler, U., et al. (2017). Induction therapy with the selective interleukin-23 inhibitor risankizumab in patients with moderate-to-severe Crohn’s disease: a randomised, double-blind, placebo-controlled phase 2 study. *Lancet* 389, 1699–1709.
- Feng, W., Ao, H., and Peng, C. (2018). Gut microbiota, short-chain fatty acids, and herbal medicines. *Front. Pharmacol.* 9, 1354.
- Feoktistova, M., Geserick, P., Kellert, B., Dimitrova, D.P., Langlais, C., Hupe, M., Cain, K., MacFarlane, M., Häcker, G., and Leverkus, M. (2011). CIAPs Block Ripoptosome Formation, a RIP1/Caspase-8 Containing Intracellular Cell Death Complex Differentially Regulated by cFLIP

Isoforms. *Mol. Cell* 43, 449–463.

Flajnik, M.F. (2018). A cold-blooded view of adaptive immunity. *Nat. Rev. Immunol.* 18, 438–453.

Flajnik, M.F., and Kasahara, M. (2010a). Origin and evolution of the adaptive immune system: Genetic events and selective pressures. *Nat. Rev. Genet.* 11, 47–59.

Flajnik, M.F., and Kasahara, M. (2010b). Origin and evolution of the adaptive immune system: Genetic events and selective pressures. *Nat. Rev. Genet.* 11, 47–59.

Foley, J.F. (2015). Blocking DAMPS but not PAMPS. *Sci. Signal.* 8, ec13–ec13.

Fu, H., Shi, Y.Q., and Mo, S.J. (2004). Effect of short-chain fatty acids on the proliferation and differentiation of the human colonic adenocarcinoma cell line Caco-2. *Chin. J. Dig. Dis.* 5, 115–117.

Fulda, S., and Debatin, K.M. (2006). Extrinsic versus intrinsic apoptosis pathways in anticancer chemotherapy. *Oncogene* 25, 4798–4811.

Fuss, I.J., Becker, C., Yang, Z., Groden, C., Hornung, R.L., Heller, F., Neurath, M.F., Strober, W., and Mannon, P.J. (2006). Both IL-12p70 and IL-23 are synthesized during active Crohn's disease and are down-regulated by treatment with anti-IL-12 p40 monoclonal antibody. *Inflamm. Bowel Dis.* 12, 9–15.

Gaidt, M.M., Ebert, T.S., Chauhan, D., Schmidt, T., Schmid-Burgk, J.L., Rapino, F., Robertson, A.A.B., Cooper, M.A., Graf, T., and Hornung, V. (2016). Human Monocytes Engage an Alternative Inflammasome Pathway. *Immunity* 44, 833–846.

Gao, Z., Tian, Y., Wang, J., Yin, Q., Wu, H., Li, Y.M., and Jiang, X. (2007). A dimeric Smac/Diablo peptide directly relieves caspase-3 inhibition by XIAP: Dynamic and cooperative regulation of XIAP by Smac/Diablo. *J. Biol. Chem.* 282, 30718–30727.

Geuking, M.B., Cahenzli, J., Lawson, M.A.E., Ng, D.C.K., Slack, E., Hapfelmeier, S., McCoy, K.D., and Macpherson, A.J. (2011). Intestinal Bacterial Colonization Induces Mutualistic Regulatory T Cell Responses. *Immunity* 34, 794–806.

Glowacki, S., Synowiec, E., and Blasiak, J. (2013). The role of mitochondrial DNA damage and repair in the resistance of BCR/ABL-expressing cells to tyrosine kinase inhibitors. *Int. J. Mol. Sci.* 14, 16348–16364.

Gonçalves, P., Araújo, J.R., and Di Santo, J.P. (2018). A cross-talk between microbiota-derived short-chain fatty acids and the host mucosal immune system regulates intestinal homeostasis and inflammatory bowel disease. *Inflamm. Bowel Dis.* 24, 558–572.

Gordon, S., and Plüddemann, A. (2018). Macrophage clearance of apoptotic cells: A critical assessment. *Front. Immunol.* 9, 127.

Gordy, C., Pua, H., Sempowski, G.D., and He, Y.W. (2011). Regulation of steady-state neutrophil homeostasis by macrophages. *Blood* 117, 618–629.

Gregory, C.D., and Devitt, A. (2004). The macrophage and the apoptotic cell: An innate immune interaction viewed simplistically? *Immunology* 113, 1–14.

Guan, Q. (2019). A Comprehensive Review and Update on the Pathogenesis of Inflammatory Bowel Disease. *J. Immunol. Res.* 2019.

Gulati, A., Kaur, D., Krishna Prasad, G.V.R., and Mukhopadhaya, A. (2018). PRR function of innate immune receptors in recognition of bacteria or bacterial ligands. In *Advances in Experimental Medicine and Biology*, (Springer New York LLC), pp. 255–280.

- Gunness, P., and Gidley, M.J. (2010). Mechanisms underlying the cholesterol-lowering properties of soluble dietary fibre polysaccharides. *Food Funct.* *1*, 149–155.
- Guo, C., Fu, R., Wang, S., Huang, Y., Li, X., Zhou, M., Zhao, J., and Yang, N. (2018). NLRP3 inflammasome activation contributes to the pathogenesis of rheumatoid arthritis. *Clin. Exp. Immunol.* *194*, 231–243.
- Guo, H., Callaway, J.B., and Ting, J.P.Y. (2015). Inflammasomes: Mechanism of action, role in disease, and therapeutics. *Nat. Med.* *21*, 677–687.
- Gurcel, L., Abrami, L., Girardin, S., Tschopp, J., and van der Goot, F.G. (2006). Caspase-1 Activation of Lipid Metabolic Pathways in Response to Bacterial Pore-Forming Toxins Promotes Cell Survival. *Cell* *126*, 1135–1145.
- Gurung, P., Anand, P.K., Malireddi, R.K.S., Vande Walle, L., Van Opdenbosch, N., Dillon, C.P., Weinlich, R., Green, D.R., Lamkanfi, M., and Kanneganti, T.-D. (2014). FADD and Caspase-8 Mediate Priming and Activation of the Canonical and Noncanonical Nlrp3 Inflammasomes. *J. Immunol.* *192*, 1835–1846.
- Haar, E. Vander, Lee, S. il, Bandhakavi, S., Griffin, T.J., and Kim, D.H. (2007). Insulin signalling to mTOR mediated by the Akt/PKB substrate PRAS40. *Nat. Cell Biol.* *9*, 316–323.
- Hamarsheh, S., and Zeiser, R. (2020). NLRP3 Inflammasome Activation in Cancer: A Double-Edged Sword. *Front. Immunol.* *11*, 1444.
- Haque, M.E., Akther, M., Jakaria, M., Kim, I.S., Azam, S., and Choi, D.K. (2020). Targeting the microglial NLRP3 inflammasome and its role in Parkinson's disease. *Mov. Disord.* *35*, 20–33.
- Hartman, D.S., Tracey, D.E., Lemos, B.R., Erlich, E.C., Burton, R.E., Keane, D.M., Patel, R., Kim, S., Bhol, K.C., Harris, M.S., et al. (2016). Effects of AVX-470, an oral, locally acting anti-tumour necrosis factor antibody, on tissue biomarkers in patients with active ulcerative colitis. *J. Crohn's Colitis* *10*, 641–649.
- He, Y., Varadarajan, S., Muñoz-Planillo, R., Burberry, A., Nakamura, Y., and Núñez, G. (2014). 3,4-Methylenedioxy- β' -nitrostyrene inhibits NLRP3 inflammasome activation by blocking assembly of the inflammasome. *J. Biol. Chem.* *289*, 1142–1150.
- He, Y., Hara, H., and Núñez, G. (2016). Mechanism and Regulation of NLRP3 Inflammasome Activation. *Trends Biochem. Sci.* *41*, 1012–1021.
- Heiss, C.N., and Olofsson, L.E. (2019). The role of the gut microbiota in development, function and disorders of the central nervous system and the enteric nervous system. *J. Neuroendocrinol.* *31*.
- Hendrickson, B.A., Gokhale, R., and Cho, J.H. (2002). Clinical aspects and pathophysiology of inflammatory bowel disease. *Clin. Microbiol. Rev.* *15*, 79–94.
- Heneka, M.T., Kummer, M.P., Stutz, A., Delekate, A., Schwartz, S., Vieira-Saecker, A., Griep, A., Axt, D., Remus, A., Tzeng, T.C., et al. (2013). NLRP3 is activated in Alzheimer's disease and contributes to pathology in APP/PS1 mice. *Nature* *493*, 674–678.
- Hilgenberg, E., Shen, P., Dang, V.D., Ries, S., Sakwa, I., and Fillatreau, S. (2014). Interleukin-10-producing B cells and the regulation of immunity. *Curr. Top. Microbiol. Immunol.* *380*, 69–92.
- Hoareau, L., Bencharif, K., Rondeau, P., Murumalla, R., Ravanan, P., Tallet, F., Delarue, P., Cesari, M., and Festy, F. (2010). Signaling pathways involved in LPS induced TNF α production in human

adipocytes. *J. Inflamm.* 7, 1.

Hoffman, H.M., Mueller, J.L., Broide, D.H., Wanderer, A.A., and Kolodner, R.D. (2001). Mutation of a new gene encoding a putative pyrin-like protein causes familial cold autoinflammatory syndrome and Muckle-Wells syndrome. *Nat. Genet.* 29, 301–305.

Hou, J., Wang, L., Quan, R., Fu, Y., Zhang, H., and Feng, W.H. (2012). Induction of interleukin-10 is dependent on p38 mitogen-activated protein kinase pathway in macrophages infected with porcine reproductive and respiratory syndrome virus. *Virology* 9, 165.

Hu, J.J., Liu, X., Xia, S., Zhang, Z., Zhang, Y., Zhao, J., Ruan, J., Luo, X., Lou, X., Bai, Y., et al. (2020). FDA-approved disulfiram inhibits pyroptosis by blocking gasdermin D pore formation. *Nat. Immunol.* 21, 736–745.

Hu, Y.W., Zhang, J., Wu, X.M., Cao, L., Nie, P., and Chang, M.X. (2018). TBK1-binding kinase 1 (TBK1) isoforms negatively regulate type I interferon induction by inhibiting TBK1-IRF3 interaction and IRF3 phosphorylation. *Front. Immunol.* 9.

Huang, Q.Q., Perlman, H., Huang, Z., Birkett, R., Kan, L., Agrawal, H., Misharin, A., Gurbuxani, S., Crispino, J.D., and Pope, R.M. (2010). FLIP: A novel regulator of macrophage differentiation and granulocyte homeostasis. *Blood* 116, 4968–4977.

Huda-Faujan, N., Abdulmir, A.S., Fatimah, A.B., Anas, O.M., Shuhaimi, M., Yazid, A.M., and Loong, Y.Y. (2010). The Impact of the Level of the Intestinal Short Chain Fatty Acids in Inflammatory Bowel Disease Patients Versus Healthy Subjects. *Open Biochem. J.* 4, 53–58.

Humphries, F., Yang, S., Wang, B., and Moynagh, P.N. (2015). RIP kinases: Key decision makers in cell death and innate immunity. *Cell Death Differ.* 22, 225–236.

Hunt, R. (2011). Innate or non-specific immunity. Univ. South Carolina.

Hurtubise, R., Audiger, C., Dominguez-Punaro, M.C., Chabot-Roy, G., Chognard, G., Raymond-Marchand, L., Coderre, L., Chemtob, S., Michnick, S.W., Rioux, J.D., et al. (2019). Induced and spontaneous colitis mouse models reveal complex interactions between IL-10 and IL-12/IL-23 pathways. *Cytokine* 121, 154738.

Ihle, J.N. (1995). Cytokine receptor signalling. *Nature* 377, 591–594.

Inatomi, O., Andoh, A., Kitamura, K.I., Yasui, H., Zhang, Z., and Fujiyama, Y. (2005). Butyrate blocks interferon- γ -inducible protein-10 release in human intestinal subepithelial myofibroblasts. *J. Gastroenterol.* 40, 483–489.

Ip, W.K.E., Hoshi, N., Shouval, D.S., Snapper, S., and Medzhitov, R. (2017). Anti-inflammatory effect of IL-10 mediated by metabolic reprogramming of macrophages. *Science* (80-.). 356, 513–519.

Ishikawa, T., and Nanjo, F. (2009). Dietary cycloinulooligosaccharides enhance intestinal immunoglobulin a production in Mice. *Biosci. Biotechnol. Biochem.* 73, 677–682.

Ising, C., Venegas, C., Zhang, S., Scheiblich, H., Schmidt, S. V., Vieira-Saecker, A., Schwartz, S., Albasset, S., McManus, R.M., Tejera, D., et al. (2019). NLRP3 inflammasome activation drives tau pathology. *Nature* 575, 669–673.

Italiani, P., and Boraschi, D. (2014). From monocytes to M1/M2 macrophages: Phenotypical vs. functional differentiation. *Front. Immunol.* 5, 1–22.

Iwasaki, A., and Medzhitov, R. (2015). Control of adaptive immunity by the innate immune system.

Nat. Immunol. 16, 343–353.

Jansen, T., Klück, V., Janssen, M., Comarniceanu, A., Efdé, M., Scribner, C., Barrow, R., Skouras, D., Dinarello, C., and Joosten, L. (2019). P160 The first phase 2A proof-of-concept study of a selective NLRP3 inflammasome inhibitor, dapansutrile™ (OLT1177™), in acute gout. In *Annals of the Rheumatic Diseases*, (BMJ), pp. A70–A71.

Jennings-almeida, B., Castelpoggi, J.P., Erivan, S., Ferreira, E.D.O., Regina, M.C.P., Echevarria-lima, J., Moreira-souza, A.C.A., Mariño, E., Mackay, C.R., Zamboni, D.S., et al. (2021). Dietary Fiber Drives IL-1 β – Dependent Peritonitis Induced by *Bacteroides fragilis* via Activation of the NLRP3 Inflammasome.

Jennings-Almeida, B., Castelpoggi, J.P., Ramos-Junior, E.S., Ferreira, E. de O., Domingues, R.M.C.P., Echevarria-Lima, J., Coutinho-Silva, R., Moreira-Souza, A.C.A., Mariño, E., Mackay, C.R., et al. (2021). Dietary Fiber Drives IL-1 β –Dependent Peritonitis Induced by *Bacteroides fragilis* via Activation of the NLRP3 Inflammasome. *J. Immunol.* 206, 2441–2452.

Jiang, X., and Wang, X. (2004). Cytochrome C-mediated apoptosis. *Annu. Rev. Biochem.* 73, 87–106.

Jofra, T., Galvani, G., Cosorich, I., De Giorgi, L., Annoni, A., Vecchione, A., Sorini, C., Falcone, M., and Fousteri, G. (2019). Experimental colitis in IL-10-deficient mice ameliorates in the absence of PTPN22. *Clin. Exp. Immunol.* 197, 263–275.

Jounai, N., Kobiyama, K., Takeshita, F., Ishii, K.J., Gekara, N., Zamboni, D.S., and Shi, Y. (2013). Recognition of damage-associated molecular patterns related to nucleic acids during inflammation and vaccination.

Juliana, C., Fernandes-Alnemri, T., Wu, J., Datta, P., Solorzano, L., Yu, J.W., Meng, R., Quong, A.A., Latz, E., Scott, C.P., et al. (2010). Anti-inflammatory compounds parthenolide and bay 11-7082 are direct inhibitors of the inflammasome. *J. Biol. Chem.* 285, 9792–9802.

Julien, O., and Wells, J.A. (2017). Caspases and their substrates. *Cell Death Differ.* 24, 1380–1389.

Kaisar, M.M.M., Pelgrom, L.R., van der Ham, A.J., Yazdanbakhsh, M., and Everts, B. (2017). Butyrate conditions human dendritic cells to prime type 1 regulatory T cells via both histone deacetylase inhibition and G protein-coupled receptor 109A signaling. *Front. Immunol.* 8, 1–14.

Kalina, U., Koyama, N., Hosoda, T., Nuernberger, H., Sato, K., Hoelzer, D., Herweck, F., Manigold, T., Singer, M. V., Rossol, S., et al. (2002). Enhanced production of IL-18 in butyrate-treated intestinal epithelium by stimulation of the proximal promoter region. *Eur. J. Immunol.* 32, 2635–2643.

Karaghiosoff, M., Neubauer, H., Lassnig, C., Kovarik, P., Schindler, H., Pircher, H., McCoy, B., Bogdan, C., Decker, T., Brem, G., et al. (2000). Partial impairment of cytokine responses in Tyk2-deficient mice. *Immunity* 13, 549–560.

Kashani, A., and Schwartz, D.A. (2019). The expanding role of anti-IL-12 and/or anti-IL-23 antibodies in the treatment of inflammatory bowel disease. *Gastroenterol. Hepatol.* 15, 255–265.

Kasten, K.R., Muenzer, J.T., and Caldwell, C.C. (2010). Neutrophils are significant producers of IL-10 during sepsis. *Biochem. Biophys. Res. Commun.* 393, 28–31.

Kaufmann, F.N., Costa, A.P., Ghisleni, G., Diaz, A.P., Rodrigues, A.L.S., Peluffo, H., and Kaster, M.P. (2017). NLRP3 inflammasome-driven pathways in depression: Clinical and preclinical findings. *Brain*.

Behav. Immun. 64, 367–383.

Kawai, T., and Akira, S. (2009). The roles of TLRs, RLRs and NLRs in pathogen recognition. *Int. Immunol.* 21, 317–337.

Kelley, N., Jeltema, D., Duan, Y., and He, Y. (2019). The NLRP3 inflammasome: An overview of mechanisms of activation and regulation. *Int. J. Mol. Sci.* 20.

Kessler, B., Rinchai, D., Kewcharoenwong, C., Nithichanon, A., Biggart, R., Hawrylowicz, C.M., Bancroft, G.J., and Lertmemongkolchai, G. (2017). Interleukin 10 inhibits pro-inflammatory cytokine responses and killing of *Burkholderia pseudomallei*. *Sci. Rep.* 7, 1–11.

Keubler, L.M., Buettner, M., Häger, C., and Bleich, A. (2015). A multihit model: Colitis lessons from the interleukin-10-deficient mouse. *Inflamm. Bowel Dis.* 21, 1967–1975.

Khaw-on, P., and Banjerdpongchai, R. (2012). Induction of intrinsic and extrinsic apoptosis pathways in the human leukemic MOLT-4 cell line by terpinen-4-ol. *Asian Pacific J. Cancer Prev.* 13, 3073–3076.

Kim, D., Langmead, B., and Salzberg, S.L. (2015). HISAT: A fast spliced aligner with low memory requirements. *Nat. Methods* 12, 357–360.

Kim, J.Y., Morgan, M., Kim, D.G., Lee, J.Y., Bai, L., Lin, Y., Liu, Z.G., and Kim, Y.S. (2011). TNF α -induced noncanonical NF- κ B activation is attenuated by RIP1 through stabilization of TRAF2. *J. Cell Sci.* 124, 647–656.

Kimberley, F.C., Lobito, A.A., Siegel, R.M., and Sreaton, G.R. (2007). Falling into TRAPS - Receptor misfolding in the TNF receptor 1-associated periodic fever syndrome. *Arthritis Res. Ther.* 9.

Kingsbury, S.R., Conaghan, P.G., and McDermott, M.F. (2011). The role of the NLRP3 inflammasome in gout. *J. Inflamm. Res.* 4, 39–49.

Kinsella, R.J., Kähäri, A., Haider, S., Zamora, J., Proctor, G., Spudich, G., Almeida-King, J., Staines, D., Derwent, P., Kerhornou, A., et al. (2011). Ensembl BioMarts: A hub for data retrieval across taxonomic space. *Database* 2011.

Kluck, R.M., Bossy-Wetzell, E., Green, D.R., and Newmeyer, D.D. (1997). The release of cytochrome c from mitochondria: A primary site for Bcl-2 regulation of apoptosis. *Science* (80-.). 275, 1132–1136.

Koelink, P.J., Bloemendaal, F.M., Li, B., Westera, L., Vogels, E.W.M., Van Roest, M., Gludemans, A.K., Van 'T Wout, A.B., Korf, H., Vermeire, S., et al. (2020). Anti-TNF therapy in IBD exerts its therapeutic effect through macrophage IL-10 signalling. *Gut* 69, 1053–1063.

Kontoyiannis, D., Kotlyarov, A., Carballo, E., Alexopoulou, L., Blackshear, P.J., Gaestel, M., Davis, R., Flavell, R., and Kollias, G. (2001). Interleukin-10 targets p38 MAPK to modulate ARE-dependent TNF mRNA translation and limit intestinal pathology. *EMBO J.* 20, 3760–3770.

Kopitar-Jerala, N. (2017). The role of interferons in inflammation and inflammasome activation. *Front. Immunol.* 8, 873.

Kourtzelis, I., Hajishengallis, G., and Chavakis, T. (2020). Phagocytosis of Apoptotic Cells in Resolution of Inflammation. *Front. Immunol.* 11, 553.

Koussounadis, A., Langdon, S.P., Um, I.H., Harrison, D.J., and Smith, V.A. (2015). Relationship between differentially expressed mRNA and mRNA-protein correlations in a xenograft model system.

Sci. Rep. 5, 1–9.

Krebs, H.A., Gurevich, P., Camacho, M., Bonete, M.J., Lambie, H.J., Hough, D.W., Biology, C., Cavicchioli, R., Fuchs, G., Alber, B.E., et al. (2011). Induction of colonic regulatory T cells by indigenous *Clostridium* species. *Sci. ...* 337–341.

Kubelkova, K., and Macela, A. (2019). Innate Immune Recognition: An Issue More Complex Than Expected. *Front. Cell. Infect. Microbiol.* 9, 241.

Kuriakose, T., Man, S.M., Subbarao Malireddi, R.K., Karki, R., Kesavardhana, S., Place, D.E., Neale, G., Vogel, P., and Kanneganti, T.D. (2016). ZBP1/DAI is an innate sensor of influenza virus triggering the NLRP3 inflammasome and programmed cell death pathways. *Sci. Immunol.* 1.

Kwaik, Y.A., Haribabu, B., Vankayalapati, R., Kanneganti, T.-D., Samir, P., and Malireddi, R.K.S. (2020). The PANoptosome: A Deadly Protein Complex Driving Pyroptosis, Apoptosis, and Necroptosis (PANoptosis). *Front. Cell. Infect. Microbiol.* | www.frontiersin.org 1, 238.

Labzin, L.I., Lauterbach, M.A.R., and Latz, E. (2016). Interferons and inflammasomes: Cooperation and counterregulation in disease. *J. Allergy Clin. Immunol.* 138, 37–46.

Lacy, P., and Stow, J.L. (2011). Cytokine release from innate immune cells: Association with diverse membrane trafficking pathways. *Blood* 118, 9–18.

Lal, H., Ahmad, F., Woodgett, J., and Force, T. (2015). The GSK-3 family as therapeutic target for myocardial diseases. *Circ. Res.* 116, 138–149.

Lamkanfi, M., and Dixit, V.M. (2009). Inflammasomes: Guardians of cytosolic sanctity. *Immunol. Rev.* 227, 95–105.

Lamkanfi, M., and Kanneganti, T.D. (2010). Nlrp3: An immune sensor of cellular stress and infection. *Int. J. Biochem. Cell Biol.* 42, 792–795.

Land, W.G. (2020). Use of DAMPs and SAMPs as Therapeutic Targets or Therapeutics: A Note of Caution. *Mol. Diagnosis Ther.* 24, 251–262.

Lerner, A.C., David, M., Feldman, G.M., Igarashi, K.I., Hackett, R.H., Webb, D.S.A., Sweitzer, S.M., Petricoin, E.F., and Finbloom, D.S. (1993). Tyrosine phosphorylation of DNA binding proteins by multiple cytokines. *Science* (80-). 261, 1730–1733.

Latres, E., Amini, A.R., Amini, A.A., Griffiths, J., Martin, F.J., Wei, Y., Hsin, C.L., Yancopoulos, G.D., and Glass, D.J. (2005). Insulin-like growth factor-1 (IGF-1) inversely regulates atrophy-induced genes via the phosphatidylinositol 3-kinase/Akt/mammalian target of rapamycin (PI3K/Akt/mTOR) pathway. *J. Biol. Chem.* 280, 2737–2744.

Lee, T.S., and Chau, L.Y. (2002). Heme oxygenase-1 mediates the anti-inflammatory effect of interleukin-10 in mice. *Nat. Med.* 8, 240–246.

Lee, H.M., Kim, J.J., Kim, H.J., Shong, M., Ku, B.J., and Jo, E.K. (2013). Upregulated NLRP3 inflammasome activation in patients with type 2 diabetes. *Diabetes* 62, 194–204.

Lee, S.H., Kwon, J. eun, and Cho, M. La (2018). Immunological pathogenesis of inflammatory bowel disease. *Intest. Res.* 16, 26–42.

Legler, D.F., Micheau, O., Doucey, M.A., Tschopp, J., and Bron, C. (2003). Recruitment of TNF receptor 1 to lipid rafts is essential for TNF α -mediated NF- κ B activation. *Immunity* 18, 655–664.

Li, L., Wang, X.C., Gong, P.T., Zhang, N., Zhang, X., Li, S., Li, X., Liu, S.X., Zhang, X.X., Li, W., et al.

- (2020). ROS-mediated NLRP3 inflammasome activation participates in the response against *Neospora caninum* infection. *Parasites and Vectors* 13, 449.
- Li, M., van Esch, B.C.A.M., Henricks, P.A.J., Folkerts, G., and Garsen, J. (2018). The anti-inflammatory effects of short chain fatty acids on lipopolysaccharide- or tumor necrosis factor α -stimulated endothelial cells via activation of GPR41/43 and inhibition of HDACs. *Front. Pharmacol.* 9, 1–12.
- Li, Y., De Haar, C., Peppelenbosch, M.P., and Van Der Woude, C.J. (2012). New insights into the role of STAT3 in IBD. *Inflamm. Bowel Dis.* 18, 1177–1183.
- Liberzon, A., Birger, C., Thorvaldsdóttir, H., Ghandi, M., Mesirov, J.P., and Tamayo, P. (2015). The Molecular Signatures Database Hallmark Gene Set Collection. *Cell Syst.* 1, 417–425.
- Limdi, J.K. (2018). Dietary practices and inflammatory bowel disease. *Indian J. Gastroenterol.* 37, 284–292.
- Lin, W.W., and Karin, M. (2007). A cytokine-mediated link between innate immunity, inflammation, and cancer. *J. Clin. Invest.* 117, 1175–1183.
- Littman, D.R., and Pamer, E.G. (2011). Role of the commensal microbiota in normal and pathogenic host immune responses. *Cell Host Microbe* 10, 311–323.
- Liu, J., Yuan, C., Pu, L., and Wang, J. (2017). Nutrient deprivation induces apoptosis of nucleus pulposus cells via activation of the BNIP3/AIF signalling pathway. *Mol. Med. Rep.* 16, 7253–7260.
- Liu, W., Luo, X., Tang, J., Mo, Q., Zhong, H., Zhang, H., and Feng, F. (2020). A bridge for short-chain fatty acids to affect inflammatory bowel disease, type 1 diabetes, and non-alcoholic fatty liver disease positively: by changing gut barrier. *Eur. J. Nutr.* 1–14.
- Liu, X., Zhang, Z., Ruan, J., Pan, Y., Magupalli, V.G., Wu, H., and Lieberman, J. (2016a). Inflammasome-activated gasdermin D causes pyroptosis by forming membrane pores. *Nature* 535, 153–158.
- Liu, Y., Beyer, A., and Aebersold, R. (2016b). On the Dependency of Cellular Protein Levels on mRNA Abundance. *Cell* 165, 535–550.
- Llorens-Martín, M., Jurado, J., Hernández, F., and Ávila, J. (2014). GSK-3 β , a pivotal kinase in Alzheimer disease. *Front. Mol. Neurosci.* 7, 46.
- Lopez-Castejon, G. (2020). Control of the inflammasome by the ubiquitin system. *FEBS J.* 287, 11–26.
- Lu, A., Magupalli, V.G., Ruan, J., Yin, Q., Atianand, M.K., Vos, M.R., Schröder, G.F., Fitzgerald, K.A., Wu, H., and Egelman, E.H. (2014). Unified polymerization mechanism for the assembly of asc-dependent inflammasomes. *Cell* 156, 1193–1206.
- Lukens, J.R., Gross, J.M., and Kanneganti, T.D. (2012). IL-1 family cytokines trigger sterile inflammatory disease. *Front. Immunol.* 3.
- Lupp, C., Robertson, M.L., Wickham, M.E., Sekirov, I., Champion, O.L., Gaynor, E.C., and Finlay, B.B. (2007). Host-Mediated Inflammation Disrupts the Intestinal Microbiota and Promotes the Overgrowth of Enterobacteriaceae. *Cell Host Microbe* 2, 119–129.
- Ma, W., Lim, W., Gee, K., Aucoin, S., Nandan, D., Kozlowski, M., Diaz-Mitoma, F., and Kumar, A. (2001a). The p38 Mitogen-activated Kinase Pathway Regulates the Human Interleukin-10 Promoter

- via the Activation of Sp1 Transcription Factor in Lipopolysaccharide-stimulated Human Macrophages. *J. Biol. Chem.* 276, 13664–13674.
- Ma, W., Lim, W., Gee, K., Aucoin, S., Nandan, D., Kozlowski, M., Diaz-Mitoma, F., and Kumar, A. (2001b). The p38 Mitogen-activated Kinase Pathway Regulates the Human Interleukin-10 Promoter via the Activation of Sp1 Transcription Factor in Lipopolysaccharide-stimulated Human Macrophages. *J. Biol. Chem.* 276, 13664–13674.
- Macia, L., Tan, J., Vieira, A.T., Leach, K., Stanley, D., Luong, S., Maruya, M., Ian McKenzie, C., Hijikata, A., Wong, C., et al. (2015a). Metabolite-sensing receptors GPR43 and GPR109A facilitate dietary fibre-induced gut homeostasis through regulation of the inflammasome. *Nat. Commun.* 6, 1–15.
- Macia, L., Tan, J., Vieira, A.T., Leach, K., Stanley, D., Luong, S., Maruya, M., Ian McKenzie, C., Hijikata, A., Wong, C., et al. (2015b). Metabolite-sensing receptors GPR43 and GPR109A facilitate dietary fibre-induced gut homeostasis through regulation of the inflammasome. *Nat. Commun.* 6, 1–15.
- Maier, T., Güell, M., and Serrano, L. (2009). Correlation of mRNA and protein in complex biological samples. *FEBS Lett.* 583, 3966–3973.
- Man, S.M., Karki, R., and Kanneganti, T.D. (2017). Molecular mechanisms and functions of pyroptosis, inflammatory caspases and inflammasomes in infectious diseases. *Immunol. Rev.* 277, 61–75.
- Mangan, M.S.J., Olhava, E.J., Roush, W.R., Seidel, H.M., Glick, G.D., and Latz, E. (2018). Targeting the NLRP3 inflammasome in inflammatory diseases. *Nat. Rev. Drug Discov.* 17, 588–606.
- Mao, L., Kitani, A., Strober, W., and Fuss, I.J. (2018). The role of NLRP3 and IL-1 β in the pathogenesis of inflammatory bowel disease. *Front. Immunol.* 9, 2566.
- Mariathasan, S., Weiss, D.S., Newton, K., McBride, J., O'Rourke, K., Roose-Girma, M., Lee, W.P., Weinrauch, Y., Monack, D.M., and Dixit, V.M. (2006a). Cryopyrin activates the inflammasome in response to toxins and ATP. *Nature* 440, 228–232.
- Mariathasan, S., Weiss, D.S., Newton, K., McBride, J., O'Rourke, K., Roose-Girma, M., Lee, W.P., Weinrauch, Y., Monack, D.M., and Dixit, V.M. (2006b). Cryopyrin activates the inflammasome in response to toxins and ATP.
- Marizzoni, M., Cattaneo, A., Mirabelli, P., Festari, C., Lopizzo, N., Nicolosi, V., Mombelli, E., Mazzelli, M., Luongo, D., Naviglio, D., et al. (2020). Short-Chain Fatty Acids and Lipopolysaccharide as Mediators between Gut Dysbiosis and Amyloid Pathology in Alzheimer's Disease. *J. Alzheimer's Dis.* 78, 683–697.
- Marlow, G.J., van Gent, D., and Ferguson, L.R. (2013). Why interleukin-10 supplementation does not work in Crohn's disease patients. *World J. Gastroenterol.* 19, 3931–3941.
- Martinon, F., Burns, K., and Tschopp, J. (2002). The Inflammasome: A molecular platform triggering activation of inflammatory caspases and processing of proIL- β . *Mol. Cell* 10, 417–426.
- Martinon, F., Pétrilli, V., Mayor, A., Tardivel, A., and Tschopp, J. (2006). Gout-associated uric acid crystals activate the NALP3 inflammasome.
- Matthews, G.M., Newbold, A., and Johnstone, R.W. (2012). Intrinsic and Extrinsic Apoptotic Pathway

Signaling as Determinants of Histone Deacetylase Inhibitor Antitumor Activity. In *Advances in Cancer Research*, (Academic Press Inc.), pp. 165–197.

McKenzie, B.A., Mamik, M.K., Saito, L.B., Boghuzian, R., Monaco, M.C., Major, E.O., Lu, J.Q., Branton, W.G., and Power, C. (2018). Caspase-1 inhibition prevents glial inflammasome activation and pyroptosis in models of multiple sclerosis. *Proc. Natl. Acad. Sci. U. S. A.* *115*, E6065–E6074.

McNeela, E.A., Burke, Á., Neill, D.R., Baxter, C., Fernandes, V.E., Ferreira, D., Smeaton, S., El-Rachkidy, R., McLoughlin, R.M., Mori, A., et al. (2010). Pneumolysin activates the NLRP3 inflammasome and promotes proinflammatory cytokines independently of TLR4. *PLoS Pathog.* *6*, 1001191.

Melillo, J.A., Song, L., Bhagat, G., Blazquez, A.B., Plumlee, C.R., Lee, C., Berin, C., Reizis, B., and Schindler, C. (2010). Dendritic Cell (DC)-Specific Targeting Reveals Stat3 as a Negative Regulator of DC Function. *J. Immunol.* *184*, 2638–2645.

Mentella, M.C., Scaldaferri, F., Pizzoferrato, M., Gasbarrini, A., and Miggiano, G.A.D. (2020). Nutrition, IBD and Gut Microbiota: A Review. *Nutrients* *12*.

Menu, P., Mayor, A., Zhou, R., Tardivel, A., Ichijo, H., Mori, K., and Tschopp, J. (2012). ER stress activates the NLRP3 inflammasome via an UPR-independent pathway. *Cell Death Dis.* *3*.

Di Meo, S., Reed, T.T., Venditti, P., and Victor, V.M. (2016). Role of ROS and RNS Sources in Physiological and Pathological Conditions. *Oxid. Med. Cell. Longev.* *2016*.

Micheau, O., and Tschopp, J. (2003). Induction of TNF receptor I-mediated apoptosis via two sequential signaling complexes. *Cell* *114*, 181–190.

Michielan, A., and D'Inca, R. (2015). Intestinal Permeability in Inflammatory Bowel Disease: Pathogenesis, Clinical Evaluation, and Therapy of Leaky Gut. *Mediators Inflamm.* *2015*.

Mion, F., Tonon, S., Toffoletto, B., Cesselli, D., Pucillo, C.E., and Vitale, G. (2014). IL-10 production by B cells is differentially regulated by immune-mediated and infectious stimuli and requires p38 activation. *Mol. Immunol.* *62*, 266–276.

Misselwitz, B., Juillerat, P., Sulz, M.C., Siegmund, B., and Brand, S. (2020). Emerging Treatment Options in Inflammatory Bowel Disease: Janus Kinases, Stem Cells, and More. *Digestion* *101*, 69–82.

Mitsuyama, K., Matsumoto, S., Masuda, J., Yamasaki, H., Kuwaki, K., Takedatsu, H., and Sata, M. (2007). Therapeutic strategies for targeting the IL-6/STAT3 cytokine signaling pathway in inflammatory bowel disease. *Anticancer Res.* *27*, 3749–3756.

Mogensen, T.H. (2009). Pathogen recognition and inflammatory signaling in innate immune defenses. *Clin. Microbiol. Rev.* *22*, 240–273.

Mondot, S., De Wouters, T., Doré, J., and Lepage, P. (2013). The human gut microbiome and its dysfunctions. In *Digestive Diseases*, (S. Karger AG), pp. 278–285.

Morgan, M.J., and Liu, Z.G. (2011). Crosstalk of reactive oxygen species and NF- κ B signaling. *Cell Res.* *21*, 103–115.

Moriwaki, K., Bertin, J., Gough, P.J., and Chan, F.K.-M. (2015). A RIPK3–Caspase 8 Complex Mediates Atypical Pro-IL-1 β Processing. *J. Immunol.* *194*, 1938–1944.

Mueller, S.N., Gebhardt, T., Carbone, F.R., and Heath, W.R. (2013). Memory T cell subsets, migration patterns, and tissue residence. *Annu. Rev. Immunol.* *31*, 137–161.

- Muendlein, H.I., Jetton, D., Connolly, W.M., Eidell, K.P., Magri, Z., Smirnova, I., and Poltorak, A. (2020). CFLIPL protects macrophages from LPS-induced pyroptosis via inhibition of complex II formation. *Science* (80-.). 367, 1379–1384.
- Mukhopadhyay, S., Heinz, E., Porreca, I., Alasoo, K., Yeung, A., Yang, H.T., Schwerd, T., Forbester, J.L., Hale, C., Agu, C.A., et al. (2020). Loss of IL-10 signaling in macrophages limits bacterial killing driven by prostaglandin E2. *J. Exp. Med.* 217.
- Muñoz-Planillo, R., Kuffa, P., Martínez-Colón, G., Smith, B.L., Rajendiran, T.M., and Núñez, G. (2013). K⁺ Efflux Is the Common Trigger of NLRP3 Inflammasome Activation by Bacterial Toxins and Particulate Matter. *Immunity* 38, 1142–1153.
- Nagini, S., Sophia, J., and Mishra, R. (2019). Glycogen synthase kinases: Moonlighting proteins with theranostic potential in cancer. *Semin. Cancer Biol.* 56, 25–36.
- Nakaya, Y., Lilue, J., Stavrou, S., Moran, E.A., and Ross, S.R. (2017). AIM2-like receptors positively and negatively regulate the interferon response induced by cytosolic DNA. *MBio* 8.
- Nepstad, I., Hatfield, K.J., Grønningsæter, I.S., Aasebø, E., Hernandez-Valladares, M., Hagen, K.M., Rye, K.P., Berven, F.S., Selheim, F., Reikvam, H., et al. (2019). Effects of insulin and pathway inhibitors on the PI3K-Akt-mTOR phosphorylation profile in acute myeloid leukemia cells. *Signal Transduct. Target. Ther.* 4.
- Neudecker, V., Haneklaus, M., Jensen, O., Khailova, L., Masterson, J.C., Tye, H., Biette, K., Jedlicka, P., Brodsky, K.S., Gerich, M.E., et al. (2017). Myeloid-derived miR-223 regulates intestinal inflammation via repression of the NLRP3 inflammasome. *J. Exp. Med.* 214, 1737–1752.
- Neunlist, M., and Schemann, M. (2014). Nutrient-induced changes in the phenotype and function of the enteric nervous system. *J. Physiol.* 592, 2959–2965.
- Neurath, M.F. (2014). Cytokines in inflammatory bowel disease. *Nat. Rev. Immunol.* 14, 329–342.
- Neurath, M.F. (2017). Current and emerging therapeutic targets for IBD. *Nat. Rev. Gastroenterol. Hepatol.* 14, 269–278.
- Newton, K. (2015). RIPK1 and RIPK3 : critical regulators of inflammation and cell death. *Trends Cell Biol.* 25, 347–353.
- Nguyen, L.H., Örtqvist, A.K., Cao, Y., Simon, T.G., Roelstraete, B., Song, M., Joshi, A.D., Staller, K., Chan, A.T., Khalili, H., et al. (2020). Antibiotic use and the development of inflammatory bowel disease: a national case-control study in Sweden. *Lancet Gastroenterol. Hepatol.* 5, 986–995.
- Nishida, A., Inoue, R., Inatomi, O., Bamba, S., Naito, Y., and Andoh, A. (2018). Gut microbiota in the pathogenesis of inflammatory bowel disease. *Clin. J. Gastroenterol.* 11.
- Nishiwaki, H., Hamaguchi, T., Ito, M., Ishida, T., Maeda, T., Kashihara, K., Tsuboi, Y., Ueyama, J., Shimamura, T., Mori, H., et al. (2020). Short-Chain Fatty Acid-Producing Gut Microbiota Is Decreased in Parkinson's Disease but Not in Rapid-Eye-Movement Sleep Behavior Disorder. *MSystems* 5.
- Norbury, C.J., and Zhivotovsky, B. (2004). DNA damage-induced apoptosis. *Oncogene* 23, 2797–2808.
- Ochoa-Repáraz, J., and Kasper, L.H. (2016). The Second Brain: Is the Gut Microbiota a Link Between Obesity and Central Nervous System Disorders? *Curr. Obes. Rep.* 5, 51–64.
- Ofengeim, D., and Yuan, J. (2013). Regulation of RIP1 kinase signalling at the crossroads of

- inflammation and cell death. *Nat. Rev. Mol. Cell Biol.* *14*, 727–736.
- Öztürk Akcora, B., Vassilios Gabriël, A., Ortiz-Perez, A., and Bansal, R. (2020). Pharmacological inhibition of STAT3 pathway ameliorates acute liver injury in vivo via inactivation of inflammatory macrophages and hepatic stellate cells. *FASEB BioAdvances* *2*, 77–89.
- Pellegrini, C., Antonioli, L., Lopez-Castejon, G., Blandizzi, C., and Fornai, M. (2017). Canonical and non-canonical activation of NLRP3 inflammasome at the crossroad between immune tolerance and intestinal inflammation. *Front. Immunol.* *8*.
- Perera, A.P., Fernando, R., Shinde, T., Gundamaraju, R., Southam, B., Sohal, S.S., Robertson, A.A.B., Schroder, K., Kunde, D., and Eri, R. (2018). MCC950, a specific small molecule inhibitor of NLRP3 inflammasome attenuates colonic inflammation in spontaneous colitis mice. *Sci. Rep.* *8*.
- Perregaux, D., and Gabel, C.A. (1994). Interleukin-1 β maturation and release in response to ATP and nigericin. Evidence that potassium depletion mediated by these agents is a necessary and common feature of their activity. *J. Biol. Chem.* *269*, 15195–15203.
- Peter, M.E. (2011). Programmed cell death: Apoptosis meets necrosis. *Nature* *471*, 310–312.
- Phillips, T.A., Ni, J., and Hunt, J.S. (2001). Death-inducing tumour necrosis factor (TNF) superfamily ligands and receptors are transcribed in human placentae, cytotrophoblasts, placental macrophages and placental cell lines. *Placenta* *22*, 663–672.
- Pithadia, A.B., and Jain, S. (2011). Treatment of inflammatory bowel disease (IBD). *Pharmacol. Reports* *63*, 629–642.
- Place, D.E., Lee, S.J., and Kanneganti, T.D. (2021). PANoptosis in microbial infection. *Curr. Opin. Microbiol.* *59*, 42–49.
- Pressman, B.C. (1976). Biological applications of ionophores. *Annu. Rev. Biochem.* *Vol. 45*, 501–530.
- Próchnicki, T., and Latz, E. (2017). Inflammasomes on the Crossroads of Innate Immune Recognition and Metabolic Control. *Cell Metab.* *26*, 71–93.
- Prow, N.A., Hirata, T.D.C., Tang, B., Larcher, T., Mukhopadhyay, P., Alves, T.L., Le, T.T., Gardner, J., Poo, Y.S., Nakayama, E., et al. (2019). Exacerbation of Chikungunya Virus Rheumatic Immunopathology by a High Fiber Diet and Butyrate. *Front. Immunol.* *10*, 2736.
- Puddu, A., Sanguineti, R., Montecucco, F., and Viviani, G.L. (2014). Evidence for the gut microbiota short-chain fatty acids as key pathophysiological molecules improving diabetes. *Mediators Inflamm.* *2014*.
- Py, B.F., Kim, M.S., Vakifahmetoglu-Norberg, H., and Yuan, J. (2013). Deubiquitination of NLRP3 by BRCC3 Critically Regulates Inflammasome Activity. *Mol. Cell* *49*, 331–338.
- Ramos, G.P., and Papadakis, K.A. (2019). Mechanisms of Disease: Inflammatory Bowel Diseases. *Mayo Clin. Proc.* *94*, 155–165.
- Raulet, D.H. (2004). Interplay of natural killer cells and their receptors with the adaptive immune response. *Nat. Immunol.* *5*, 996–1002.
- Riera Romo, M., Pérez-Martínez, D., and Castillo Ferrer, C. (2016). Innate immunity in vertebrates: An overview. *Immunology* *148*, 125–139.
- Robinson, M.D., and Oshlack, A. (2010). A scaling normalization method for differential expression analysis of RNA-seq data. *Genome Biol.* *11*, 1–9.

- Robinson, M.D., McCarthy, D.J., and Smyth, G.K. (2009). edgeR: A Bioconductor package for differential expression analysis of digital gene expression data. *Bioinformatics* 26, 139–140.
- Round, J.L., and Palm, N.W. (2018). Causal effects of the microbiota on immune-mediated diseases. *Sci. Immunol.* 3, o1603.
- Rundquist, S., Sachs, M.C., Eriksson, C., Olén, O., Montgomery, S., and Halfvarson, J. (2021). Drug survival of anti-TNF agents compared with vedolizumab as a second-line biological treatment in inflammatory bowel disease: results from nationwide Swedish registers. *Aliment. Pharmacol. Ther.* 53, 471–483.
- Russo, E., Giudici, F., Fiorindi, C., Ficari, F., Scaringi, S., and Amedei, A. (2019). Immunomodulating Activity and Therapeutic Effects of Short Chain Fatty Acids and Tryptophan Post-biotics in Inflammatory Bowel Disease. *Front. Immunol.* 10, 2754.
- Sagulenko, V., Thygesen, S.J., Sester, D.P., Idris, A., Cridland, J.A., Vajjhala, P.R., Roberts, T.L., Schroder, K., Vince, J.E., Hill, J.M., et al. (2013). AIM2 and NLRP3 inflammasomes activate both apoptotic and pyroptotic death pathways via ASC. *Cell Death Differ.* 20, 1149–1160.
- Sai, K., Parsons, C., House, J.S., Kathariou, S., and Ninomiya-Tsuji, J. (2019). Necroptosis mediators RIPK3 and MLKL suppress intracellular *Listeria* replication independently of host cell killing. *J. Cell Biol.* 218, 1994–2005.
- Sanchez-Muñoz, F., Dominguez-Lopez, A., and Yamamoto-Furusho, J.K. (2008). Role of cytokines in inflammatory bowel disease. *World J. Gastroenterol.* 14, 4280–4288.
- Sandborn, W.J., Colombel, J.F., Ghosh, S., Sands, B.E., Dryden, G., Hébuterne, X., Leong, R.W., Bressler, B., Ullman, T., Lakatos, P.L., et al. (2016). Eldelumab [Anti-IP-10] induction therapy for ulcerative colitis: A randomised, placebo-controlled, phase 2b study. *J. Crohn's Colitis* 10, 418–428.
- Sandborn, W.J., Ferrante, M., Bhandari, B.R., Berliba, E., Feagan, B.G., Hibi, T., Tuttle, J.L., Klekotka, P., Friedrich, S., Durante, M., et al. (2020). Efficacy and Safety of Mirikizumab in a Randomized Phase 2 Study of Patients With Ulcerative Colitis. *Gastroenterology* 158, 537-549.e10.
- Santos, M.P.C., Gomes, C., and Torres, J. (2018). Familial and ethnic risk in inflammatory bowel disease. *Ann. Gastroenterol.* 31, 14–23.
- Saraste, A., and Pulkki, K. (2000). Morphologic and biochemical hallmarks of apoptosis. *Cardiovasc. Res.* 45, 528–537.
- Sarkar, A., Lehto, S.M., Harty, S., Dinan, T.G., Cryan, J.F., and Burnet, P.W.J. (2016). Psychobiotics and the Manipulation of Bacteria–Gut–Brain Signals. *Trends Neurosci.* 39, 763–781.
- Schrecengost, R.S., Green, C.L., Zhuang, Y., Keller, S.N., Smith, R.A., Maines, L.W., and Smith, C.D. (2018a). In Vitro and In Vivo Antitumor and Anti-Inflammatory Capabilities of the Novel GSK3 and CDK9 Inhibitor ABC1183 s. *J. Pharmacol. Exp. Ther. J Pharmacol Exp Ther* 365, 107–116.
- Schrecengost, R.S., Green, C.L., Zhuang, Y., Keller, S.N., Smith, R.A., Maines, L.W., and Smith, C.D. (2018b). In vitro and in vivo antitumor and anti-inflammatory capabilities of the novel GSK3 and CDK9 inhibitor ABC1183s. *J. Pharmacol. Exp. Ther.* 365, 107–116.
- Schroeder, B.O., and Bäckhed, F. (2016). Signals from the gut microbiota to distant organs in physiology and disease. *Nat. Med.* 22, 1079–1089.
- Schulthess, J., Pandey, S., Capitani, M., Arancibia-ca, C. V, Uhlig, H.H., Powrie, F., Schulthess, J.,

- Pandey, S., Capitani, M., Rue-albrecht, K.C., et al. (2019). The Short Chain Fatty Acid Butyrate Imprints an Antimicrobial Program in Macrophages. 1–14.
- Shaw, M.H., Freeman, G.J., Scott, M.F., Fox, B.A., Bzik, D.J., Belkaid, Y., and Yap, G.S. (2006a). Tyk2 Negatively Regulates Adaptive Th1 Immunity by Mediating IL-10 Signaling and Promoting IFN- γ -Dependent IL-10 Reactivation. *J. Immunol.* 176, 7263–7271.
- Shaw, M.H., Freeman, G.J., Scott, M.F., Fox, B.A., Bzik, D.J., Belkaid, Y., and Yap, G.S. (2006b). Tyk2 Negatively Regulates Adaptive Th1 Immunity by Mediating IL-10 Signaling and Promoting IFN- γ -Dependent IL-10 Reactivation. *J. Immunol.* 176, 7263–7271.
- Shi, C.S., Shenderov, K., Huang, N.N., Kabat, J., Abu-Asab, M., Fitzgerald, K.A., Sher, A., and Kehrl, J.H. (2012). Activation of autophagy by inflammatory signals limits IL-1 β production by targeting ubiquitinated inflammasomes for destruction. *Nat. Immunol.* 13, 255–263.
- Shi, J., Zhao, Y., Wang, Y., Gao, W., Ding, J., Li, P., Hu, L., and Shao, F. (2014). Inflammatory caspases are innate immune receptors for intracellular LPS. *Nature* 514, 187–192.
- Shi, J., Zhao, Y., Wang, K., Shi, X., Wang, Y., Huang, H., Zhuang, Y., Cai, T., Wang, F., and Shao, F. (2015). Cleavage of GSDMD by inflammatory caspases determines pyroptotic cell death. *Nature* 526, 660–665.
- Shim, J.O., and Seo, J.K. (2014). Very early-onset inflammatory bowel disease (IBD) in infancy is a different disease entity from adult-onset IBD; One form of interleukin-10 receptor mutations. *J. Hum. Genet.* 59, 337–341.
- Shio, M.T., Christian, J.G., Jung, J.Y., Chang, K.P., and Olivier, M. (2015). PKC/ROS-mediated NLRP3 inflammasome activation is attenuated by leishmania zinc- metalloprotease during infection. *PLoS Negl. Trop. Dis.* 9.
- Shouval, D.S., Biswas, A., Kang, Y.H., Griffith, A.E., Konnikova, L., Mascanfroni, I.D., Redhu, N.S., Frei, S.M., Field, M., Doty, A.L., et al. (2016). Interleukin 1 β Mediates Intestinal Inflammation in Mice and Patients With Interleukin 10 Receptor Deficiency. *Gastroenterology* 151, 1100–1104.
- Siegel, C.A., and Melmed, G.Y. (2009). Predicting response to anti-TNF agents for the treatment of Crohn's disease. *Therap. Adv. Gastroenterol.* 2, 245–251.
- Silva, L.G., Ferguson, B.S., Avila, A.S., and Faciola, A.P. (2018). Sodium propionate and sodium butyrate effects on histone deacetylase (HDAC) activity, histone acetylation, and inflammatory gene expression in bovine mammary epithelial cells. *J. Anim. Sci.* 96, 5244–5252.
- Silva, Y.P., Bernardi, A., and Frozza, R.L. (2020). The Role of Short-Chain Fatty Acids From Gut Microbiota in Gut-Brain Communication. *Front. Endocrinol. (Lausanne).* 11, 25.
- Simon, E.G., Ghosh, S., Iacucci, M., and Moran, G.W. (2016). Ustekinumab for the treatment of Crohn's disease: Can it find its niche? *Therap. Adv. Gastroenterol.* 9, 26–36.
- Singh, U.P., Singh, N.P., Murphy, E.A., Price, R.L., Fayad, R., Nagarkatti, M., and Nagarkatti, P.S. (2016). Chemokine and cytokine levels in inflammatory bowel disease patients. *Cytokine* 77, 44–49.
- Singh, V., Yeoh, B.S., Walker, R.E., Xiao, X., Saha, P., Golonka, R.M., Cai, J., Bretin, A.C.A., Cheng, X., Liu, Q., et al. (2019). Microbiota fermentation-NLRP3 axis shapes the impact of dietary fibres on intestinal inflammation. *Gut* 68, 1801–1812.
- De Smedt, T., Van Mechelen, M., De Becker, G., Urbain, J., Leo, O., and Moser, M. (1997). Effect of

- interleukin-10 on dendritic cell maturation and function. *Eur. J. Immunol.* 27, 1229–1235.
- Stammler, D., Eigenbrod, T., Menz, S., Frick, J.S., Sweet, M.J., Shakespear, M.R., Jantsch, J., Siegert, I., Wolffe, S., Langer, J.D., et al. (2015). Inhibition of Histone Deacetylases Permits Lipopolysaccharide-Mediated Secretion of Bioactive IL-1 via a Caspase-1-Independent Mechanism. *J. Immunol.* 195, 5421–5431.
- Statovci, D., Aguilera, M., MacSharry, J., and Melgar, S. (2017). The impact of western diet and nutrients on the microbiota and immune response at mucosal interfaces. *Front. Immunol.* 8, 838.
- Steen, E.H., Wang, X., Balaji, S., Butte, M.J., Bollyky, P.L., and Keswani, S.G. (2020). The Role of the Anti-Inflammatory Cytokine Interleukin-10 in Tissue Fibrosis. *Adv. Wound Care* 9, 184–198.
- Striz, I., Brabcova, E., Kolesar, L., and Sekerkova, A. (2014). Cytokine networking of innate immunity cells: A potential target of therapy. *Clin. Sci.* 126, 593–612.
- Stutz, A., Kolbe, C.-C., Stahl, R., Horvath, G.L., Franklin, B.S., van Ray, O., Brinkschulte, R., Geyer, M., Meissner, F., and Latz, E. (2017). NLRP3 inflammasome assembly is regulated by phosphorylation of the pyrin domain. *J. Exp. Med.* 214, 1725–1736.
- Subramanian, A., Tamayo, P., Mootha, V.K., Mukherjee, S., Ebert, B.L., Gillette, M.A., Paulovich, A., Pomeroy, S.L., Golub, T.R., Lander, E.S., et al. (2005). Gene set enrichment analysis: A knowledge-based approach for interpreting genome-wide expression profiles. *Proc. Natl. Acad. Sci. U. S. A.* 102, 15545–15550.
- Sugimoto, K. (2008). Role of STAT3 in inflammatory bowel disease. *World J. Gastroenterol.* 14, 5110–5114.
- Swann, O.G., Kilpatrick, M., Breslin, M., and Oddy, W.H. (2020). Dietary fiber and its associations with depression and inflammation. *Nutr. Rev.* 78, 394–411.
- Taabazuig, C.Y., Okondo, M.C., and Bachovchin, D.A. (2017). Pyroptosis and Apoptosis Pathways Engage in Bidirectional Crosstalk in Monocytes and Macrophages. *Cell Chem. Biol.* 24, 507-514.e4.
- Tai, Y.H., Tsai, R.Y., Lin, S.L., Yeh, C.C., Wang, J.J., Tao, P.L., and Wong, C.S. (2009). Amitriptyline suppresses neuroinflammation-dependent interleukin-10-p38 mitogen-activated protein kinase-heme oxygenase-1 signaling pathway in chronic morphine-infused rats. *Anesthesiology* 110, 1379–1389.
- Takahashi, N., Vereecke, L., Bertrand, M.J.M., Duprez, L., Berger, S.B., Divert, T., Gonçalves, A., Sze, M., Gilbert, B., Kourula, S., et al. (2014a). The epithelium against apoptosis.
- Takahashi, N., Vereecke, L., Bertrand, M.J.M., Duprez, L., Berger, S.B., Divert, T., Gonçalves, A., Sze, M., Gilbert, B., Kourula, S., et al. (2014b). RIPK1 ensures intestinal homeostasis by protecting the epithelium against apoptosis. *Nature* 513, 95–99.
- Takiishi, T., Fenero, C.I.M., and Câmara, N.O.S. (2017). Intestinal barrier and gut microbiota: Shaping our immune responses throughout life. *Tissue Barriers* 5.
- Tang, Y., Chen, Y., Jiang, H., and Nie, D. (2011). Short-chain fatty acids induced autophagy serves as an adaptive strategy for retarding mitochondria-mediated apoptotic cell death. *Cell Death Differ.* 18, 602–618.
- Telle-Hansen, V.H., Holven, K.B., and Ulven, S.M. (2018). Impact of a healthy dietary pattern on gut microbiota and systemic inflammation in humans. *Nutrients* 10.
- Thomas, M., Wrzosek, L., Miquel, S., Noordine, M.-L., Bouet, S., Chevalier-Curt, M.J., Robert, V.,

- Philippe, C., Bridonneau, C., Cherbuy, C., et al. (2013). 264 *Bacteroides Thetaiotaomicron* and *Faecalibacterium prausnitzii* Shape the Mucus Production and Mucin O-Glycosylation in Colon Epithelium. *Gastroenterology* 144, S-59.
- Tokuhira, N., Kitagishi, Y., Suzuki, M., Minami, A., Nakanishi, A., Ono, Y., Kobayashi, K., Matsuda, S., and Ogura, Y. (2015). PI3K/AKT/PTEN pathway as a target for Crohn's disease therapy (Review). *Int. J. Mol. Med.* 35, 10–16.
- Toldo, S., and Abbate, A. (2018). The NLRP3 inflammasome in acute myocardial infarction. *Nat. Rev. Cardiol.* 15, 203–214.
- Trinchieri, G. (2007). Interleukin-10 production by effector T cells: Th1 cells show self control. *J. Exp. Med.* 204, 239–243.
- Trompette, A., Gollwitzer, E.S., Pattaroni, C., Lopez-Mejia, I.C., Riva, E., Pernot, J., Ubags, N., Fajas, L., Nicod, L.P., and Marsland, B.J. (2018). Dietary Fiber Confers Protection against Flu by Shaping Ly6c⁺ Patrolling Monocyte Hematopoiesis and CD8⁺T Cell Metabolism. *Immunity* 48, 992-1005.e8.
- Tsugawa, H., Kabe, Y., Kanai, A., Sugiura, Y., Hida, S., Shun'ichiro Taniguchi, Takahashi, T., Matsui, H., Yasukawa, Z., Itou, H., et al. (2020). Short-chain fatty acids bind to apoptosis-associated speck-like protein to activate inflammasome complex to prevent *Salmonella* infection. *PLoS Biol.* 18.
- Ugucioni, M., Gionchetti, P., Robbiani, D.F., Rizzello, F., Peruzzo, S., Campieri, M., and Baggiolini, M. (1999). Increased expression of IP-10, IL-8, MCP-1, and MCP-3 in ulcerative colitis. *Am. J. Pathol.* 155, 331–336.
- Vanaja, S.K., Russo, A.J., Behl, B., Banerjee, I., Yankova, M., Deshmukh, S.D., and Rathinam, V.A.K. (2016). Bacterial Outer Membrane Vesicles Mediate Cytosolic Localization of LPS and Caspase-11 Activation. *Cell* 165, 1106–1119.
- Vandanmagsar, B., Youm, Y.H., Ravussin, A., Galgani, J.E., Stadler, K., Mynatt, R.L., Ravussin, E., Stephens, J.M., and Dixit, V.D. (2011). The NLRP3 inflammasome instigates obesity-induced inflammation and insulin resistance. *Nat. Med.* 17, 179–189.
- VanDeusen, J.B., Shah, M.H., Beknell, B., Blaser, B.W., Ferketich, A.K., Nuovo, G.J., Ahmer, B.M.M., Durbin, J., and Caligiuri, M.A. (2006). STAT-1-mediated repression of monocyte interleukin-10 gene expression in vivo. *Eur. J. Immunol.* 36, 623–630.
- Venegas, D.P., De La Fuente, M.K., Landskron, G., González, M.J., Quera, R., Dijkstra, G., Harmsen, H.J.M., Faber, K.N., and Hermoso, M.A. (2019). Short chain fatty acids (SCFAs) mediated gut epithelial and immune regulation and its relevance for inflammatory bowel diseases. *Front. Immunol.* 10, 277.
- Verhoef, J., van Kessel, K., and Snippe, H. (2019). Immune Response in Human Pathology: Infections Caused by Bacteria, Viruses, Fungi, and Parasites. In Nijkamp and Parnham's Principles of Immunopharmacology, (Springer International Publishing), pp. 165–178.
- Vignali, D.A.A., Collison, L.W., and Workman, C.J. (2008). How regulatory T cells work. *Nat. Rev. Immunol.* 8, 523–532.
- Villagra, A., Cheng, F., Wang, H.W., Suarez, I., Glozak, M., Maurin, M., Nguyen, D., Wright, K.L., Atadja, P.W., Bhalla, K., et al. (2009). The histone deacetylase HDAC11 regulates the expression of interleukin 10 and immune tolerance. *Nat. Immunol.* 10, 92–100.

- Vinolo, M.A.R., Rodrigues, H.G., Nachbar, R.T., and Curi, R. (2011). Regulation of inflammation by short chain fatty acids. *Nutrients* 3, 858–876.
- Vivier, E., and Malissen, B. (2005). Innate and adaptive immunity: Specificities and signaling hierarchies revisited. *Nat. Immunol.* 6, 17–21.
- Vogel, C., and Marcotte, E.M. (2012). Insights into the regulation of protein abundance from proteomic and transcriptomic analyses. *Nat. Rev. Genet.* 13, 227–232.
- Vulliemoz, M., Brand, S., Juillerat, P., Mottet, C., Ben-Horin, S., and Michetti, P. (2020). TNF-Alpha Blockers in Inflammatory Bowel Diseases: Practical Recommendations and a User's Guide: An Update. *Digestion* 101, 16–26.
- Waldecker, M., Kautenburger, T., Daumann, H., Busch, C., and Schrenk, D. (2008). Inhibition of histone-deacetylase activity by short-chain fatty acids and some polyphenol metabolites formed in the colon. *J. Nutr. Biochem.* 19, 587–593.
- Wang, G., Huang, S., Wang, Y., Cai, S., Yu, H., Liu, H., Zeng, X., Zhang, G., and Qiao, S. (2019a). Bridging intestinal immunity and gut microbiota by metabolites. *Cell. Mol. Life Sci.* 76, 3917–3937.
- Wang, K., Yao, Y., Zhu, X., Zhang, K., Zhou, F., and Zhu, L. (2017). Amyloid β induces NLRP3 inflammasome activation in retinal pigment epithelial cells via NADPH oxidase- and mitochondria-dependent ROS production. *J. Biochem. Mol. Toxicol.* 31.
- Wang, S., Yuan, Y.H., Chen, N.H., and Wang, H.B. (2019b). The mechanisms of NLRP3 inflammasome/pyroptosis activation and their role in Parkinson's disease. *Int. Immunopharmacol.* 67, 458–464.
- Wang, X., Jiang, W., Yan, Y., Gong, T., Han, J., Tian, Z., and Zhou, R. (2014). RNA viruses promote activation of the NLRP3 inflammasome through a RIP1-RIP3-DRP1 signaling pathway. *Nat. Immunol.* 15, 1126–1133.
- Wang, X., He, G., Peng, Y., Zhong, W., Wang, Y., and Zhang, B. (2015). Sodium butyrate alleviates adipocyte inflammation by inhibiting NLRP3 pathway. *Sci. Rep.* 5, 1–10.
- Wang, Z., Zhang, S., Xiao, Y., Zhang, W., Wu, S., Qin, T., Yue, Y., Qian, W., and Li, L. (2020). NLRP3 Inflammasome and Inflammatory Diseases. *Oxid. Med. Cell. Longev.* 2020.
- Wannamaker, W., Davies, R., Namchuk, M., Pollard, J., Ford, P., Ku, G., Decker, C., Charifson, P., Weber, P., Germann, U.A., et al. (2007a). (S)-1-((S)-2-[[1-(4-amino-3-chloro-phenyl)-methanoyl]-amino]-3, 3-dimethyl-butanoyl)-pyrrolidine-2-carboxylic acid ((2R,3S)-2-ethoxy-5-oxo-tetrahydrofuran-3-yl)-amide (VX-765), an orally available selective interleukin (IL)-converting enzyme/caspase-1 inhibitor. *J. Pharmacol. Exp. Ther.* 321, 509–516.
- Wannamaker, W., Davies, R., Namchuk, M., Pollard, J., Ford, P., Ku, G., Decker, C., Charifson, P., Weber, P., Germann, U.A., et al. (2007b). (S)-1-((S)-2-[[1-(4-amino-3-chloro-phenyl)-methanoyl]-amino]-3, 3-dimethyl-butanoyl)-pyrrolidine-2-carboxylic acid ((2R,3S)-2-ethoxy-5-oxo-tetrahydrofuran-3-yl)-amide (VX-765), an orally available selective interleukin (IL)-converting enzyme/caspase-1 inhibitor. *J. Pharmacol. Exp. Ther.* 321, 509–516.
- Wehinger, J., Gouilleux, F., Groner, B., Finke, J., Mertelsmann, R., and Weber-Nordt, R.M. (1996). IL-10 induces DNA binding activity of three STAT proteins (Stat1, Stat3, and Stat5) and their distinct combinatorial assembly in the promoters of selected genes. *FEBS Lett.* 394, 365–370.

- Weinlich, R., Oberst, A., Beere, H.M., and Green, D.R. (2017). Necroptosis in development, inflammation and disease. *Nat. Rev. Mol. Cell Biol.* 18, 127–136.
- West, N.R., Hegazy, A.N., Owens, B.M.J., Bullers, S.J., Linggi, B., Buonocore, S., Coccia, M., Görtz, D., This, S., Stockenhuber, K., et al. (2017). Oncostatin M drives intestinal inflammation and predicts response to tumor necrosis factor–neutralizing therapy in patients with inflammatory bowel disease. *Nat. Med.* 23, 579–589.
- Wilbers, R.H.P., Van Raaij, D.R., Westerhof, L.B., Bakker, J., Smant, G., and Schots, A. (2017a). Re-evaluation of IL-10 signaling reveals novel insights on the contribution of the intracellular domain of the IL-10R2 chain. *PLoS One* 12, e0186317.
- Wilbers, R.H.P., Van Raaij, D.R., Westerhof, L.B., Bakker, J., Smant, G., and Schots, A. (2017b). Re-evaluation of IL-10 signaling reveals novel insights on the contribution of the intracellular domain of the IL-10R2 chain.
- Wilkins, L.J., Monga, M., and Miller, A.W. (2019). Defining Dysbiosis for a Cluster of Chronic Diseases. *Sci. Rep.* 9, 1–10.
- Willemsen, L.E.M., Koetsier, M.A., Van Deventer, S.J.H., and Van Tol, E.A.F. (2003). Short chain fatty acids stimulate epithelial mucin 2 expression through differential effects on prostaglandin E1 and E2 production by intestinal myofibroblasts. *Gut* 52, 1442–1447.
- Williams, L.M., Ricchetti, G., Sarma, U., Smallie, T., and Foxwell, B.M.J. (2004). Interleukin-10 suppression of myeloid cell activation - A continuing puzzle. *Immunology* 113, 281–292.
- Wu, D., and Smyth, G.K. (2012). Camera: A competitive gene set test accounting for inter-gene correlation. *Nucleic Acids Res.* 40.
- Wu, M., Tian, T., Mao, Q., Zou, T., Zhou, C. Juan, Xie, J., and Chen, J. jun (2020). Associations between disordered gut microbiota and changes of neurotransmitters and short-chain fatty acids in depressed mice. *Transl. Psychiatry* 10, 1–10.
- Wu, W., Sun, M., Chen, F., Cao, A.T., Liu, H., Zhao, Y., Huang, X., Xiao, Y., Yao, S., Zhao, Q., et al. (2017). Microbiota metabolite short-chain fatty acid acetate promotes intestinal IgA response to microbiota which is mediated by GPR43. *Mucosal Immunol.* 10, 946–956.
- Xiao, Y., Zou, Q., Xie, X., Liu, T., Li, H.S., Jie, Z., Jin, J., Hu, H., Manyam, G., Zhang, L., et al. (2017a). The kinase TBK1 functions in dendritic cells to regulate T cell homeostasis, autoimmunity, and antitumor immunity. *J. Exp. Med.* 214, 1493–1507.
- Xiao, Y., Zou, Q., Xie, X., Liu, T., Li, H.S., Jie, Z., Jin, J., Hu, H., Manyam, G., Zhang, L., et al. (2017b). The kinase TBK1 functions in dendritic cells to regulate T cell homeostasis, autoimmunity, and antitumor immunity. *J. Exp. Med.* 214, 1493–1507.
- Xu, D., Jin, T., Zhu, H., Chen, H., Ofengeim, D., Zou, C., Mifflin, L., Pan, L., Amin, P., Li, W., et al. (2018). TBK1 Suppresses RIPK1-Driven Apoptosis and Inflammation during Development and in Aging. *Cell* 174, 1477-1491.e19.
- Yang, R., and Rincon, M. (2016). Mitochondrial Stat3, the need for design thinking. *Int. J. Biol. Sci.* 12, 532–544.
- Yang, J., Zhao, Y., and Shao, F. (2015). Non-canonical activation of inflammatory caspases by cytosolic LPS in innate immunity. *Curr. Opin. Immunol.* 32, 78–83.

- Yilma, A.N., Singh, S.R., Fairley, S.J., Taha, M.A., and Dennis, V.A. (2012). The anti-inflammatory cytokine, interleukin-10, inhibits inflammatory mediators in human epithelial cells and mouse macrophages exposed to live and UV-inactivated chlamydia trachomatis. *Mediators Inflamm.* 2012.
- Yu, T., Yi, Y.S., Yang, Y., Oh, J., Jeong, D., and Cho, J.Y. (2012). The pivotal role of TBK1 in inflammatory responses mediated by macrophages. *Mediators Inflamm.* 2012.
- Yuan, X., Wang, L., Bhat, O.M., Lohner, H., and Li, P.L. (2018). Differential effects of short chain fatty acids on endothelial Nlrp3 inflammasome activation and neointima formation: Antioxidant action of butyrate. *Redox Biol.* 16, 21–31.
- Zanoni, I., Tan, Y., Gioia, M. Di, Broggi, A., Ruan, J., Shi, J., Donado, C.A., Shao, F., Wu, H., Springstead, J.R., et al. (2016). An endogenous caspase-11 ligand elicits interleukin-1 release from living dendritic cells. *Science (80-.)*. 352, 1232–1236.
- Zanoni, I., Tan, Y., Di Gioia, M., Springstead, J.R., and Kagan, J.C. (2017). By Capturing Inflammatory Lipids Released from Dying Cells, the Receptor CD14 Induces Inflammasome-Dependent Phagocyte Hyperactivation. *Immunity* 47, 697-709.e3.
- Zhang, Q., Wu, Y., Wang, J., Wu, G., Long, W., Xue, Z., Wang, L., Zhang, X., Pang, X., Zhao, Y., et al. (2016). Accelerated dysbiosis of gut microbiota during aggravation of DSS-induced colitis by a butyrate-producing bacterium. *Sci. Rep.* 6, 1–11.
- Zhen, Y., and Zhang, H. (2019). NLRP3 inflammasome and inflammatory bowel disease. *Front. Immunol.* 10, 276.
- Zhou, R., Tardivel, A., Thorens, B., Choi, I., and Tschopp, J. (2010). Thioredoxin-interacting protein links oxidative stress to inflammasome activation. *Nat. Immunol.* 11, 136–140.
- Zhu, L., Shi, T., Zhong, C., Wang, Y., Chang, M., and Liu, X. (2017). IL-10 and IL-10 Receptor Mutations in Very Early Onset Inflammatory Bowel Disease. *Gastroenterol. Res.* 10, 65–69.
- Ziegler, S.F. (2016). Division of labour by CD4+ T helper cells. *Nat. Rev. Immunol.* 16, 403.
- Zuo, T., and Ng, S.C. (2018). The Gut Microbiota in the Pathogenesis and Therapeutics of Inflammatory bowel disease. *Front. Microbiol.* 9, 2247.

10. Acknowledgement

I would like to thank my supervisor Prof. Dr. Eicke Latz for giving me the opportunity to conduct my PhD study in the Institute of Innate Immunity. I have learnt a lot from you in both work and life in the past five years, which will be beneficial to me the whole life. Because of you, I have the chance to meet so many nice people, to listen to different languages and to have ice-cream at 1 am in Vibo Valentia (Italy). In addition, I want to say thanks to you for your encouragement in science and life, you opened a new world to me and also changed the way I see the world. Thank you very much!

I would like to especially thank Dr. Bianca Martin for allowing me to take over this amazing project, for your supervision and helpful discussions.

I would like to thank Dr. Susanne Schmidt for her supervision at the beginning of my PhD study, Dr. Matthew S. Mangan for his great help and discussions on my PhD project.

I would like to say thanks to two brilliant students supervised by me, Yubell Patricia Alvarez Valdivia and Alesja Dernst, it is you two who make me more and more confident.

I would like to thank all the technical assistants in the AG Latz, Fraser G. Duthie, Maximilian Rothe, Romina Kaiser, Gudrun Engels and Rainer Stahl for your help with plasmid designing, mice experiments, monocytes purification, L929 generation and software setup.

I would like to express my gratitude to my office family (past and present) in BMZ1 and BMZ2, Dr. Mario Lauterbach, Dr. James Stunden, Carl Christian Kolbe, Lena Standke, Marta Lovotti, Ornina Marma, Tobias Dierkes, Fraser G. Duthie, Maximilian Rothe, for giving me so many good memories, for all the translations and for all the care to my family, it was a great pleasure in the same office with you.

Many thanks to Dr. Pia Langhoff, Dr. Damien Bertheloot, Dr. Anette Christ, Dr. Alena Grebe, Dr. Florian Hoß, Dr. Christina Budden for all the conversations and encouragement during my PhD study. Special thanks to Dr. Christina Budden for all the fantastic RNA-seq and MS data analyses and explanations.

Many thanks to all collaborators involved in my project, Neil Stair, Prof. Manolis Pasparakis, Meera Phulphagar, Prof. Felix Meissner, Debjani Biswas, Dr. Peter Düwell, Dr. Ashley

Mansell. All the experiments performed by you are of great importance for me to finish my PhD thesis.

Many thanks to my Brazilian colleagues and friends, Dr. Laura Migliari Branco, Dr. Marina Lima Silva Santos, Dr. Tarcio Braga and Dr. Lucas Secchim Ribeiro for all the help in my study and life.

I would like to thank Dr. Tomasz Prochnicki, Dr. Juan Francisco Rodríguez Alcazár and Eike Geissmar for proofreading my thesis. Many thanks to Dr. Tomasz Prochnicki for all the discussions about my project, I can't find anyone who is as cool as you. A big thank you to Juan and Eike, you make me feel like at home in Bonn.

I would like to thank my Thesis Committee: Prof. Joachim Schultze, Prof. Matthias Geyer and Prof. Wolfgang Kastenmüller for agreeing to review and evaluate my thesis.

我要感谢我的家人, 爸爸王丙中, 妈妈计秀勤, 哥哥王伸和王春魏, 谢谢你们这么多年来照顾, 关心, 支持和理解, 希望你们看到我的博士毕业会感到这么多年来付出是值得的, 我没有让你们失望。

感谢我的岳父杨正尚和岳母陈艳这几年来宽容和支持。

感谢我的女儿妙妙和六六, 你们让我懂得了尊重, 理解和宽容, 我爱你们。

感谢高田子阿姨这十年来的鼓励, 教导和厚爱, 我从中受益良多。

最后, 我要感谢我的妻子杨珊珊, 感谢你这么多年来陪伴, 照顾, 宽容, 理解和支持, 我很幸运有你在身边。

11. Curriculum Vitae